Electric Technology U.S.S.R.

ЭЛЕКТРИЧЕСТВО

Volume 3, November, 1959

Selected papers from
Elektrichestvo Nos. 7, 8 and 9, 1958

Published by

PERGAMON · PRESS NEW YORK LONDON OXFORD PARIS LOS ANGELE

for Pergamon Institute, Washington and Oxfor

ELECTRIC TECHNOLOGY, U.S.S.R.

EDITORIAL BOARD

H. M. Barlow, *London;* F. W. Bowden, *San Luis Obispo;* F. Brailsford, *London;* G. S. Brown, *Cambridge, Mass.;* F. M. Bruce, *Glasgow;* C. C. Carr, *Brooklyn;* G. W. Carter, *Leeds;* A. G. Conrad, *New Haven, Conn.;* G. F. Corcoran, *College Park, Md.;* J. D. Craggs, *Liverpool;* A. L. Cullen, *Sheffield;* G. E. Dreifke, *St. Louis;* V. Easton, *Birmingham;* A. R. Eckels, *Vermont;* W. Fishwick, *Swansea;* C. Froehlich, *New York;* C. G. Garton, *Leatherhead;* J. Greig, *London;* L. D. Harris, *Salt Lake City;* J. D. Horgan, *Milwaukee;* E. C. Jones, *Morgantown;* E. C. Jordan, *Urbana;* I. H. Lovett, *Rolla, Missouri;* J. M. Meek, *Liverpool;* J. H. Mulligan, Jnr., *N.Y.;* W. A. Murray, *Blacksburg, Virginia;* J. E. Parton, *Nottingham;* H. A. Peterson, *Madison;* A. Porter, *London;* J. C. Read, *Rugby;* W. G. Shepherd, *Minneapolis;* W. P. Smith, *Lawrence, Kansas;* Philip Sporn (Chairman), *New York;* J. A. Strelzoff, *East Lansing;* F. W. Tatum, *Dallas, Texas;* C. V. O. Terwilliger, *Monterey;* D. H. Tompsett, *Stafford;* A. Tustin, *London;* S. Reid Warren Jnr., *Philadelphia;* A. R. van C. Warrington, *Stafford;* A. H. Waynick, *Pa.;* E. M. Williams, *Pittsburgh;* F. C. Williams, *Manchester;* H. I. Wood, *Manchester;* C. M. Zieman, *Ohio.*

PERGAMON INSTITUTE

A DIVISION OF PERGAMON INTERNATIONAL CORPORATION, OPERATED IN THE PUBLIC SERVICE FOR THE FURTHERANCE AND DISSEMINATION OF SCIENTIFIC KNOWLEDGE

President of the Scientific Advisory Council:
Sir Robert Robinson, O.M., F.R.S.

Executive Director: Captain I. R. Maxwell, M.C.

Scientific Secretary: Dr. D. J. Hughes

1404 New York Avenue, N.W., WASHINGTON, 5, D.C. (Telephone No. Metropole No. 8-5382)
Headington Hill Hall, OXFORD. (Telephone No. Oxford 64881)

Pergamon Institute can occasionally use additional translators for science and engineering material to assist with this programme of translation from Russian and other Slavonic languages.

Scientists and engineers who have a knowledge of Russian, and who are willing to assist with this work, should apply to the Administrative Secretary of the Institute. They should write to either Washington, D.C., or Oxford for rates of payment and other details.

Financial assistance has also been received from A.S.E.A., Sweden

Four volumes per annum. Approximately 700 pages per annum.
Annual Subscription Rate £20 ($56).
Single volumes may be purchased for £6 ($14).

Orders should be sent to the distributors at either of the following addresses

4 & 5 Fitzroy Square, London W.1
122 East 55th Street, New York 22, N.Y.

PUBLISHED BY

PERGAMON PRESS LTD.

NEW YORK · LONDON · OXFORD · PARIS · LOS ANGELES

February 1960

THE UTILIZATION OF SEMICONDUCTORS IN RELAY PROTECTION*

V.L. FABRIKANT

(Received 8 October 1957)

The utilization of semiconductors permits the improvement of many aspects of relay protection. However, as the first results of developments indicate, the most substantial changes have occurred in the power consumption and overall size of individual relays and protective gear. So with a certain increase in operation speed and a decrease in accurate operation voltage, the power consumption in an impedance relay circuit can be decreased from 60 to 5 W. With the decrease in power consumption there is a reduction in the dimensions of all auxiliary devices, and the overall relay size can on the whole be reduced 3-4 times.

Such a substantial reduction in the power consumption and size of relays make it possible to decrease the dimensions of relay panels and the space reserved for them, and also to revise the construction of current and voltage metering transformers. Possibly the application of metering transformers without steel cores or gap cores will become expedient, which would eliminate distortion in secondary circuits due to metering transformer non-linearity.

The great possibilities which lie in the use of semiconductors in relay protection must be seriously applied to the development of relays and protective gear based on this principle.

It seems that at first it is most desirable to conduct research in various directions so that when the most rational principles have been exposed, all effort can be concentrated on their utilization. Some preliminary results of the developments in relays and protective gear using semiconductors can in our opinion already be appreciated.

As is known, protection comprises three types of dissimilar components:

---

* *Elektrichestvo* No. 7, 42-45, 1958.

1. Complex protective devices (impedance relays, power directional relays, etc.). These units use the two electrical quantities: voltage and current. Electromechanically the counter-torque is small and plays a secondary role.

2. Simple protective devices (current and voltage relays). These members use a single electrical quantity. Electromechanically, the counter-torque determines the primary parameter of operation.

3. The logical section of the circuit, (intermediate relays and time relays). This section of the circuit must ensure the transmission of a braking pulse with given combinations of the action of the complex and simple units, and the absence of a braking pulse with other combinations.

Let us consider each of these protection components separately.

The design of complex protection units

Two principles are possible for the design of these members: (1) comparison of the vectors $\dot{A}$ and $\dot{B}$ of the two electrical quantities according to absolute magnitude; (2) comparison of the vectors $\dot{A}$ and $\dot{B}$ of the two electrical quantities according to phase.

In the first case the relay must act where $|\dot{A}| < |\dot{B}|$ or $|\dot{A}| / |\dot{B}| \leqslant 1$ independently of the angle between $\dot{A}$ and $\dot{B}$. The boundary characteristic of such a relay in the complex plane $\dot{A}/\dot{B}$ will be expressed by a circle with a centre at the origin and a radius equal to unity.

If the vector $\dot{A}$ represents a voltage $\dot{U}$, and vector $\dot{B}$ is proportional to the current, a total impedance relay with setting resistance Z_y is obtained.

If vector $\dot{A}$ represents the braking current $\dot{I}_m$, and vector $\dot{B}$ is proportional to the operating current $\dot{I}_r$, a differential relay with braking is obtained.

If each of the vectors $\dot{A}$ and $\dot{B}$ is a linear function of two electrical quantities, for example, voltage and current, i.e.

$$\left.\begin{aligned} \dot{A} &= K_1\dot{U} + K_2\dot{I}; \\ \dot{B} &= K_3\dot{U} + K_4\dot{I}, \end{aligned}\right\} \tag{1}$$

then the quantity

$$\frac{\dot{A}}{\dot{B}} = \frac{K_1\dot{U} + K_2\dot{I}}{K_3\dot{U} + K_4\dot{I}} = \frac{K_1Z + K_2}{K_3Z + K_4}, \tag{2}$$

where

$$Z = \frac{\dot{U}}{\dot{I}}.$$

Expression (2) shows that $\dot{A}/\dot{B}$ is a fractional linear function of the quantity Z. As is known in this case the characteristic, having the form of a circle or straight line in the plane $\dot{A}/\dot{B}$, forms another circle or straight line in the plane Z. By a corresponding selection of coefficients K_1, K_2, K_3 and K_4, a given circle in the plane $\dot{A}/\dot{B}$ can be transformed into any given circle or straight line in plane Z. Thus, an impedance relay can be obtained with a characteristic in the complex plane in the form of a circle or a straight line.

It must be noted that the same characteristic can be obtained with different combinations of coefficients K_1, K_2, K_3, and K_4. In particular, for obtaining a characteristic in the form of a straight line which does not pass through the origin, or in the form of a circle, one of the coefficients can be taken as equal to zero; i.e. one of the quantities $\dot{A}$ or $\dot{B}$ can depend only on the current or only on the voltage.

A block diagram of any complex unit based on the comparison of absolute magnitudes is shown in Fig. 1.

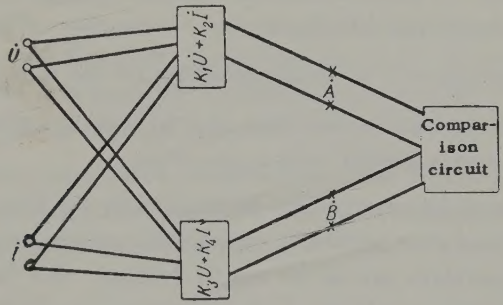

Fig. 1

The devices for obtaining the quantities $\dot{A}$ and $\dot{B}$ are extremely simple, and consist of voltage autotransformers, transreactors and intermediate current transformers. As a rule there are not more than three of these units in both devices, for example, one voltage autotransformer and two transreactors. For directional relays it is sometimes necessary to have an extra slugging circuit to provide for the action of the relay in the presence of faults near the location where it is set up.

However, the chief section, the comparison circuit, can be made up the same for all or almost all complex protective devices, which is a considerable advantage, and at the same time makes the development of this device particularly reliable.

In order to decrease the power consumption and overall size of the circuit, the secondary devices for obtaining the quantities $\dot{A}$ and $\dot{B}$ must have a small power. Then the resulting power at the outlet will be extremely small, and a sensitive responding unit will be required to provide sufficiently high relay parameters.

It is known that in a number of countries [3, 6, 7] highly sensitive moving-coil or polarized relays with an operating power of the order of 10^{-6}W are used for this end. It seems to us, however, that a more reliable, simpler and more economical solution lies in the application of coarser relays with a semiconductor triode as a d.c. amplifier and an operating power of about 10^{-2}W. With this the responding unit can be made sufficiently reliable and quick-acting.

The final solution to the question of which of the relays indicated should be used as the responding unit can be obtained in our opinion only after comparing the best models of these relays.

Two methods different in principle for making up a comparison circuit are possible with the use of semiconductor triodes as d.c. amplifiers: (1) amplification of each of the quantities to be compared and subsequent subtraction of these amplified quantities; (2) subtraction of the quantities to be compared and subsequent amplification of this difference.

The first method appears to be inappropriate for the following reasons:

1. The amplifier is used in this case as a measuring component, and an error in the amplifier creates a similar error in the relay.

2. This deficiency is considerably heightened by the fact that the amplification factor of semiconductor triodes is variable for various specimens, and depends on the temperature and on the supply voltage. The fulfilment of temperature stabilization requiring individual adjustment and temperature testing for each specimen is not practicable.

3. The use of an amplifier as a measuring component not only fails to simplify the circuit, but complicates it somewhat.

The second method by which a semiconductor triode is used for difference amplification, i.e. in the capacity of a null-detector relay, is more expedient since a variation in the amplification characteristics results only in a change in the insensitivity zone and has comparatively little effect on the primary parameters of the relay. The more sensitive the circuit, the less the zone of insensitivity and the less the value of the change in the triode characteristics.

A possible principal circuit for the comparison of vectors $\dot{A}$ and $\dot{B}$ according to absolute magnitude with a triode amplifier as a null-detector relay is shown in Fig. 2.

With phase comparison of the vectors $\dot{A}$ and $\dot{B}$ the relay must act when

$$\psi < \widehat{(\dot{A}, \dot{B})} < \psi + 180^\circ, \qquad (3)$$

where ψ is a certain constant angle.

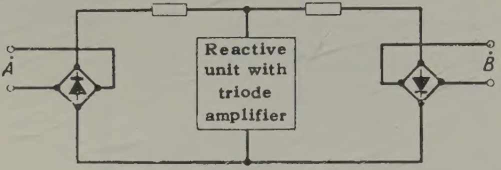

Fig. 2

The boundary line corresponding to expression (3) in the plane $\dot{A}/\dot{B}$ will be expressed as a straight line passing through the origin at an angle ψ to the positive axis of the abcissa. If the vector $\dot{A}$ represents the voltage and vector $\dot{B}$ the current, then the relay becomes a power directional relay. However, if each of the vectors $\dot{A}$ and $\dot{B}$ represents a linear function of the two electrical quantities, for example, voltage and current (1), the quantity $\dot{A}/\dot{B}$, as follows from expression (2), is a fractional linear function of Z. By selecting corresponding coefficient values it is possible to transform the straight line representing the boundary line in the plane $\dot{A}/\dot{B}$ into any circle or straight line in the plane Z.

Thus, the angular comparison of quantities $\dot{A}$ and $\dot{B}$, like their comparison according to absolute magnitude, makes it possible to obtain an impedance relay with a characteristic in the complex plane in the form of a circle or a straight line.

Comparison by phase can be performed by determining the fraction of the cycle during which the signs of the compared quantities coincide. So, if the two quantities coincide in phase, their signs are similar during the whole cycle. With an increase in phase divergence, the fraction of the cycle during which the signs of the values coincide decreases, and with divergence equal to 180° it is equal to zero.

Measurement of the fraction of the cycle during which both values coincide in phase can be accomplished by various methods. One of the possible methods is shown in Fig. 3.

Quantities $\dot{A}$ and $\dot{B}$ rectified in a half-wave rectifier are fed into circuit E. The signal appears at the output of this circuit only in that case where both signals were fed into the input; i.e. if quantities $\dot{A}$ and B are positive. A responding unit is set at the output whose action depends on the time of pulse flow. In Fig. 3 a relay with a triode amplifier is used in this capacity.

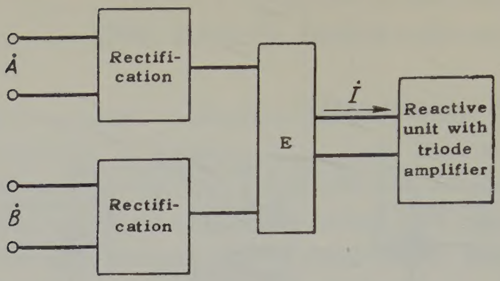

Fig. 3

In the circuit in Fig. 3 the relay with a triode amplifier is used as a measuring component. The inadequacies of such a solution were indicated above.

In the circuit in Fig. 4 [1 and 2], the same time measurement is accomplished by means of a comparison of the voltage on a charged capacitor with the voltage taken from a potentiometer. Since condensor charge and potentiometer feeding are accomplished from the same source, the sign of the voltage difference is independent of the magnitude of the supply voltage, and depends only on the charging time. A relay with a triode amplifier is used in this system as a null-detector relay. As has already been indicated, the relay with a triode amplifier as a null-detector relay must be given preference in our opinion.

In the circuit in Fig. 4, as in the circuit in Fig. 3, the time is measured during which both quantities are positive, which is fully permissible since this time amounts to half the time during which the quantities *A* and *B* have the same sign. With this there will be a delayed action of the protective gear. To increase the speed of this circuit an analagous circuit for negative values can be added.

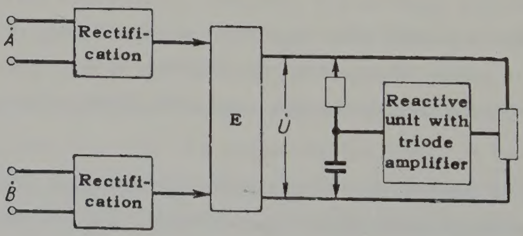

Fig. 4

The pulse principle can also be used for phase comparison, [4]. Here, one of the quantities compared is transformed into short pulses and the other into rectangular pulses, (Fig. 5). Phase comparison is accomplished by determining the sign of the quantity *B* at the instant when a positive pulse of quantity *A* appears. An overall view of the block diagram, constructed on the pulse principle is shown in Fig. 6.

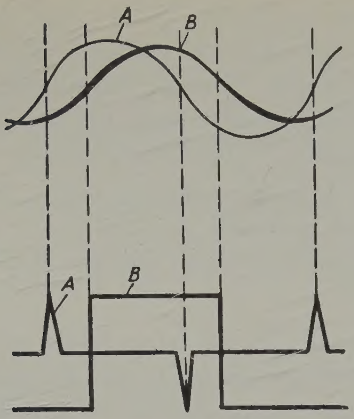

Fig. 5

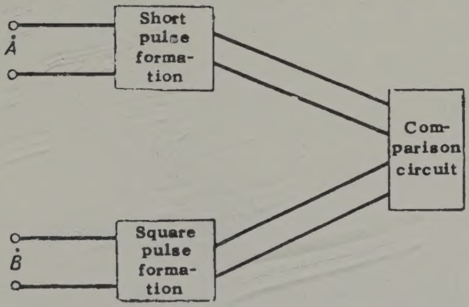

Fig. 6

In principle, the pulse circuit should be the more rapid. However, in the tests made up to now it has been necessary to delay its action in order to tune out transients. Due to this it has not yet been possible to make use of its advantages. In addition, this circuit is more complicated than the others.

It must be noted that circuits comparing absolute magnitudes and phases make it possible to produce any characteristic in the form of a straight line or a circle in a complex plane, and make it possible to have a universal comparison device. However, up to now this unit is produced more simply in an absolute magnitude comparison circuit than in a phase comparison circuit.

Considering the fact that there is not a great deal of experience with new developments, it is our opinion that work must be continued in both directions.

Design of simple devices

Simple units would be produced more simply if the effective electrical quantity were directly supplied to the responding unit which would at the same time be used as a measuring component. In this case, the use of the responding unit as a measuring component results in a substantial simplification and also an improvement of the parameters. However, considering the essential instability at present of triode amplifier characteristics, it is our opinion that it is impossible even in this case to make use of them as measuring components in relays requiring accurate setting. In order to obtain a setting accuracy within the limits of ± 5 per cent, which is already unacceptable for many relays, the amplification factor must be constant to a degree which is at the present time impossible in practice.

The possibility of obtaining simple relays based on the principle of the comparison of the outputs from linear and non-linear components supplied from a common source was examined. As is seen from Fig. 7, with comparatively small values for a certain quantity, for example current, the non-linear component output is greater than the linear. With large values, however, the linear component output is greater. A block diagram of a simple unit based on this principle is shown in Fig. 8.

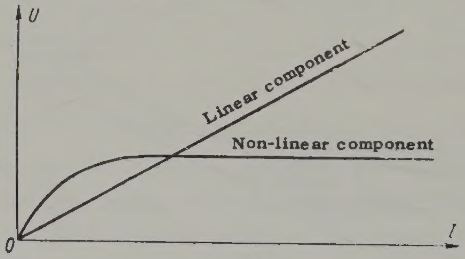

Fig. 7

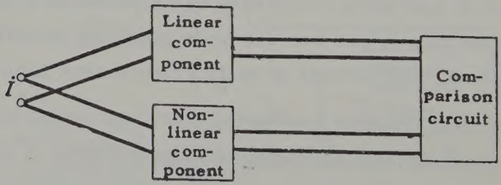

Fig. 8

As tests have shown, the power consumption of such units is greater than for corresponding electromechanical relays. Their application can be justified only for protective gear in which they simplify the complete circuit.

A certain stabilized voltage, fed from an outside source, can also be used as a non-linear component. Here, the difficulty lies in obtaining a sufficiently durable and accurate stabilizer in which capacity a Zener diode might possibly be used.

It must be noted that in the use of semiconductors as null-detector relays, complex units are obtained which are no more complex than simple units. In this connexion, a relay with braking must more frequently be applied. So, a negative sequence current relay is not apparently complicated if phase current braking is used for it. In addition, its characteristics can be improved by this.

The design of the logical section of the circuit

The functions performed by intermediate relays and time relays are reduced to a series of logical operations, for example, "or", "and" and "not", and to the introduction of time.

So, operation "or" is fulfilled by parallel connected intermediate relay contacts which are normally open, and the operation "and" by the same contacts connected in series. These operations can be carried out by the use of semiconductors, [5].

In our opinion, in the design of protection circuits it would be undesirable to seek to exclude all electromechanical relays, replacing them by semiconductors. Intermediate relays or logical semiconductor circuits must be applied depending on which of them give the best solution for the circuit as a whole.

Translated by F.J.C. Griffiths

REFERENCES

1. C. Adamson and L.M. Wedepohl; Power system protection with particular reference to the application of junction transistors to distance relays. *The Proceedings of the Institution of Electrical Engineers;* Pt. A. No. 10 (1956).
2. C. Adamson and L.M. Wedepohl; A dual-comparator mho-type distance relay utilizing transistors. *The Proceedings of the Institution of Electrical Engineers;* Pt. A. September (1956).
3. G.I. Atabekov; Application of moving-coil and polarized relays to relay protection circuits. *Elektrichestvo;* No. 7 (1956).
4. H.C. Barnes and R.H. Macpherson; Field experience-electronic mho distance relay. *Trans. Amer. Inst. elect. Engrs.*, Vol. 72, Pt. III (1953).
5. A.I. Kitov; *Elektronnye tsifrovye meshiny, (Electronic digital computers).*
6. H. Nengebauer; *Gleichstrom-Drehspulelais mit Gleichrichter fur die Seletivschutztechnik.* (D.C. moving-coil Relay and Rectifier for Selective Protective Gear). ETZ; No. 12 (1950).
7. Stark; Neuzeitliche Relaiskonstruktionen. *(Contemporary Relay Designs). Deutsche elektrotechnik*, No. 6 (1955).

CONTROLLED REACTORS FOR LONG-DISTANCE TRANSMISSION *

I.S. BRUK

(Received 29 July 1957)

At the present time the construction of large-scale hydroelectric stations and the connexion of energy systems into a single h.v. system are widespread occurrences. In this regard the development of measures for further increases in the power and distance of electrical energy transmission is of great significance. The majority of transmissions in time lose their initial "through" nature as power is drained off and other systems are connected at intermediate points. In these cases an economical solution can be obtained by the use of three-phase current; however, with long transmission distances this meets serious difficulties which are not to be overcome by only stepping up the voltage.

Economic requirements dictate the necessity of amplifying the transmitted power which flows in one circuit of a transmission line in order to compensate for the cost of the line which increases with the length. However, stability conditions prevent this. At the same time underloading the line in relation to its natural power causes an unfavourable voltage condition. Thus we encounter a serious contradiction which can be resolved only by shortening the electrical length of the line. One way or another all the means of increasing line capacity have been applied at various times.

The electrical length of a line, equal to 2π times the ratio of its geometric length to its wavelength, is directly proportional to the current frequency and $\sqrt{L_0C_0}$. To reduce it, either its capacitive susceptance, or its inductive resistance per unit length or both must be reduced.

In actual practice, as is known, there has been an increase in the use of reactors for capacitive current compensation and capacitors to compensate for the inductive drop in voltage in the line. As shunt compensation with the aid of reactors and series compensation with the aid of capacitors are not simple conceptions, many problems arise in their application in practical conditions. Some of them, relative to the use of reactors, are considered below. The reactor power necessary for full compensation of discharge current for each thousand kilometres overhead line is slightly greater than the natural power of the line. For example, for a h.v. line with split conductors (wave resistance 300 Ω) with voltage 600 kV for a length of 2,000 km the necessary reactor power is about 2.5 GVA for one circuit. With the distribution of this power at several points to distances of 300-400 km, extremely powerful reactor groups are required with a unit power of 200-300 MVA.

---

* *Elektrichestvo*, No.7, 14-19, 1958.

The creation of powerful reactors presents a complex technical problem. A reactor possessing a linear volt-ampere characteristic should operate with a magnetic circuit containing air gaps of considerable volume in which almost all the energy of the magnetic circuit is concentrated. With a frequency of 50 c/s and power of 100 MVA the magnetic energy maximum is:

$$A_m = \frac{100\,000}{314} = 319 \text{ kW hr}$$

The air gap volume

$$\frac{A_m\, 10^{11}}{0.4 B_m^2} = \frac{319 \cdot 10^{11}}{0.4 \times 256 \times 10^6} = 311 \times 10^3 \text{ cm}^3,$$

i.e. almost 1/3 m³, corresponds to this with a maximum induction of $B_m = 16{,}000$ G.

It is obvious that the concentration of such a volume in one gap with a core diameter of the order of 0.8 - 1.0 m is unsuitable, and it must be distributed at several gaps according to core height. Serious difficulties (apart from obtaining a stable construction) are caused by heating due to additional losses in the copper of the winding and in the construction elements.

However, a linear volt-ampere reactor characteristic is not the best solution to the problem of increasing line capacity for long distances. For example, compensation of 50 per cent of the capacitive current with an unchanged value for the natural power reduces the electrical length of the line to half the length of a non-compensated line. With a great line length, for example 2000 km, it would be unsuitable to confine oneself to only one compensation for reactance and capacitive current. The subdivision of a long line into a number of 400 - 600 km sections at the ends of which voltage is maintained independently of changes in line loading, for example with the aid of synchronous compensators, imparts to it the stability characteristics of a line one section long. Here, the desired results are attained more fully the more the separate sections of the line are independent; i.e. the more stably the voltage is maintained.

The voltage can be maintained at support points with the aid of reactors possessing a sufficiently steep characteristic for the dependence of reactive current on voltage, (according to r.m.s. value); here both methods of shortening the electrical length of a line are combined in one device.

With this in mind we suggested a system of two three-phase transformer groups whose cores are premagnetized by a direct current according to the circuit shown in Fig. 1*. Varying the direct premagnetizing current makes it possible to displace the operating point on the magnetization curve, thereby altering the reactive power Q required by the reactor with a given voltage U, and simultaneously the steepness of the characteristic $Q(U)$.

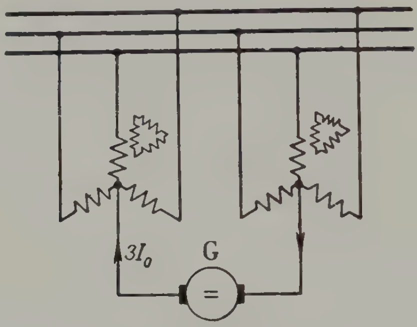

FIG. 1. Transformer premagnetization system

The increase in the power of the combined systems necessarily involves a rise in the general level of transmission voltage and an increase in the requirements made on the compensating reactors. Therefore, combining a reactor and transformer in one unit presents certain economical advantages, particularly in those cases where a consumer or source of energy is connected to the line at the location of the reactor assembly.

The characteristic of a three-phase transformer group with premagnetization

The characteristic of a reactor whose core is premagnetized by a direct current is determined only as the magnetic characteristic of the core if active losses are disregarded. If the average value for the magnetic flux (Φ_1) in the core is found, then by calculation or graph it is easy also to find the value for the m.f. constant component for a given amplitude value (Φ_m) of a sinusoidally alternating magnetic flux.

---

[*] I.S. Bruk. Author's certificate No. 75749 (1948).

With the replacement of the magnetic characteristic shown in Fig. 2 by a straight line $i = K(\Phi - \Phi_0)$, the current curve will consist of sinusoid and rectilinear sections varying in dependence on the constant displacement flux Φ_1, and the sinusoidal flux amplitude Φ_m (Fig. 3). When the reactor terminal voltage and premagnetization are so correlated that the condition $\Phi_m - \Phi_2/\Phi_0 < 1$ is fulfilled, the expression for the nth harmonic of the magnetizing current (Fig. 4) assumes the simple form:

$$\pi I_n = K\Phi_m \int_{t_1}^{\pi - t_1} (\sin t - \sin t_1) \sin nt \, dt, \tag{1}$$

from whence

$$2\pi I_1 = K\Phi_m (\pi - 2t_1 - \sin 2t_1), \tag{2}$$

and for premagnetizing current I_0

$$2\pi I_0 = K\Phi [2 \cos t_1 - \sin t_1 (\pi - 2t_1)], \tag{3}$$

where

$$\sin t_1 = \frac{1 - \Phi_1/\Phi_0}{\Phi_m/\Phi_0}. \tag{4}$$

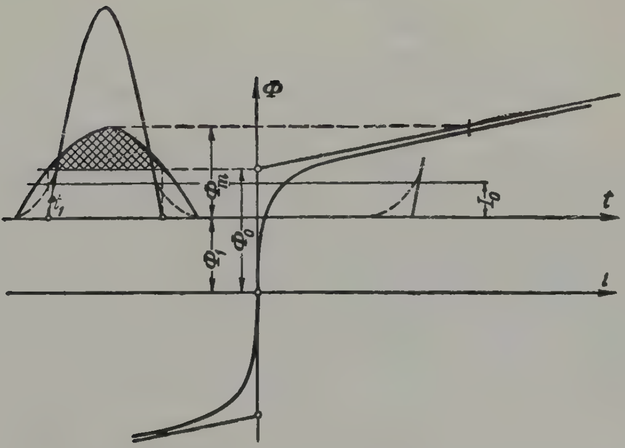

FIG. 2. Graph plotted to determine magnetizing current components

The conventional current curves shown in Fig. 3 will in reality be rounded as the dotted lines show. However, current "cut-off" is clearly indicated. On the basis of this system other phenomena are explained which are to be observed in steel circuits.

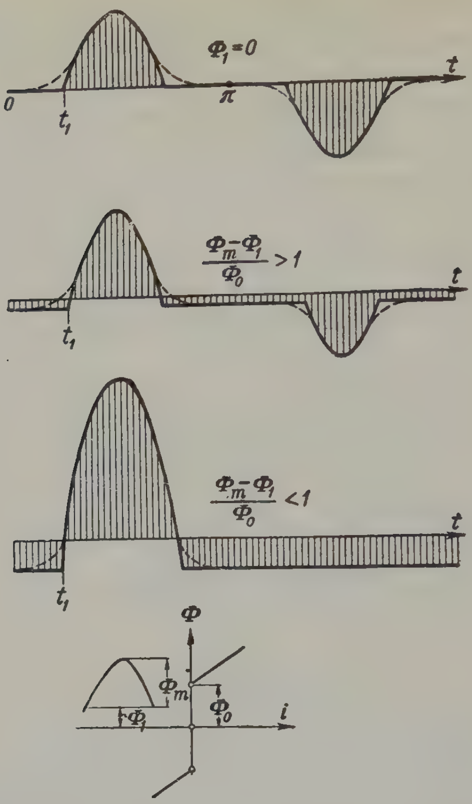

FIG. 3. Characteristic curve forms for the magnetizing current

In connecting the windings of the two three-phase groups, as shown in Fig. 1, all the even harmonics of the magnetizing current are in opposition and cannot develop in the external circuits when the transformers are identical which in actual practice is the case for large transformers. These harmonics are localized in the transformer windings and are distributed in inverse proportion to their dispersion resistance. The double frequency component grows together with the premagnetizing current. Certain data for rating the value of the second harmonic are introduced below.

The third harmonic and its uneven multiples are localized chiefly in the lower voltage delta winding. The amplitude of the third harmonic depends strongly on premagnetization. With a certain small value for the premagnetizing current, the third harmonic amplitude is at a minimum. It increases with further increase in premagnetization. These relationships can be obtained from the magnetic characteristic; they are explained by the mechanism of third harmonic formation:

its strong dependence on the "cut-off" angle t_1 which can be demonstrated by calculating the amplitude of this harmonic according to formula (1).

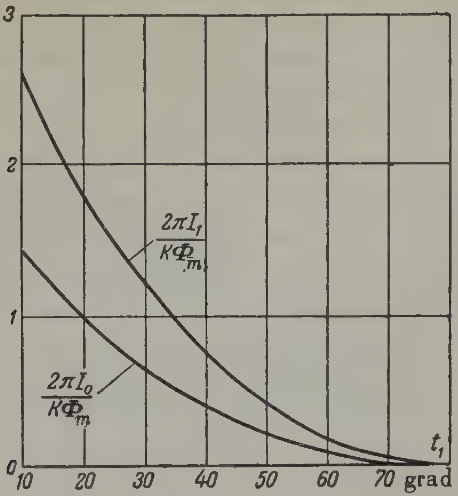

FIG. 4. Graph for determining the premagnetization current and the basic harmonic of magnetizing current

The fifth and seventh current harmonics penetrate into the external circuit (into the line), and their distribution according to the separate circuits (windings) depends on the connexion of the circuit being considered with the magnetic flux of the transformer core, the reactor. Here, it is obviously necessary to consider the reactance for the given harmonic and also for the external circuit connected at the transformer terminals (line, load, etc.).

We present some of the results of the calculation for the reactive power characteristic of a reactor with premagnetization. A rectilinear magnetic characteristic with a steepness of $K = 7$ is the basis of the calculation which makes a good approximation of the actual magnetic characteristic of large transformers. Expressing all values in relative units we obtain, for example, for $\Phi_m = 0.8$ ($U = 0.8$), $I_1 = 0.23$ and $K = 7$, the "cut-off" angle $t_1 = 56°$ according to formula (2), and according to formula (3) $I_0 = 7 \times 0.8 \times 0.135/2\pi = 0.120$ or $0.120 \times \sqrt{2} = 0.170$ (r.m.s. value). Analogously for $I_1 = 0.366$, we find $t_1 = 50°$, $I_0 = 0.193$ (0.273), and for $I_1 = 0.675$ we obtain $t_1 = 40°$; $I_0 = 0.368$ (0.52).

These results agree with experimental data. The dependence of reactive power on voltage with constant premagnetization is approximately parabolic. Thus Thus, a reactor with premagnetization, if it is diverted from higher harmonics, acquires the properties of a reactor with a linear characteristic whose steepness is controlled.

It is possible to put transformer premagnetization into actual practice by various methods. One of the systems is shown in Fig. 5 for earthed neutral transformers. Here two d.c. sources are used, preferably controlled rectifiers. The d.c. source must be shunted for the passage of alternating current. The shunting resistance must be selected several times greater than the transformer winding resistance. The power of the d.c. source for premagnetization is negligible. If the losses in power transformer windings are rated at ¼ per cent for premagnetization by a ⅓ rated current, it would be sufficient to have a d.c. source of approximately 0.05 per cent of the transformer group power. In fact a greater power must be provided: double, and with a reserve according to the voltage, bearing in mind control requirements. A source having a total output of approximately 200 kW would be required for a group with an output of 180 MVA.

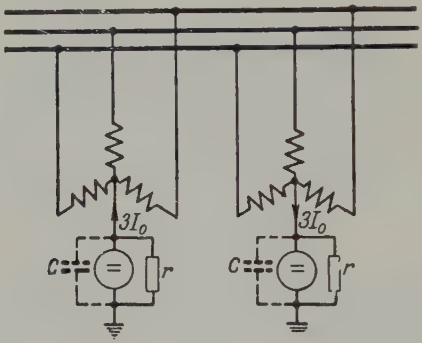

FIG. 5. One of the premagnetization circuits with earth neutral

The possibility of evenly varying the reactive power required by the reactor by varying premagnetization makes it comparatively easy to control the line voltage automatically with the object of increasing the stability, above all static stability. Here known difficulties arise in connexion with control lag. The fact is that with variation of the premagnetizing current the direct magnetic flux in the cores varies considerably more slowly since it is impeded by currents developing in the lower voltage delta winding. The time constant of this process, the true steadying time, amounts to more than 10 sec. Therefore, in order to quicken up control, forcing must be used, and the system must be constructed to avoid overshoot and swings in the complex oscillatory system which is formed by the synchronous machines at the ends of the line together with the reactors.

Results of tests

In order to determine the electromagnetic characteristics of large transformers premagnetized by a direct current, and the feasibility of prolonged transformer operation under such conditions, tests were made on ODTG-60000/220 transformers at the Noginsk substation, Mosenergo,* in March 1956.

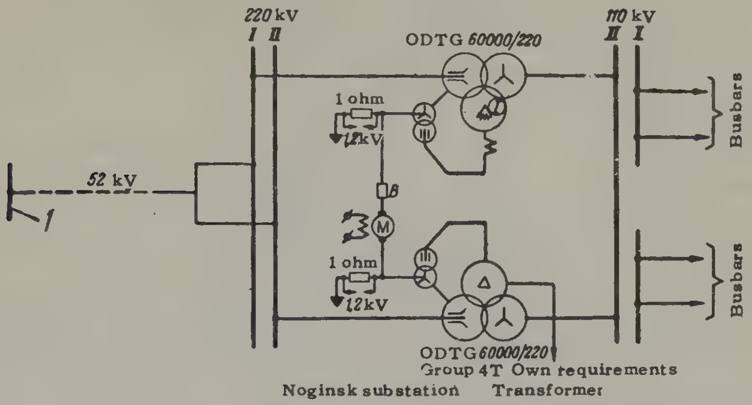

FIG. 6. Circuit for connecting transformers during tests
1 – supply substation

The following characteristics were determined:

1. The dependence of the reactive power required by the transformers on the premagnetizing direct current.

2. Voltage and current curve forms.

3. The time for the system to be steadied when making and breaking the d.c. circuit.

It was suggested that the basis of the tests should be an attempt to reveal to what extent local heating of the transformer magnetic circuit and the elements of its construction can be caused by stray losses. The tests were performed with the system shown in Fig. 6. The voltage at the busbars amounted to 110 kV and was controlled with the aid of series connected transformers. An exciter of a synchronous compensator served as the d.c. source.

The dependence of the reactive power required by the test transformers on the applied alternating voltage and the premagnetizing direct current are shown in Figs. 7 and 8 (conveniently: $U_{baz} = 115$ kV; $Q_{baz} = 360$ MVA; $I_{baz} = 472.5$ A).

From Fig. 8 it is seen that with a constant alternating voltage, the reactive power varies almost directly with direct current I_0 at an average steepness of 1.2 per cent for 1 per cent of the direct current, when $U = 0.75 - 0.9$.

---

* The tests were made by S.S. Vorob'ev and Iu.S. Vukolov with the participation and guidance of M.S. Libkind who carried out all the work in preparing the tests.

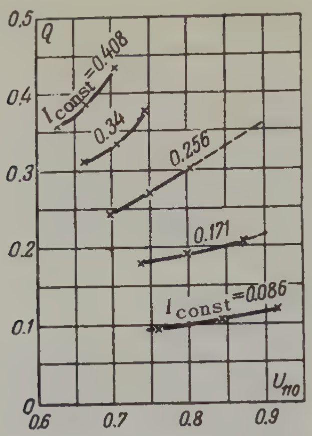

FIG. 7. Dependence of reactive power on voltage on 110 kV busbars

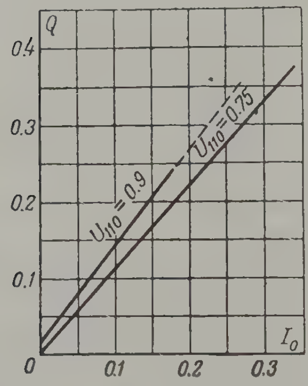

FIG. 8. Dependence of reactive power on premagnetization current

The maximum value for the reactive power $Q = 156$ MVA was obtained with an alternating voltage of $U = 81.2$ kV (0.71) and direct current of $I_0 = 193$ A (0.408). Here the power supplied by the d.c. source amounted to 141 kW; i.e. less than 0.1 per cent of the required reactive power.

The voltage at the supply substation during the experiments was almost unchanged. The currents which flowed in the 220 kV line contained the fifth higher harmonic.

With a premagnetizing current of $I_0 = 120$ A (0.256) in phase and an alternating voltage at the 110 kV busbars, a value of $U = 92$ kV (0.8) was obtained which corresponded to the reactive power demand $Q = 108$ MVA (0.3). The voltage curves at the Noginsk substation had the following harmonic composition:

Phase voltage at 220 kV busbars

$U_1 = 110$ kV; $U_2 \approx 4$ kV; $U_3 \approx 5$ kV; $U_5 = 4$ kV; $U_7 = 1$ kV; $U_9 = 6$ kV;

Phase voltage at 110 kV busbars

$U_1 = 53$ kV; $U_2 \approx 1.5$ kV; $U_3 \approx 0.5$ kV; $U_5 \approx 7$ kV; $U_7 \approx 3$ kV; $U_9 \approx 1$ kV;

Harmonic analysis of the curve for the current in the 220 kV windings gave the following results (r.m.s. values):

$I_1 = 181$ A; $I_2 \approx 23$ A; $I_3 \approx 9$ A; $I_5 \approx 46$ A; $I_7 \approx 5$ A.

A current of predominately double frequency flowed in the 110 kV windings. Triple frequency currents were almost completely localized in 11 kV delta windings.

A full double frequency current applied to the 220 kV winding amounted to 150 A (r.m.s. value) in one of the operations which gives 150/120 = 1.25 A per 1 A direct current. In other conditions, other relative values for double frequency current were obtained; however, in all cases they were close to unity.

It is desirable to pass a direct current through the higher voltage windings. Then a double frequency current will flow in the medium voltage windings, the r.m.s. value of which is approximately equal to the applied d.c. value. The triple frequency current is concentrated basically in the lower voltage delta windings.

Quintuple frequency currents, as has already been noted, flowed in all windings connected with external circuits. During the experiments only 220 kV windings were so affected. Therefore, the amplitude of the fifth harmonic of the current in these windings reached approximately 25 per cent of the first harmonic amplitude in one set of conditions.

As a first approximation it can be considered that 0.3 - 0.5 A of quintuple frequency current was generated for each ampere of premagnetizing direct current. The current flowing in the 220 kV line also contained the fifth higher harmonic. In one of the operations the relative amplitude of the fifth harmonic in the current measured at the supply substation amounted to 10 per cent.

A transient process was created by means of closing and breaking circuit-breaker V in the d.c. circuit (Fig. 6) with a previously excited generator. Direct currents established up to 160 A were tripped in phase.

Oscillographic recordings indicated that the duration of the transient process in the a.c. circuit (of the 220 kV winding), depending on the value of the supply voltage and the direct premagnetizing current, amounts to 20 to 40 sec. The direct current is established in 5 - 7 sec.

The heating of the magnetic circuit was observed with the aid of resistance thermometers set in the tank and in the output section of one transformer of the group.

Extended premagnetization was carried out under the conditions shown in Table 1.

TABLE 1

Voltage kV	Current A	Power MVA	Oil temperature at beginning of experiment °C	Duration of experiment, hr	Oil temperature at end of experiment °C
103	40.7	41	35...40	4	35...40
101	80.8	75	37...40	5	49...56
92	121	121	36...38	Total 4.5 hr with interval of 2.5 hr	43...46

It can be concluded from the experiments that with premagnetization by a direct current, the total losses in the transformer were slightly increased in comparison with no load losses. Measurements showed that the rate of increase of the yoke temperature was approximately the same as for oil; this is substantiated by the absence of local heating in the yoke.

The steel pressing limbs of the upper yoke were heated under the first set of conditions to 75°C, under the second to 90°, and under the third set, the limb temperature could be expected to reach 100 - 105°C. Rapid limb heating was conditioned by eddy currents caused by the field of magnetic circuit dispersion.

The experiments indicated the following facts:

1. The electromagnetic characteristics of the Noginsk substation transformers under conditions of premagnetization by direct current, correspond basically to the theoretical propositions and results of the experimental study made in 1954 at Hydro-electric station — 13, Mosenergo.

2. With short transformer premagnetization (10 - 15 min.) the reactive power required can be brought up to at least half the rated power of the two groups;

3. With prolonged premagnetization, the reactive power required by ODTG - 60000/220 transformers can be brought up to approximately 25 per cent of their rated power. Further increase in premagnetization is limited by heating of the magnetic circuit steel yoke limbs.

Conclusion

Transformer premagnetization by a direct current is an economical solution to the problem of obtaining a powerful controlled reactor for long-distance a.c. transmission.

Premagnetization is also applicable to power autotransformers which, undoubtedly, will be widely used for connecting long-distance transmission with intermediary systems in the U.S.S.R.

Here it must be remembered that direct current for all practical purposes will flow in only the main section of an autotransformer winding, since the resistance of the connecting busbars is small in comparison to the resistance of the remaining part of the winding. This does not affect the electromagnetic characteristic of an autotransformer as a reactor, if the windings are distributed with sufficient evenness.

A detailed consideration of the effect of a transformer (reactor) with premagnetization on the course of transient processes during line making and breaking, and on dynamic overvoltages is beyond the scope of this paper. This effect can be roughly evaluated by comparing it with the connexion of a choke reactor premagnetized from an independent source.

At the present, work is being done which is connected with the examination of these questions as well as the permissible load of multi-winding transformers and autotransformers.

Additional experimental studies must also be carried out on the interaction of the reactor and the long-distance line, as well as the constructive development of magnetic circuit parts in order to decrease additional losses and heating.

Translated by F.J.C. Griffiths

NEW METHODS OF CONNECTING STARTER-CONTROL RESISTANCES OF ASYNCHRONOUS MOTORS*

I.K. KHRUSTALEV

Siberian Metallurgical Institute

(Received 9 July 1957)

In contemporary methods of relay switch control of asynchronous motors there is a considerable array of switch connexions of rotor magnetic sets by means of which disconnexion or connexion in series of resistance steps in the engine rotor circuit take place. In this case the number of resistance steps and, consequently, the number of rheostat characteristics of the motor are equal to the number of contactors. Just as two out of 5 ...... 9 rheostat steps are usually preliminary, the number of working steps does not exceed 3 ..... 9. The presence of a relatively small number of resistance steps produces a deterioration in the performance of the starter and brake action of the motor, irregularity in its speed control and also contributes to the emergence in the system of intolerable dynamic loads. An increase in the number of steps as a result of an increased number of contactors in a magnetic set makes the starter systems of the motor less reliable and is not usually implemented.

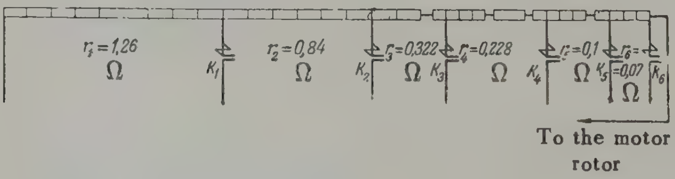

FIG. 1. Method of equipping a single-phase rheostat by means of contactor-connexion in series
$K_1 \ldots\ldots K_6$ = contactors

It is possible to eliminate the defects of existing systems of resistance connexions in the case of switch connexions in parallel and parallel-series.

---

* *Electrichestvo* No. 7, 55-56, 1958.

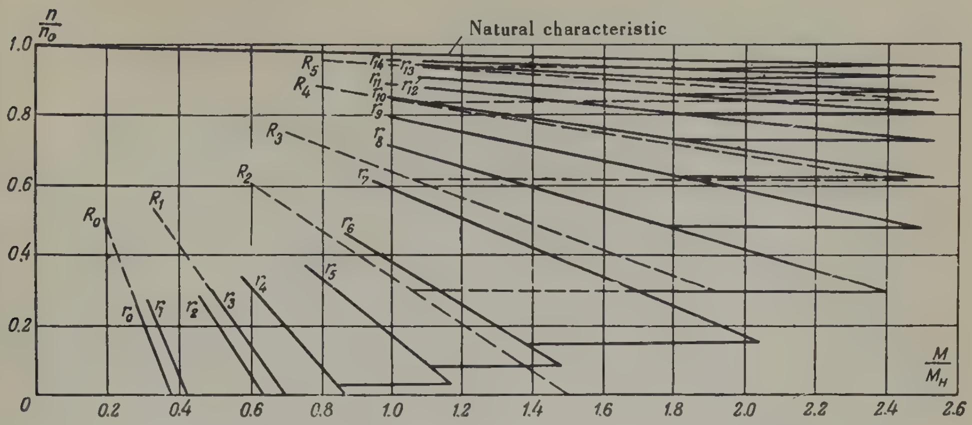

FIG. 2. A series of rheostatic and mechanical characteristics of an induction motor by means of contactor connexions in series ($R_0 \dots R_5$) and in parallel-series ($r_0 \dots\dots r_{14}$)

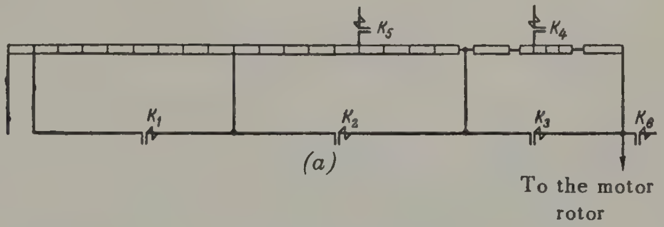

(a)

Contactor	Number of step															
	1	2	3	4	5	6	7	8	9	10	11	12	13	14	15	16
K_1	—	—	×	—	—	—	—	×	×	—	—	×	—	—	×	×
K_2	—	—	—	×	×	—	—	×	×	×	—	×	—	×	×	×
K_3	—	×	—	—	×	—	×	—	—	×	—	×	×	×	×	×
K_4	—	—	—	—	—	—	—	—	—	—	×	—	×	×	×	×
K_5	—	—	—	—	—	×	×	—	×	×	—	—	—	×	×	×
K_6	—	—	—	—	—	—	—	—	—	—	—	—	—	—	—	×

(b)

FIG. 3. Method of equipping a single-phase of resistances and a diagram of commutation of switches when connected in parallel-series. × = closed contact

Thus, by one of the methods of parallel switch connexions of a six-contactor rotor set one can obtain 18 rheostat ratings of the motor instead of six obtained by the standard method of switch connexion.

TABLE 1

Schedule of resistances of a single-phase rheostat with switch connexion in parallel-series

Number of step	Resistance of step, Ω	Number of step	Resistance of step, Ω
1	2.82	9	0.396
2	2.52	10	0.253
3	1.70	11	0.170
4	1.56	12	0.14
5	2.26	13	0.074
6	0.902	14	0.0595
7	0.602	15	0.0416
8	0.44		

A six-step metallic rheostat has been designed and equipped for one of the coal-mines in the Karaganda coal-field. The method of complementing a single-phase rheostat is shown in Fig. 1 and a series of rheostatic mechanical characteristics of an induction winding motor is represented in Fig. 2 by dotted lines (characteristics $R_0 \dots R_5$). By another method of connecting resistances of this rheostat and by parallel-series switch-connexion, 15 rheostat mechanical characteristics of the motor are obtained, (characteristics $r_0 \dots r_{14}$ in Fig. 2). The method of equipping a single-phase of resistances for this instance and the diagram of switch commutation are produced in Table 1 and in Fig. 3.

Conclusion

It is possible to obtain a greater number of rheostat mechanical characteristics of a motor with a small number of contactors, resulting in an increased reliability in the motor control system, by means of metallic rheostats inserted in accordance with the resistance connexion methods which have been suggested.

TRANSIENT PROCESSES IN A MAGNETIC BOOSTER WORKING IN A RELAY SYSTEM*†

R.A. LIPMAN and I.B. NEGNEVITSKI

Moscow Institute of Energy

(Received 17 February 1958)

Transient processes in an actively loaded magnetic booster working in a relay system (non-contact magnetic relay) are examined by the authors in comparative detail in [1, 2]. It is, however, well known from practical experience that in certain cases considerable retardation in the operation and release of the relay is observed which is somewhat higher than the values determined by the formulae produced in [1].

In the work under consideration a physical explanation and a rigid mathematical analysis of the effect of delay on an example of a most elementary non-contact magnetic relay are provided. Formulae have been deduced by which it is possible to calculate the time of delay and also the total time of operation and release at initial displacement.

For simplification, the magnetization curve is assumed to be perfect. The main relay system with an external return connexion is shown in Fig. 1a, and with an internal and auxiliary feedback in Fig. 1b. In studying the effects in a non-contact magnetic relay we assume that the rectifiers are perfect and do not take into account the influence of eddy currents.

Transient processes in an ordinary magnetic booster without feedback are examined by the authors in [5] and in half-phase (high-speed) boosters in [4]. In both cases it was shown that provided the maximum amplitude of the alternating component induction B_m is less than the saturation induction B_s the indicated effect of delay in a transient process can take place. The reasons for delay in a transient process in a relay system are of that particular nature.

---

* *Electrichestvo* No. 7, 25-30, 1958.

† From a report on magnetic boosters in the Seminar at the Institute of Automation and Telemechanics Akad. Nauk U.S.S.R.

In this way an essential (but not always adequate) condition for the presence of delay is as follows:

$$B_m < B_s \text{ or } E < 2E_s, \tag{1}$$

where E_s = the e.m.f. of saturation of one choking-coil, determined by the formula:

$$E_s = 4fw_{\sim}SB_s \times 10^{-8}\,* \tag{2}$$

Condition (1) is conveniently written in the form:

$$\varepsilon = \frac{E}{2E_s} < 1^{\dagger} \tag{3}$$

and the relative value ϵ called the degree of saturation [3].

When $\epsilon < 1$ during the transient process, there is an interval of time when, for instance, an increase in the constant component of induction B_0 occurs in one core, but the absolute value of induction still does not amount to the induction of saturation. During all this time the cores are not saturated and we may assume that the current in the load remains at zero. This in fact also explains the presence of delay.

Transient processes in a relay are examined in respect of current and inductive values averaged per phase (or half-phase) on the supposition that the "natural magnetization process" takes place, and on those assumptions which are usually obtained by analysis of transient processes in magnetic boosters [1]. In addition, it is possible to assume that the static dependence of mean values of the current in the load I on the control current I_y and of the constant component of induction B_0 on the current I_y are maintained in the transient process for averaged values.

The dependence of B_0 on I_y for various ϵ for a magnetic booster with a feedback is shown in [5]. Below, the dependence of B_0 on I_y is produced in the relay system when $\epsilon < 1$, which determines the course of the transient process and graphically illustrates the presence of delay.

---

* Here and below the mean values of e.m.f., currents, and induction will basically apply. Index (av) omitted.

† For the method with internal feedback $\epsilon = E/E_s$

Relay system

At initial displacement the magnetic booster possesses the relay rating shown in Fig. 2a in relative units. Here the ratings of the booster without feedback and direct feedback are shown.

We shall determine in relative units the basic parameters which characterize the performance of a non-contact magnetic relay. The load current and the inductive currents in other circuits we shall refer to as the maximum load current $I_{\max}$ when $\epsilon = 1$, and the induction as the saturation induction B_s.

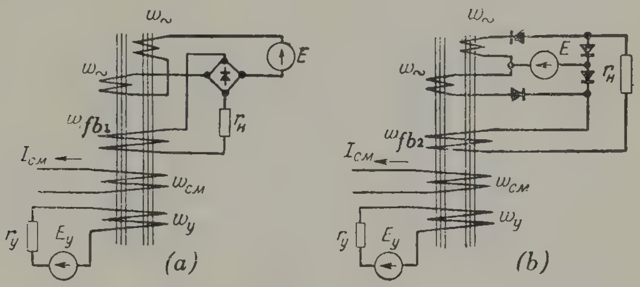

FIG. 1. Principal non-contact magnetic relay systems
a – relay with external feedback
b – relay with internal and auxiliary additional external feedback
E – e.m.f. of alternating current feed of frequency f
E_y – e.m.f. of direct current control (signal)
r_H – resistance of load
r_y – total resistance of control circuit

At full saturation the following relationship between the parameters of the system takes place:

$$I_{\max} = \frac{E}{r}; \; I^0_{\max} = \frac{Er}{2E_s r} = \varepsilon. \tag{4}$$

The width of the relay rating (loop):

$$\Delta = I_{\max} \frac{w_\sim}{w_y} (k_{fb} - 1); \qquad \Delta^0 = \varepsilon (k_{fb} - 1). \tag{5}$$

The relative displacement current* =

* Anywhere below I_{cm} is the absolute volume of displacement current.

$$I^0_{\text{см}} = I_{\text{см}} \frac{w_{\text{см}}}{w_{\sim}} \cdot \frac{r}{2E_s}\,. \tag{6}$$

The operating and release currents:

$$\begin{aligned} I^0_{op} &= I^0_{\text{см}}; \\ I^0_{rel} &= I^0_{\text{см}} - \Delta^0 = I^0_{\text{см}} - \varepsilon(k_{fb} - 1). \end{aligned} \tag{7}$$

The reset factor of the relay:

$$k_{\text{reset}} = \frac{I_{rel}}{I_{op}} = 1 - \varepsilon \frac{k_{fb} - 1}{I^0_{\text{см}}}\,. \tag{8}$$

The reserve factor is determined by the formula:

$$\begin{aligned} k_{\text{reserve}} &= \frac{I_y}{I_{op}} = \frac{I^0_y}{I^0_{op}} = \frac{E^0_y}{I^0_{\text{см}}} = \\ &= \frac{E^0_y(1 - k_{\text{reset}})}{\varepsilon(k_{fb} - 1)}, \end{aligned} \tag{9}$$

where

$$E^0_y = \frac{E_y w_y}{r_y w_{\sim} I_{\max}}\,.$$

The initial value of the load current:

$$\begin{aligned} I_0 &= \frac{I_{\text{см}} w_{\text{см}}}{w_{\sim}} \cdot \frac{1}{k_{fb} + 1}; \\ I^0_0 &= \frac{I^0_{\text{см}}}{k_{fb} + 1}\,. \end{aligned} \tag{10}$$

In these formulae r is the total resistance of the alternating current circuit.

The dependence of the constant component of induction on the control current is produced in comparative units in Fig. 2b which corresponds with the relay rating of the booster represented in Fig. 2a when $\varepsilon < 1$. This dependence can easily be represented by the curve $B_0 = B_0(I_y)$, which is familiar for a procedure without feedback, and with a direct feedback Fig. 2b.

Section 2-3 corresponds with the performance of a relay with a negative feedback. For this section the following relationship takes place:

$$B_0^0 = \frac{B_0}{B_s} = -(1-\varepsilon) + \frac{I_y^0 - I_{cм}^0}{k_{fb}+1} \tag{11}$$

and

$$\frac{dB_0^0}{dI_y^0} = \frac{1}{k_{fb}+1}. \tag{12}$$

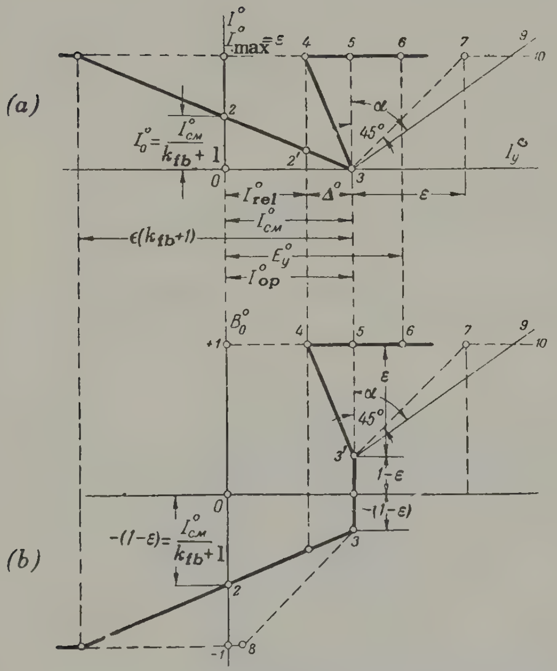

FIG. 2. a – relay rating in relative units at initial displacement, corresponding to normal open contact operation (lines 2-3-4-6): booster rating without feedback (lines 3-7-10); direct feedback (lines 3-9); b – dependence of direct component of induction on control current in relative units, corresponding to relay rating 2-3-4-6; line 8-3-3′-7-10 is the dependence of B_0^0 on I_y^0 of the booster without feedback when $\epsilon < 1$; line 3′-9 is the direct feedback. The scales along the axes of the ordinates; $\tan \alpha = k_{\text{feedback}}$

Section 3′-4 corresponds with the region of unstable relay operation. For this section it is possible to write:

$$B_0^0 = 1 - \varepsilon + \frac{I_{cм}^0 - I_y^0}{k_{fb}-1} \tag{13}$$

and

$$\frac{dB_0^0}{dI_y^0} = -\frac{1}{k_{fb} - 1} \cdot$$

Transient process

Let us consider a transient process in a non-contact magnetic relay with instantaneous connexion of the e.m.f. of the signal E_y, assuming that the displacement circuit is fed from the source of the current. At positive displacement (Fig. 2a), the relay will have a "normal open contact".

The transient process in the control circuit is described by the following differential equation:

$$2w_y S \cdot 10^{-8} \frac{dB_0}{dt} + i_y r_y = E_y. \tag{14}$$

It is convenient to express the time in the number of frequency cycles of the supply voltage, (relative time t^0):

$$t^0 = \frac{t}{T} = tf. \tag{15}$$

The equation (14) in relative units takes the form:

$$\frac{k}{4} \cdot \frac{dB_0^0}{dt^0} + i_y^0 = E_y^0; \tag{16}$$

$$k = \frac{w_y^2 r}{w_\sim^2 r_y}, \tag{17}$$

where k is the power amplification factor (for mean values) of a booster without feedback.

It is evidently necessary to examine the transient process in separate stages to correspond with the various sections of the curves in Fig. 2.

The transient process is analysed in the appendix; only the final expressions for determining the duration of separate stages is produced below.

Duration of first stage (Section 2-3):

$$t_1^0 = \frac{k}{4(k_{fb} + 1)} \ln \frac{k_{\text{reserve}}}{k_{\text{reserve}} - 1} \tag{18}$$

Duration of the delay stage (section 3-3′):

$$t_2^0 = \frac{k\,(1-\epsilon)}{2\epsilon} \times \frac{1-k_{\text{reset}}}{(k_{fb}-1)\,(k_{\text{reserve}}-1)} \tag{19}$$

Duration of third stage (section 3′-4):

$$t_3^0 = \frac{k}{4\,(k_{fb}-1)} \ln \frac{k_{\text{reserve}}-k_{\text{reset}}}{(k_{\text{reserve}}-1)} \tag{20}$$

Towards the end of the third stage the load current reaches a steady value and in the fourth stage remains constant.

In this way the relative operating time equals:

$$t_{op}^0 = t_1^0 + t_2^0 + t_3^0 \tag{21}$$

or

$$t_{op}^0 = \frac{k}{4}\quad \frac{1}{k_{fb}+1} \ln \frac{k_{\text{reserve}}}{k_{\text{reserve}}-1} + \frac{2\,(1-\epsilon)\,(1-k_{\text{reset}})}{\epsilon\,(k_{fb}-1)\,(k_{\text{reserve}}-1)} + \\ + \frac{1}{k_{fb}-1} \ln \frac{k_{\text{reserve}}-k_{\text{reset}}}{k_{\text{reserve}}-1} \tag{22}$$

When disconnecting the control signal (without breaking the control circuit), the transient process in the booster continues in the following manner. The electro-motive force E_y decreases in a jump to zero which corresponds in section 6-4 with the intermittent decrease of the control current to the magnitude:

$$I_{\text{rel}}^0 = \epsilon\,(k_{fb}-1)\,\frac{k\,k_{\text{reset}}}{1-k_{\text{reset}}} \tag{23}$$

During this time the current in the load and the induction B_0 remain constant.

Equation (16) is actually in respect of section 4-3 and its solution in conjunction with the calculation of (13) when $E_y = 0$ and with the initial condition $i_y^0(0) = I_{\text{rel}}^0$ takes the form:

$$i_y^0 = I_{\text{rel}}^0\, e^{\frac{t^0}{\tau_3^0}}\,. \tag{24}$$

At the end of section 4-3 the current i_y^0 increases to I_{cm}^0, and the current in the load decreases to zero. The duration of this stage is determined by the equality:

$$t_4^0 = \frac{k}{4\,(k_{fb}-1)} \ln \frac{1}{k_{\text{reset}}} \tag{25}$$

Section 3′-3 corresponds with the delay of variation of the control current. In solving equation (16) when $E_y = 0$ and $i_y^0 = I^0_{\mathrm{cm}} = \mathrm{const.}$, the initial condition $B_0^0(0) = 1-\epsilon$ and the final condition $B_0^0(t_5^0) = -(1-\epsilon)$, we find that the time of delay =

$$t_5^0 = \frac{k(1-\epsilon)}{2I^0_{\mathrm{cm}}} = \frac{k(1-\epsilon)}{2\epsilon} \times \frac{1-k_{\mathrm{reset}}}{k_{fb}-1} \tag{26}$$

The time of delay at the release of the relay t_5^0 generally differs from the time of delay t_2^0 on operation.

In the last section (3-2) the control current decreases from the value $i_y^0 = I^0_{\mathrm{cm}}$ to zero, and the current in the load increases to the initial value I_0, which is determined by equality (10). These variations take place in accordance with the law of exponents with the time constant τ_1^0 (cf. appendix). Theoretically the duration of the last stage is equal to infinity. It is not usually possible in a relay system to take into consideration the time of the increase of the current in the load in section 3-2, and then one may assume that the delay in the variation of the current of the load is not indicated and the release time of the relay:

$$t^0_{\mathrm{rel}} = t_4^0 = \frac{k}{4(k_{fb}-1)} \ln \frac{1}{k_{\mathrm{reset}}} \tag{27}$$

Similarly expressions for determining the operating and release times of a relay can be obtained for the occasion, when the displacement winding works in accordance with the feedback winding, (a relay with a "normal closed contact"):

$$t^0_{\mathrm{rel}} = \frac{k}{4} \quad \frac{1}{k_{fb}+1} \ln \frac{k_{\mathrm{reserve}}}{k_{\mathrm{reset}}} + \frac{2(1-\epsilon)(1-k_{\mathrm{reset}})}{\epsilon k_{\mathrm{reset}}(k_{fb}-1)} + \frac{1}{k_{fb}-1} \ln \frac{1}{k_{\mathrm{reset}}}\ ; \tag{28}$$

$$t^0_{op} = \frac{k}{4(k_{fb}-1)} \ln \frac{k_{\mathrm{reserve}} - k_{\mathrm{reset}}}{k_{\mathrm{reserve}} - 1}\ , \tag{29}$$

where,

$$k_{\mathrm{reserve}} = \frac{E \quad E_y^0}{I^0_{\mathrm{cm}} + \Delta^0}; \quad k_{\mathrm{reset}} = \frac{I^0_{\mathrm{cm}}}{I^0_{\mathrm{cm}} + \Delta^0} \tag{30}$$

In formulae (22) and (27)-(29) it is possible to calculate the operating and release times of a relay by the known reserve factor k_{reserve}, reset factor k_{reset}, the feedback k_{fb}, the power amplification factor without feedback k, and by the magnitude of the relative supply voltage $\epsilon = B_m/B_s$. All these quantities are usually ascertained from the static ratings of the relay. The determination of the operating and release times of a relay by means of relative coefficients, and not by the absolute values of the control and operating currents, etc. is, in our opinion, a very convenient method for calculating and analysing the influence of various parameters on t_{op} and t_{rel}.

Results of experimental verification

A quantitative check on the theoretical results obtained has been carried out in a number of boosters designed according to the systems represented in Fig. 1. One of these boosters had the following data. Each core consisted of 18 rings of molybdenum permalloy measuring 34 × 50 mm and 0.25 mm thick. The number of winding turns: $w_{\sim} = 300$; $w_{\text{feedback 1}} = 340$; $w_y = 400$; $w_{\text{feedback 2}} = 40$. The supply frequency was 500 c/s. Saturation induction was taken to be equal to 6300 G; e.m.f. of saturation of one choking coil $E_s = 13.6$ V; the total resistance of the load circuit for the method in Fig. 1a amounted to 44 Ω, but for the method in Fig. 1b, 21 Ω; the total resistance of the control circuit in all cases was $r_y = 7\,\Omega$. The germanium rectifiers were of the DG - TS23 type.

Results of calculation and experiment for five different relay procedures are reproduced in Table 1. The duration of each stage in the transient process was determined by oscillograms. The oscillogram currents on operation and release of the relay for systems 1, 4 and 5 are shown in Fig. 3.

Three quantities for each time component of the transient process are produced in Table 1. The first column contains quantities calculated by (18), (19), (20) and (25) on the basis of the rated static characteristics for a perfect magnetization curve. The quantities given in the second column, which are calculated by those formulae, but which enter into the formulae of the coefficients k_{reserve}, k_{reset}, k_{feedback} are determined by the experimental static relay ratings of the booster. The experimental quantities are given in the third column. The variation of experimental volumes from those calculated in the second column does not exceed the limits of accurate measurement.

It is apparent from analysis of the oscillograms in Fig. 3, that the vibrators of the oscillograph in the control and load circuits are shunted by capacitances to reduce the even harmonics of current in the vibrators. With sufficiently large capacitances the variations of the stubs are practically proportional to the mean values of the current (provided the circuit resistance is considerably greater than the resistance of the vibrator). An oscillograph of momentary values of currents can produce a misrepresentation of the character of the transient process and operating and release times. In Fig. 4 oscillograms of relay operation and release are provided for comparison. They were taken in system 3 in the presence and absence of capacitance shunting the vibrator in the load circuit. An examination of oscillograms taken without shunting capacity can create the false impression that on operation of the relay, delayed variation of the load current takes place, and that on release, the load current reaches a steady value sooner than the control current. This case is explained by the considerable difference in the laws of variation of amplitude and mean values of currents in magnetic boosters in a transient process, [5].

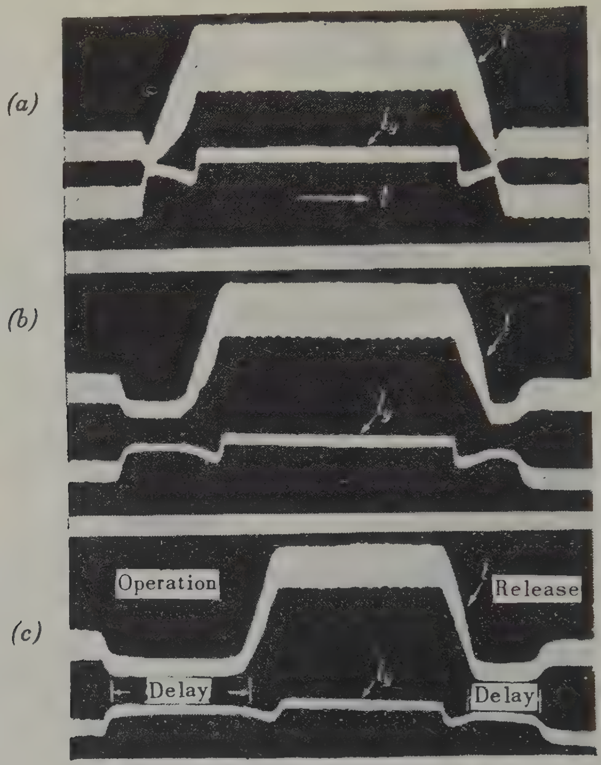

FIG. 3. Oscillograms of currents in the load i and in the control circuit i_y during relay operation and release a – system 1; b – system 4; c – system 5. The vibrators are shunted by capacitance

Conclusion

The delay effect on operation (or release) of a non-contact magnetic relay can be utilized to create non-contact time relays, which will profitably differ from similar non-contact relays, in that in the passage of time the current in the load practically does not vary.

In spite of the accepted perfection of the magnetization curve, calculated formulae for determining the operating and release times of a relay are more in conformity with experiment, if the values k_{reserve}, k_{reset}, Δ^0 are determined by the experimental static ratings of the relay. Without the latter, the calculation of the operating and release times by means of derived formulae produce satisfactory results given a sufficiently accurate calculation of the static ratings. Conversely, if in devising a relay, the requisite values of k_{reserve}, k_{reset}, k and Δ^0 are given, then the calculation thereby of the operating and release times is more in conformity with experiment, provided that after the approximate calculation of the relay experimentally, the given values of k_{reserve}, k_{reset}, k and Δ^0 are ensured. This conformity of experimental and calculated values of the operating and release times is explained by the fact that the static ratings of the relay entirely determine the actual dependence of the direct component of induction on the control current and, consequently, determine the course of the transient process.

It is natural that the results obtained can also be used to solve the problem of determining the possible values of k_{reserve}, k_{reset}, ϵ and Δ^0 by means of the given operating and release times.

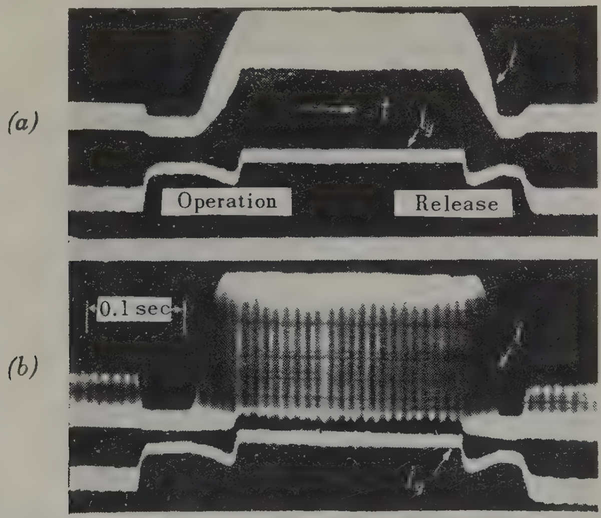

FIG. 4. Oscillograms of currents in the load i and in the control circuit i_y during relay operation and release in system 3 with the vibrator shunted by capacitance in the control circuit
a - vibrator shunted by capacitance in the load circuit
b - vibrator in load circuit not shunted by capacitance

Appendix

Let us examine the transient process on operation of the relay by separate stages in accordance with the various sections of the curves, represented in Fig. 2.

The first section, (section 2-3). Here the control current varies within

TABLE 1

Operating condition	Figure	E, V	ε	$I_{cм}$, ma	E_y/r_y, ma	t_1, msec			t_2, msec			t_3, msec			t_{op}, msec			$t_4 = t_{rel}$, msec		
						1	2	3	1	2	3	1	2	3	1	2	3	1	2	3
1	1, *a*	27	1	425	124	5.2	3.3	6.8	—	—	—	61	49	48	66	52	55	34	35	36
2	1, *b*	12.6	0.93	405	121	4.3	3.5	6.6	17	11	14	53	46	48	74	61	69	36	37	39
3	1, *a*	16	0.75	300	92	4.4	3.3	5.5	72	47	50	53	49	45	129	99	101	34	35	36
4	1, *b*	14.8	0.70	300	92	4.2	3.2	6.6	89	60	55	51	47	42	144	110	104	36	37	38
5	1, *b*	5	0.465	200	62	4.2	3.2	7	240	146	140	51	44	38	295	193	185	36	31	33

limits from zero to I^0_{cm}.

Taking (12) into consideration we should write equation (16) in the form:

$$\frac{k}{4(k_{fb}+1)}\cdot\frac{di^0_y}{dt^0}+i^0_y=E^0_y. \qquad (I,1)$$

The solution of (I,1), with the initial condition $i^0_y(0)=0$, is:

$$i^0_y=E^0_y\left(1-e^{-\frac{t^0}{\tau^0_1}}\right);\quad \tau^0_1=\frac{k}{4(k_{fb}+1)}. \qquad (I,2)$$

The current in the load and direct component of induction vary in accordance with the following equations:

$$i^0=\frac{I^0_{cm}-i^0_y}{k_{fb}+1};\quad B^0_0=-\left(1-\varepsilon+\frac{I^0_{cm}-i^0_y}{(k_{fb}+1)}\right). \qquad (I,3)$$

In time t_1 this stage terminates. Here the following dependences take place:

$$i^0_y(t^0_1)=I^0_{cm};\quad i^0(t^0_1)=0;\quad B^0_0(t^0_1)=-(1-\varepsilon). \qquad (I,4)$$

The duration of the first stage:

$$t^0_1=\frac{k}{4(k_{fb}+1)}\ln\frac{E^0_y}{E^0_y-I^0_{cm}}$$

or

$$t^0_1=\frac{k}{4(k_{fb}+1)}\ln\frac{k_{\text{reserve}}}{k_{\text{reserve}}-1} \qquad (I,5)$$

The second section, (section 3 - 3′). In this stage the delay of variation of the control current takes place until the direct component of induction increases to the value: $(1-\epsilon)$. In the second section:

$$i^0_y=I^0_{cm}=\text{const};\quad i^0=0. \qquad (I,6)$$

Equation (16) takes the form:

$$\frac{k}{4}\cdot\frac{dB^0_0}{dt^0}=E^0_y-I^0_{cm}. \qquad (I,7)$$

The solution of (I,7) with the initial condition $B^0_0(0)=-(1-\epsilon)$, is:

$$B^0_0=\frac{4}{k}(E^0_y-I^0_{cm})t^0-(1-\varepsilon). \qquad (I,8)$$

Induction B^0_0 at the end of the second stage increases according to linear law and reaches the value $B^0_0(t^0_2) = \xi - \epsilon$; consequently, the duration of the second stage is as follows:

$$t^0_2 = \frac{k(1-\varepsilon)}{2(E^0_y - I^0_{\text{см}})}$$

$$t^0_2 = \frac{k(1-\varepsilon)}{2\varepsilon} \cdot \frac{1 - k_{\text{reset}}}{(k_{fb}-1)(k_{\text{reserve}}-1)} \tag{I,9}$$

The third section (section 3′-4). By taking (13) into account we may write equation (16) in the form:

$$-\frac{k}{4(k_{fb}-1)} \cdot \frac{di^0_y}{dt^0} + i^0_y = E^0_y. \tag{I,10}$$

The solution of (I,10), with the initial condition $i^0_y(0) = I^0$, is as follows:

$$i^0_y = E^0_y + (I^0_{\text{см}} - E^0_y)\, e^{-\frac{t^0}{\tau^0_3}};$$

$$\tau^0_3 = \frac{k}{4(k_{fb}-1)}. \tag{I,11}$$

The current in the load and induction B^0_0 vary in accordance with the following equations:

$$i^0 = \frac{I^0_{\text{см}} - i^0_y}{k_{fb}-1}; \quad B^0_0 = 1 - \varepsilon + \frac{I^0_{\text{см}} - i^0_y}{k_{fb}-1}. \tag{I,12}$$

We shall note than an exponential term with a positive characteristic enters into the equations of all the values. At the end of the third section a total saturation of the cores takes place:

$$B^0_0(t^0_3) = 1; \; i(t^0_3) = \varepsilon; \; i^0_y(t^0_3) = I^0_{\text{см}} - \varepsilon(k_{fb}-1). \tag{I,13}$$

The duration of the third stage:

$$t^0_3 = \frac{k}{4(k_{fb}-1)} \ln \frac{I^0_{\text{см}} - \varepsilon(k_{fb}-1) - E^0_y}{I^0_{\text{см}} - E^0_y}$$

or

$$t^0_3 = \frac{k}{4(k_{fb}-1)} \ln \frac{k_{\text{reserve}} - k_{\text{reset}}}{k_{\text{reserve}} - 1} \tag{I,14}$$

In fact, the transient process comes to an end after the third stage - the current in the load has reached a fixed value.

The fourth section (section 4-6, Fig. 2). The control current (on accepted hypotheses) reaches the fixed value $i_y^0 = I_y^0 = E_y^0$ in a jump, but the current in the load and induction B_0^0 remain constant. The qualitative character of current and inductive variations in a transient process during relay operation and release is shown in Fig. 5.

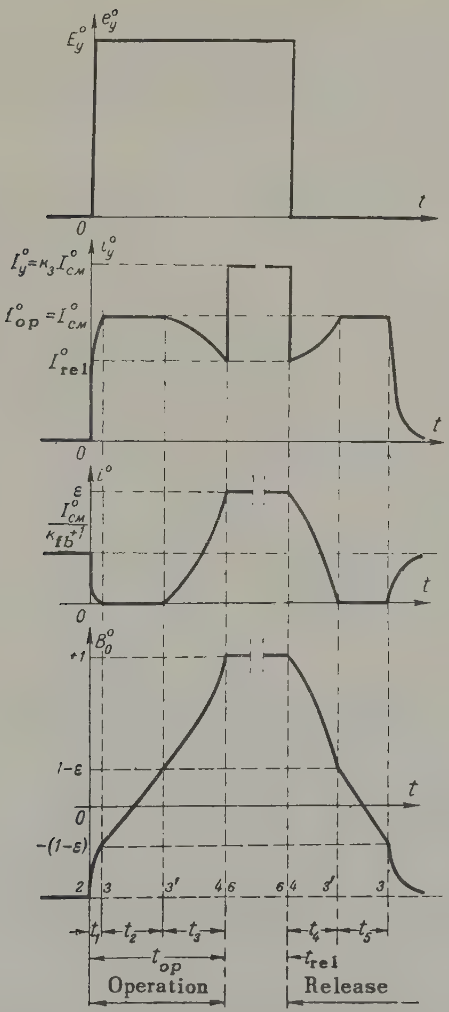

FIG. 5. Qualitative character of the variation of the direct component of induction and of the control and load currents in the transient process during relay operation and release with normally open contact

Translated by J.F. Boyland

REFERENCES

1. M.A. Rozenblat; Magnitnye usiliteli. (Magnetic amplifiers). *"Sovetskoe radio"* (1956).
2. I.B. Negnevitskii and L.L. Samurina; Experimental'noe issledovanie perekhodnykh protsessov V deskon-taktnykh magnitnykh rele (Experimental investigation of transients in contactless magnetic relays). *Elektrichestvo*, No. 9 (1953).
3. R.A. Lipman and I.B. Negnevitskii; K teorii ideal'novo drossel'novo magnitnovo usilitelya, (Theory of the ideal choke magnetic relay). *Elektrichestvo*, No. 1 (1956).
4. R.A. Lipman and I.B. Negnevitskii; k teorii odnopoluperiodnovo magnitnovo usilitelya, ch. 1. (Theory of the single half-period magnetic amplifier). *Avtomatika i Telemekhanika*, No. 4 (1957).
5. R.A. Lipman and I.B. Negnevitskii; Drossel'nyi magnitnyi usilitel. (Choke magnetic amplifier). *Elektrichestvo*, No. 6 (1958).

ABSTRACTS FROM PAPERS PUBLISHED IN ELEKTRICHESTVO No. 7, 1958

General questions of the theory of electric motors: A.N. Larionov, N.Z. Mastiaev, I.N. Orlov and D.N. Panov. (pp 1-6)

The first work on the theory of hysteresis motors was begun in the U.S.S.R. in 1950. These motors have been widely applied as their power indices have been improved. The article considers the method of operation of the motors, the character of magnetic polarity reversal and the distribution of the field in the rotor. Expressions for the electromagnetic hysteresis torque and parameters of the rotor circuit in the equivalent network are shown. Diagrams are presented showing the mechanical characteristic of a hysteresis machine; the spatial arrangement of the induction vectors B, field strength H and intensity of magnetization J at a point of the rotor during magnetic polarity reversal; the dependance of losses in the ferromagnetic material during rotary magnetic polarity reversal and magnetic polarity in the alternating field and the sine of the hysteresis angle γ on the induction of the magnetic field; the equivalent network of a hysteresis motor; the operating characteristics of an ideal hysteresis motor; experimental characteristics of a four pole hysteresis motor and rotor of a hysteresis motor with regions of different magnetic permeability. An appendix deals with the region of the hysteresis layer which is of interest.

Currents of tooth frequency in the damping winding and damping losses of a synchronous generator: P.M. Ipatov. (pp 7-10)

Damping losses in a synchronous machine can cause distortion and pulsation of the field in an air gap leading to the distortion of the shape of the e.m.f. curve of a generator. Expedient choice of the tooth division of a damping winding can considerably reduce higher harmonics in the e.m.f. curve of the generator. The author concentrates on the currents in the transverse axis of the poles and the additional losses caused by these currents.

Measurement of the strength of the electromagnetic field using the auxiliary electrode method: M.I. Sysoev. (pp 11-14)

A new method is described for the experimental investigation of the field, making it possible for high voltage installations to measure directly and simply the field strength in complex insulation, compared with the probe method or modelling of the field in an electrolytic tank. The method consists of introducing a small auxiliary electrode at the point of the field under investigation, the electrode preferably being in the form of a sphere, washer with rounded edges, or a semi-ellipsoid made of steel, or better, refractory metals. If the voltage is increased gradually between the main electrodes then a discharge arises from the auxiliary electrode. The author shows that the rise of the discharge can be taken as the signal of the attainment of a value of strength of the main field at the point where the auxiliary electrode is inserted. This method has an accuracy of ± 5 per cent when the field is uniform. It is specially useful for apparatus insulated with compressed gas.

Compensation of the resistance in the rotor circuit of synchronous generators of electrodynamic models: V.V. Pruss-Zhukouskii and V.V. Fetisov. (pp 19-24)

A special difficulty arises when modelling synchronous machines having comparatively low inertia constants (M= 4-6 sec) and high time-constants, (T_{do} = 10-12 sec), e.g. for turbogenerators and synchronous compensators. It is, therefore, necessary to compensate excess resistance by means of special electrical machines or devices. The authors here consider experience with single-phase commutator generators in connexion with long distance transmission. Provided (1) the resistance to be compensated is constant in static and dynamic conditions, (2) the magnitude of the resistance can be smoothly regulated, (3) operation is stable, (4) self-excitation is absent, (5) and given the permissible magnitude of the inductive resistance in the conditions of modelling the parameters of the generator, the single phase commutator generator can ensure high stability of operation and constant compensation of resistance at a degree of compensation up to 0.75-0.85 and even higher values.

Oscillographing the electromagnetic torque in electrical d.c. machines with the aid of the Hall effect in semiconductors: O.D. Elpat'evskaia and V.A. Perchuk. (pp 31-35)

The practical use of the Hall effect became possible only after sufficient study of the electrical properties of semiconductors with great mobility and comparatively low concentration of the current carriers in which the Hall e.m.f. is several times greater than in metals. The author here considers the use of fine plates of selenide of mercury on a micaceous backing which have the advantages of flexibility and thinness compared with monocrystals. The method of producing the plates is then considered together with the method of measurement. Zero compensation is effected by an impedance between a current and a Hall outlet allowing several activators to be connected in a bank, as illustrated graphically. Two methods of reducing interference are noted; namely, increasing the sensitivity of the plates and introducing a filtering choke in the Hall circuit. Such a method of oscillographing gives sufficiently accurate results and has other advantages.

The calculation of three phase circuits with an arbitrary number of asymmetrical short-circuits and phase breaks: N.M. Gorbatov. (pp 35 and 41)

Simple methods of calculation have still to be formulated, the criterion being the number of necessary time consuming multiplication and division operations. The use of computers and the recording of intermediate results is also considered. Tables are included and an example given of the calculation of a circuit with one short-circuit and two breaks.

A special case of synthesis of circuit schemes: V.S. Davydov. (pp 45 - 50)

The problems of the construction of electrical oscillating systems with given frequency characteristics have been dealt with elsewhere and so the author limits himself to a linear electrical system in the form of a circuit scheme formed by a number of elementary oscillating contours. He proceeds to consider how with $2n$ given natural frequencies, a circuit scheme of n elementary contours can be synthesized on the condition that n frequencies are obtained in the no-load state of the circuit system and n other frequencies are obtained in the presence of a short-circuit on the output terminals of the scheme. He bases the solution of this problem on the property of continued fractions and certain aspects of electrical circuit schemes. He then considers an analogous problem of determining the reactive parameters of a circuit scheme of both the high and low frequency filter type. The method may be extended to cases with attenuation. The paper ends with an example of the synthesis of a circuit system for a three link scheme of the low frequency filter type.

Design of heaters for thermal bi-metallic elements of thermal apparatus: IA.A. Rips. (pp 51 - 55)

An effective method of protecting electrical equipment from dangerous overloads is the use of thermal protective gear, the metering device of which reacts to the temperature developing on account of the heat due to current. The most improved gear makes use of the properties of thermal bi-metal for this purpose. As regards the planning of such gear, the first stage is to create a specimen apparatus with any magnitude of nominal current and direct heating of the thermo-bimetallic element, to choose a shape and investigate the kinematic properties common to all the planned series of apparatus. A further stage is the design of the sensitive elements for all the different models within the series. Here, no difficulties arise if the direct method of heating is employed. However, in the case of indirect or combined methods of heating, the design of the heater is complicated. The author, therefore, introduces formulae for designing heaters for the case when a series of apparatus with indirect or combined heating elements is produced from a specimen with a direct heating element, and concludes with an example of the calculations.

Neutralization of the charges of static electricity on paper: V.M. Orlov and N.I. Kromiak. (pp 56 - 58)

Electrification of paper in printing processes etc. breaks production. The Lenin Electrotechnical Institute in Leningrad has developed a neutralizer based on the principle in P.S.H. Henry's article "Electrostatic Eliminators in the textile Industry", *Brit. J. Appl. Phys.* Suppl. pages 78 - 83, 2, 1953, and applied it to printing processes.

Permissible overloads of cables in fault and operating conditions: D.S. Livshitz and S.M. Messerman. (pp 59 - 63)

In practice the problem arises of permissible short run (30 - 60 min and over) overloads of cables in fault conditions. The author reviews Soviet literature on this subject and proposes a method of calculation which will reduce capital expenditure. Taking into account ageing of the insulation, it is necessary to consider the long run operation of the cables as well as fault conditions. He concludes that the choice of cable on the "30 minute maximum load" rule leads inevitably to substantial non-utilization of the section and to an unwarranted freezing of capital expenditure.

Constant wire resistances for operation in a tropical climate: B.N. Dolgov, N.P. Kharitonov, G.V. Belinskaia and V.G. Abetikov. (pp 64 - 65)

Since in a tropical climate the resistance of insulation must be high and the equipment resistant to humidity and fungus, five constant tropical wire resistances of the P.T. series have been developed. Their general appearance is illustrated and values of rated power of dispersion (7.5 to 75W), dimensions and the rated values of resistance (5 - 30,000 Ω) are tabulated. At rated load, the surface temperature is no more than 200°C above ambient. Special thermal-humidity insulation has been developed based on silicone organic polymer compounds. The results of humidity tests thereon are tabulated and are favourable. The resistances have also undergone tests for fungus resistance and electrical and mechanical strength.

Device for measuring the angle between voltage vectors and the e.m.f. of a synchronous machine: M.Z. Gurgenidze and I.K. Servingin. (pp 65 - 67)

Experimental investigations show that indirect measurement does not reveal the overload capacity of machines. The authors propose the plotting of an angle power characteristic for different operating conditions using oscillograph recording of variations in active power and angle θ both for slow and quick load changes. A device for measuring θ produced by the Water-power Institute of the

Academy of Sciences of the Armenian S.S.R. has been modified to overcome the distortion of the linear dependence between θ and the voltage at the output of the filter. Both schemes are illustrated diagrammatically. Tests on the operation of the modified scheme in the presence of variations of the input voltage show that these variations do not affect the operation of the scheme within the limits of 100-60 V. When θ changes abruptly the lag of the scheme does not exceed 20 m sec.

HEAT RESISTANT WINDING CONDUCTORS

V.A. PREVEZENTSEV

Moscow Energy Institute*

(Received 27 February 1958)

At the present time in the U.S.S.R. and in the leading techniques of advanced countries there is a noteworthy development of conductors with enamel insulation gradually replacing winding conductors with fibrous insulation. In this direction, in the next few years we are forced to do much more, since now the total production of our enamelled conductors forms about 50 per cent of the whole output of winding conductors, while in some advanced countries it has reached 65 - 70 per cent. Much attention must be directed also to the production of aluminium enamelled conductors.

The pre-eminent development must be to produce high-stability enamelled conductors. For a long time the volume of production of these conductors with polyvinylacetate lacquers (Viniflesk and Metalvin) was very small in our country and did not reach more than 8 - 10 per cent of the total output of enamelled conductors.

The remarkable increase in the production of high-stability enamelled conductors in 1956 - 57 took place as a result of the inclusion of the output of conductors with polyamide-bakelite bases by the factories "Yuzhkabel" (Kharkov), "Estikabel" (Tallin) and "Kuibyshevkabel" as a result of much work carried out by NIIKP on the creation of formulae for a given lacquer and of the exploitation with the given factories of a new technology of enamelling with these lacquers.

The electro-insulating and physicomechanical properties of high-stability conductors with polyvinylacetate and polyamide-bakelite lacquers are well known to the many users of these conductors and are fairly widely described in our technical literature. It is only essential to remark that in accordance with GOST 7262 - 54 and with the technical conditions TUK.OMM 505.073 - 54 the long term temperature of these conductors may not exceed 110°C. For a strictly limited time of use it is permissible to increase the working temperature.

---

* *Elektrichestvo* No. 8, 5 - 11, 1958.

High-stability heat-resistors enamelled conductors class B

The organization of production of high-stability enamelled conductors in accordance with the classes B,F and H of heat-resistance is of great practical importance. Abroad, great attention is given to polyamide-epoxy enamels and in general to enamels with polyurethane and polyester bases. This is borne out, in particular, by an article by the English firm Henley †. According to the data in this article, Fig. 1 shows the relationship between the elasticity of various enamels and the duration of their exposure to a temperature of 200°C. It is not hard to see that at such a temperature the elasticity of enamelled conductors with polyvinylacetate lacquers falls fastest of all, and that for conductors with polyurethane enamels it falls noticeably slower, and least of all with silicone enamels. In comparison with the latter enamelled conductors with polyester lacquers appear more stable. In the same place follow the results of investigations of twisted samples with a voltage (a.c.) of 1 kV and a simultaneous ambient temperature of 200°C. The polyester and silicone enamels stood up to this test for about 5000 hr the polyurethane enamels about 700 hr epoxy about 500 hr and polyvinylacetate about 100 hr.

The investigatory works on the creation of high-stability enamelled conductors, in accordance with Class B heat resistance in recent times have been carried out in NIIKP in two ways: the exploitation of formulae for polyamide-epoxy lacquers and for lacquers on the basis of polyurethane resin.

For the development of polyamide-epoxy lacquers for conductor enamelling the property of epoxide resins whereby they pass into a thermoreactive condition was used, and also the property of giving, in combination with other components, lacquers of high dessication and of increased heat resistance. An enamelled conductor with insulation of polyamide-epoxy lacquers has high mechanical and electrical durability and may be used in electromechanical devices without additional protection of the enamel insulation with woven materials. In the original condition enamel conductors stand up to winding on a core of equal diameter; the enamel has good adhesion to the exterior of the wire. In the process of heat ageing at a temperature of 180°C polyamide-epoxy enamel conductors behave better than Viniflex conductors at a temperature of 150°C. Experiments at a temperature of 130°C show that over a period of 30 days polyamide-epoxy enamel films retain their elasticity at their original level.

---

† A new Henley high temperature enamelled wire. Distribution of Electricity, May 1957.

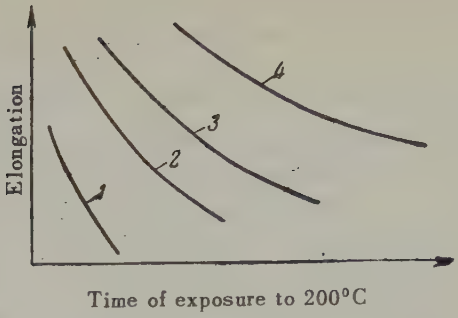

Fig. 1. Variation of elongation of enamel insulation (with stretching of the conductor) as a function of the duration of exposure to a temperature of 200°C

(1) Polyvinylacetate enamels
(2) Polyurethane enamels
(3) Silicone organic enamels
(4) Polyester enamels

The conclusions given enable one to assume that such enamel conductors may, over a protracted period, be exploited at a temperature of 130°C and for short periods at temperatures up to 150°C. This insulation has high resistance to the effects of solvents such as benzine and benzole.

A defect of enamel insulation of the first formulae for polyamide-epoxy lacquers appeared as an excessive thermoplasticity which reached 18 - 20 per cent at a temperature of 200°C. A reduction of the thermoplasticity of these materials was achieved by the introduction of polybutyltitanate. A general defect of enamelled conductors with polyamide-epoxy insulation appeared as a sharper fall in insulation resistance in conditions of high relative humidity of the air than with Viniflex enamel. Nevertheless the insulation resistance of experimental enamelled conductors remains noticeably higher than with woven insulation (Mark PBD etc.) which gives grounds for considering that the new enamel conductors are more suitable for general electromechanical apparatus.

Noticeably better results were obtained in the exploitation of a formula for polyurethane enamels. Polyurethanes appear as products of mutual reaction between diisocyanates and compounds containing hydroxyl groups. For a general picture of the reaction for the production of polyurethanes one may write the following:

$$x.\mathrm{HOROH} + x.\mathrm{OCNR'NCO} \rightarrow (\mathrm{-OROCONHR'NHCO-})_x.$$

For the preparation of polyurethanes the most suitable manner would seem to be the application of the aromatic diisocyanate – toluylenediisocyanate

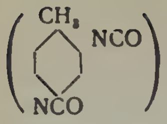

, which is produced by the reaction of toluylenediamine with phosgene and the production of which is well known to our chemical industry.

Isocyanates seem to be remarkably chemically active substances. When they are mixed with polyesters, even at room temperatures, after a short while a reaction takes place between the two. For preparation of enamels it is essential to apply stabilized ("masked") diisocyanates, by the production of which high dessication lacquers are obtained. Stabilized diisocyanates are obtained by reactions with phenols, cresols etc. according to the equation:

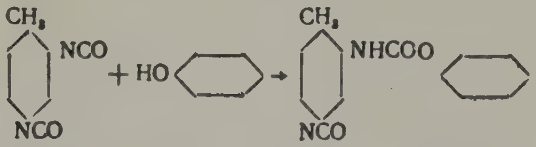

In this case one active group – NCO is blocked by the phenol and so the diisocyanate changes to monophenylurethane, losing, at ordinary temperatures, its liability to reactions. The second active group – NCO when mixed with polyesters reacts with free OH groups, as a result of which monophenylurethane becomes completely blocked and particularly inert at normal temperatures; moreover blocked diisocyanates are non-toxic.

At higher temperatures (180°C and above) monophenylurethane decomposes into its original products – phenol and diisocyanate, which is also used in enamelling, so that diisocyanate goes into a deeper reaction with the second component of the lacquer – the polyester, forming insoluble enamel films.

Enamel conductors on a basis of polyurethane resin are distinguished by high elasticity. They stand up to winding on a core the diameter of which is equal to the conductor under investigation, and under these conditions neither cracking nor damage to the enamel occurs. The thermoplasticity of these conductors is noticeably lower than the demands presented in GOST 7262-54, and is found within the limits 6-7 per cent. Insulation on the basis of polyurethanes is inert to benzine and to aliphatic hydrocarbons.

Prolonged investigations of enamelled conductors under heat ageing showed the exceptional heat resistance of enamel insulation. Thus after being thermostatically maintained at 150°C for 25 days, they showed their original elasticity and could be wound on a core of equal diameter to that of the wire. At the same time, wires with insulation of Viniflex lacquer maintained their original elasticity at 150°C for only 1-2 days.

At 180°C after five days, the elasticity of enamelled wires on a base of polyurethanes remained at the same value as at the beginning. These conductors maintained a satisfactory elasticity after eleven days exposure to the same temperatures; a further reduction of elasticity took place uniformly in the course of a comparatively long time interval. Tests on protracted ageing of enamelled conductors at a temperature of 125°C show that the elasticity of the conductors is maintained without change for a period of 150 days.

The foregoing data on the heat resistance of enamelled conductors on a polyurethane basis allows one to assume that they may be used for long periods at a temperature of 130°C (Class B insulators) and for a limited period – at higher temperatures (150 - 180°C).

Measurements have shown that enamelled conductors with polyurethane base insulation are particularly noted for high electrical insulation characteristics not only in the original condition but also in an atmosphere with high relative humidity (Fig. 2).

The information obtained permits the recommendation of enamelled conductors with a base of polyurethane for application in the radio industry or the production of high-frequency apparatus where there are specially stringent demands on the electro-insulation characteristics of the conductors.

An especially valuable property of enamelled conductors on a polyurethane base appears in that they can be covered with a layer of tin (or its alloys) without preparatory dressing of the enamel and without the use of fluxes. The temperature necessary for soldering enamelled conductors is in the range 320 - 360°C, in which the higher the temperature of the tin, the shorter is the time required for soldering. Thus, at a temperature of 360°C, 2 - 3 sec are needed for soldering enamelled wires, while at 320°C, 15 - 40 sec are needed depending on the thickness of the insulation. Wires of small diameter are much more rapidly soldered at these temperatures than wires of greater gauge.

In this manner the use of polyurethane enamelled conductors noticeably facilitates the assembly of many different types of apparatus. From this point of view, polyurethane enamelled wires are particularly desirable for the preparation of high-frequency winding conductors (Litz wires). Their current carrying elements often consist of many tens or hundreds of enamelled wires whose diameter is from 0.05 - 0.10 mm the cleaning and soldering of which is very complicated and time consuming. With the use of polyurethane enamelled conductors the necessity for cleaning vanishes, and even the soldering process may be accomplished quickly and without any difficulty.

It may also be observed that these wires may be made with the enamel films dyed in various colours, which has a special significance for mass production.

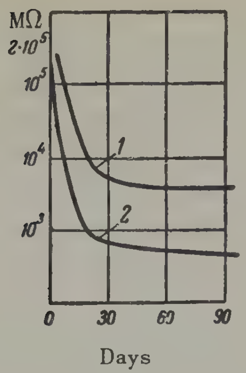

Fig. 2. Variation of insulation resistance of (1) Polyurethane and (2) Oil based enamels as a function of time of exposure to a relative humidity of 97 per cent and a temperature of 35°C (according to the Swiss firm Huber)

Enamel conductors with additional thermoplastic covering

In the production of low-power electric motors and generators and of electrical apparatus, it is often necessary that the windings of the coils be made in sections or in frames for the purpose of gluing them together without a support or other similar device. To achieve this it is essential that the wires besides their usual enamel insulation (of polyvinylacetate, oil, polyamide and other similar lacquers) should have an additional exterior thermoplastic layer, which ensures the solid adhesion of the coils one to the other if they, or other section or the spools are exposed to baking at 170 - 180°C for 3 - 5 hr. The additional coverings may be made by the use of enamels from such thermoplastic resins as polyvinylacetate, polyvinylacetal, (without hardeners) etc. with the addition of some quantity of hardening plasticizer. The prepared wires may be produced on ordinary lathes with an increase in the number of operations of 2 - 3. Work on the construction of such wires is successfully achieved in NIIKP and it is being introduced at the first opportunity into the factories “Mikroprovod” and “Moskabel”. On investigation, a thermoplastic lacquer on a polyvinylacetate basis has shown better results.

Enamel conductors with particularly high heat resistance of the enamel insulation

At the present time there is a very great demand for enamelled conductors with yet greater resistance to heat (for extended working at 150 - 300°C). One of the ways for the production of such conductors has appeared until recently to be the use of Silicone compounds. As a result of combined work the VEI, NIIKP and the cable factory "Mikroprovod" have organized the production of conductors with these lacquers (Type PETK) with diameters of 0.05 - 0.25 mm.

Frequent attempts to produce silicone lacquers for enamelling larger circular conductors and conductors with rectangular cross-sections have, until recently, not led to successful results on account of the low mechanical strength of the insulation on these wires. Moreover the wires obtained showed unsatisfactory resistance to benzene and a greatly lowered breakdown voltage after an operating temperature of 180°C. The undertaking MAP produced the silicone lacquer (Type MK-4) modified with glyptal resins. The enamelled conductors with this lacquer, as regards mechanical durability, noticeably exceed wires with similar lacquers of the VEI and for durability approach that of the wires type PEV-1; moreover, they are resistant to benzene. Nevertheless, these lacquers have less heat-resistance in comparison with VEI lacquers so that after 5 - 7 days exposure to 150°C the elasticity of the enamel insulation has noticeably decreased. The wires lose the elasticity of their insulation after 2 - 3 days at 180°C. In this way, enamelled conductors with MK-4 lacquer may be worked for limited periods at temperatures not exceeding 150 - 160°C.

Recently, fellow-workers of one of the undertakings developed the formula for this lacquer to increase its heat resistance; therefore, the new lacquer (MK-4y), suitably modified, was tested and investigated on an experimental basis for enamelled conductors. Noticeably better results were obtained with lacquers in which polyester resins were incorporated. These latter are obtained as a result of the reaction of polycondensation of double radical acids and multi-atom alcohols. Examples of such resins are the polyterephthalates (Lavsan, Mailar, Terebek, Terylene), obtained as a result of the reaction of terephthalic acid on ethyleneglycol:

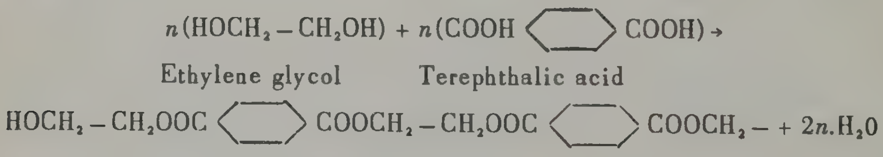
n(HOCH₂ – CH₂OH) + n(COOH COOH) →
Ethylene glycol
Terephthalic acid
HOCH₂ – CH₂OOC COOCH₂ – CH₂OOC COOCH₂ – + 2n.H₂0

Polyethyleneterephthalate

A linear molecule construction determines the properties of polymers, and often its elasticity, mechanical durability etc. For the preparation of lacquers, polymers are essential which are capable of giving a spacious structure. In connexion with this, in the molecules of the polymer, substances are introduced with groups giving possibilities of side reactions (e.g. glycerine

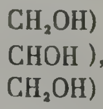

$$\begin{matrix} CH_2OH \\ CHOH \\ CH_2OH \end{matrix}$$

), enabling the function of such a structure.

Wire, enamelled with polyester lacquers is marketed in the U.S.A. under the names "Teramel" and "Levkanex".

In the German Federal Republic polyester enamels are prepared – "Terebek F-35" and "Terebek F-45" (different viscosities) with prolonged heat-resistance at 155°C. The solvent of these lacquers is tricresol. Finally, for the production of enamelled conductors with prolonged heat resistance at 155°C, within limits, enamels with a polyester base are used, in which to increase the heat resistance about 20-25 per cent silicone resin is added.

It remains to mention that some polyester enamels give films insufficiently resistant to warmth, blows and to the action of hot solvents (while bent), which reduces the use of these products. In mechanical and electrical strength of the enamel films, polyester enamelled conductors do not give rise to high resistant conductors.

In the VEI in this direction much work has been done as a result of which a modified polyester lacquer No. 124 has been developed, and the NIIKP with the factories "Moskabel" and "Mikroprovod" have produced a technique of enamelling with these lacquers.

In Fig. 3. are shown curves of the variation of elasticity of enamelled conductors in the ageing process at temperatures of 180 and 200°C. It is apparent that the elasticity of enamelled wires after 30 days ageing at a temperature of 180°C has hardly changed: the enamel films fail by cracking when the conductors are wound on a core 2-3 times the wire diameter. Holding of the conductors at a temperature of 200°C noticeably reduces their elasticity.

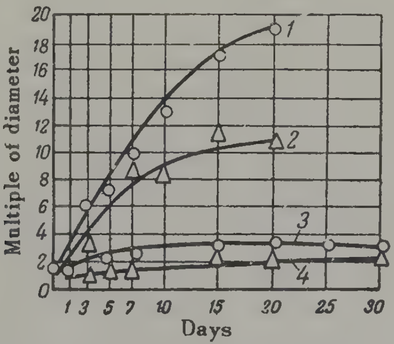

Fig. 3. Variation of elasticity of enamelled wires in lacquer No.124 as a function of the time of exposure to temperatures of 180°C and 200°C

(1) Wire diameter 0.8 mm, temperature 200°C
(2) Wire diameter 0.44 mm, temperature 200°C
(3) Wire diameter 0.8 mm, temperature 180°C
(4) Wire diameter 0.44 mm, temperature 180°C

Determination of the breakdown voltage of enamelled conductors at room temperature after they have been exposed for 1 - 20 days to a temperature of 200°C, and also indefinitely at this temperature has shown that the new insulation shows high electrical strength. The thermoplasticity of wires measured at a temperature of 200°C reaches 8.3 per cent.

It is possible that on aluminium or aluminium coated wires the heat resistance of polyester films may be increased a little as a result of the exclusion of catalytic influence of the copper during the ageing of the enamel insulation.

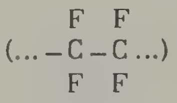

Fluoroplast - 4 $(\ldots - \underset{F}{\overset{F}{C}} - \underset{F}{\overset{F}{C}} \ldots)$ also appears as a desirable prime material for enamels on account of its lasting heat resistance in any case not less than 250 - 300°C. In connexion with this, great interest has been caused by the development of a formula for enamels on the basis of a suspension of the copolymers of Fluoroplast-4 leading to LF NIIKP. In the creation of such lacquers, high lacquer strength and humidity resistance of the enamel wires will be achieved. However, these enamels may exhibit reduced adhesive qualities and increased thermoplasticity.

Abroad, wires with especially high heat resistance of the insulation with a very thin layer of ceramic material are recommended, which is deposited from a solution by electrophoresis. Ceramic insulation is additionally supported by a suspension of a Fluoroplast-4 or Silicone base lacquer. Conductors with this type of insulation are recommended for protracted use at temperatures up to 300°C.

Conductors with heat resistance up to 250 - 300°C may be obtained in the same way by impregnation with oxide insulation by suspensions on a base of Fluoroplast-4 or of its copolymers, or indeed, with heat resistant silicone compounds or polyester lacquers, as is done on an experimental basis in the NIIPP and by some foreign firms. For the formation of the oxide insulation the copper conductors must first be covered with a thin layer of aluminium. Such conductors may only be used for the preparation of various coils, designed to work at particularly high temperatures, but the wires thus obtained exhibit limited elasticity (they stand up to winding on a core of 10 - 20 times the wire diameter), low electric strength (150 - 200 V) and an increased hygroscopic quality.

Very thin manganin* wires with continuous glass insulation

In recent times the factory "Mikroprovod" with special techniques has prepared for small scale, high ohmic resistances of increased stability, manganin wires with diameters of 6 - 10 μ with continuous glass insulation. Since measurements of the dimensions of such bare manganin wires is exceedingly laborious, these wires are classified in relationship to their electrical resistance (see Table 1).

---

* Manganin is a manganese-nickel-copper alloy.

Selection and general characteristics of very thin manganin wires with continuous glass insulation

TABLE 1

Resistance of manganin wire 1 m long (Ω)	Permissible deviations of resistance (Ω)	Maximum outside diameter of the insulated wire (μ)	Breaking strength of the wire. Not less than g (grams)
15,000	± 2500	14	8
11,000	± 1500	16	10
8000	± 1500	17	12
5500	± 1000	18	14
4000	± 500	20	18

Disregarding the very small thickness of the glass insulation the latter exhibits high electro-insulation properties (the absence of small points of damage, puncture voltage not less than 1000 V). Naturally, continuous glass insulation has less flexibility and much more brittleness than fibre-glass. In connexion with this, the wires remain wound on aluminium formers 25 - 30 mm diameter with a weight of not less than 0.5 g on one end. For 20 per cent of the total quantity a minimum weight of 0.2 g on the end is permitted.

For the determination of elasticity and strength of glass insulation the wires are tested by winding them on a core of 4 mm diameter. In general it is possible to obtain it with this sort of insulation on copper and constantan wires.

Enamelling of conductors with rectangular cross-section

In recent times, wires with rectangular cross-sections have only been made with enamelled insulation with films of Viniflex lacquer. The selection of these wires has been limited to copper about 0.5 - 1.95 mm thick and 2.10 - 8.8 mm wide. The electrical strength of the enamel insulation of the wires (175 - 250 V) is determined by the thickness of the film at the edges, so that for enamelling rectangular conductors with small radii of curvature, the film in these places runs, compacts and goes over to the flat part of the surface of the conductor. In fact, at the edges a high pressure of film p will be obtained according to the Laplace equation

$$p=\sigma\left(\frac{1}{r}+\frac{1}{r_1}\right),$$

where; σ is the surface tension

r, r_1 the radii defining the curvature of the surface.

In the case given $r=\infty$ and consequently,

$$p=\frac{\sigma}{r_1}.$$

The removal of the given defect may be achieved if for rectangular conductors with a thickness of 1.35 mm one takes a curved form for the edges (Fig. 4) with a radius of curvature of $r=a/2$, where a is the thickness of the copper conductor, and for wires of greater thickness one uses a radius of curvature about 0.7 - 2.0 mm (Fig. 5). The reduction in the calculated section for rectangular wires with a thickness less than 1.35 mm will be expressed by the following equation

$$\eta\,\%=\frac{a^2-\frac{\pi}{4}a^2-\xi}{ab-\xi}\cdot 100$$

and for wires of greater dimensions:

$$\eta\,\%=\frac{4r^2-\pi r^2-\xi}{ab-\xi}\cdot 100,$$

where ξ is the reduction of section established in the calculated tables GOST 434 - 53 and equal approximately 0.50 mm².

In principle, the value η may be further reduced, in taking an ellipsoidal form for the narrow side of the rectangular wire (Fig. 6). In this case the reduction in section as against that calculated in GOST 434 - 53 may be obtained from the equation:

$$\eta\,\%=\frac{2aq-\frac{\pi}{2}aq-\xi}{ab-\xi}\,100.$$

A given increase in the radius of curvature on the edges which is accomplished by foreign firms may increase the value of the breakdown voltage. The losses of the cross-section in a wire of small cross-section will not exceed 2 - 3 per cent. Therefore, the question relating to the change of profile of our rectangular copper and aluminium conductors must be given great attention by us.

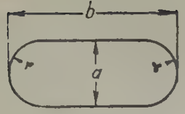

FIG. 4. "Rectangular" copper wire with semi-circular narrow sides

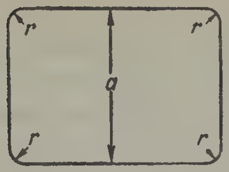

FIG. 5. "Rectangular" copper wire with increased radius of curvature at the edges

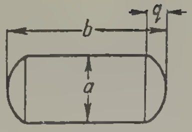

FIG. 6. "Rectangular" copper wire with semi-ellipsoidal narrow sides

The enamelling of rectangular conductors is also possible when using other enamels (Metalvin, polyamide-resol, polyester etc.). In particular, in recent times for special applications rectangular conductors of high heat resistance, which can be used for limited periods at 180 - 200°C are prepared with the use of polyester lacquers. Abroad (in Czechoslovakia, Eastern Germany etc.) for the preparation of rectangular enamelled conductors, lacquers on a polyamide-resol base are widely used. In the U.S.S.R., the production of rectangular enamelled conductors must be greatly increased rapidly since that would allow the output of wires type PBD,PDA and others to be reduced and would give new possibilities for the perfection of construction of various electrical machines.

Conductors with delta-asbestos insulation

Asbestos insulation is put on and stuck to the copper wire with a final impregnation and dessication of the insulation. At the present time, glyptal lacquer is used for sticking, but for the impregnation of the insulation for a long time, only bituminous lacquer was used. The presence of the impregnating bituminous lacquer gave difficulty in soldering wound conductors, in particular for mechanized soldering of collectors since, when heated, this lacquer melted out of the conductors and fell into the baths with the solder.

Experiments to improve the properties of delta-asbestos coated wires by completing the work on the formula for bituminous impregnating lacquers (modifications to it of quick drying vegetable fats, kanifol and other resins) did not give suitable results. Therefore an investigatory work was undertaken having for its aim the explanation of the use of other impregnating lacquers. As a result of this work it has been confirmed that in use as an impregnated and sticking lacquer more or less useful results were given by water emulsified glyptal lacquers.

When using this lacquer, particular attention must be given to its quality and careful preparation in order to exclude the possibility of the appearance of separate cracks on the bends of the insulation, in particular after prolonged storage. GOST 7019 - 54 sets forth the maximum permitted heat for these conductors at the time of use as up to 130°C. Some foreign firms allow the heating for limited periods of asbestos and delta-asbestos insulation in combination with glass-fibre to reach 200°C and even up to 250°C. Therefore the additional investigations by ourselves in these directions are undoubtedly of practical interest.

Wires with fibre-glass insulation

At the present time, a special type of conductor with fibre-glass insulation conductors type PSD has appeared, which the cable factories have produced in accordance with GOST 7019-54, which sets out the long term permissible temperature as 150°C. Past investigations show that this temperature may yet be slightly increased and raised to 160-170°C. Short term conductors may be worked at temperatures of 200-250°C.

PE′TSO type conductors, the long term permissible temperature of which is about 125°C, are as yet produced in limited quantity. At the present time, for the preparation of these conductors instead of enamelled ones type PET (with glyptal lacquer) conductors type PEV-1 (Viniflex or Metalvin) are used which only raised their quality.

The choice of covered conductors with fibre-glass insulation is now noticeably greater. As a sign of the organization of production of electric motors for tropical conditions manufactured in recent times may be given type PETSO-T and PSD-T (TUK OMM, 190-56). In these the thickness of the insulation is of the same order as with type PELBO.

In the cable factories conductors type PSDK are also made in which in the place of adhesive and impregnated substances Silicone lacquers are used. BTU MEP OAA 505.023-52 gives the long term temperature of these conductors as up to 180°C. For a limited period these conductors may be used at temperatures of 250-300°C.

Moreover, as a result of the needs of aviation electric machine construction, our cable factories produce conductors type PETKSO and PETKSOT for the preparation of which wire enamelled with Silicone lacquer is used adaptable also for sticking and impregnation with single layer fibre-glass insulation. Wires type PETKSOT are distinguished from wires PETKSO by some increase in the thickness of the insulation, which is reached by the use for all conductor dimensions 4 μ and with the presence of small holes in the insulation. These and other wires are designed for work for limited periods (500-2000 hr) at temperatures of up to 180°C.

Using fibre-glass 3 and 4μ thick in recent times NIIKP in co-operation with "Moskabel" have developed the construction of conductors type PSDK with a reduced thickness of insulation. Type PSDKT is manufactured with these conductors. With the same purpose, for the needs of the aviation industry there was developed the construction of conductors type PSOT with single layer insulation with glued and impregnated fibre-glass insulation of heat resistant Silicone lacquers. In the NIIKP and MEI, experiments were carried out which showed that these conductors, particularly type PSDKT, may for a limited time (a few hundred hours) be worked at temperatures up to 300 - 350°C. With these experiments it was determined that the action of such a temperature does not really affect the electrical properties of fibre-glass insulation; although the latter at these temperatures does lose (especially with small diameter circular conductors) a noticeable portion of its silicone impregnated lacquer. In particular, after 100 - 200 hr exposure to these temperatures, it continues to stick to the wire stably and stands up to vibratory conditions (the amplitude of oscillation 2 mm at 1350 c/s).

According to the conditions of these experiments one may consider the oscillations to proceed according to the law, $s = A \sin(\omega t + \phi)$.

The acceleration of this oscillation is:

$$s'' = -A\omega^2 \sin(\omega t + \varphi).$$

If in this equation one puts the given conditions of the test, $A = 2$ mm, $\omega = (2\pi 1350)/60$, then the maximum acceleration will be:

$$s'' \approx 4g.$$

In this way, the experiments mentioned correspond to the maximum acceleration equal to $4g$, by which in the course of 16 hr of such tests there was no noticeable decomposition of the insulation and exposure of the copper conductor. In recent times on conductors type PSDKT and PSOT the provisional technical specifications TUKP 18 - 58 and TUPK 17 - 58 were confirmed.

More stable for generally high temperatures is insulation made from windings and braids of fine fibre-glass as well as with glued and impregnated heat resistant silicone lacquers. In this case especially, the thickness of the insulation is a little increased. However, the technical process of applying braid is very tedious and slow and so conductors made in this way may only be used in very special circumstances.

According to a communication from the General Electric* Co., radio apparatus has been built allowing operation at temperatures up to 500°C. All the components in it may work at red heat and without reaction to the effects of powerful radioactive radiation. The development was made at the order of the military command of the U.S.A. for general defence purposes.

---

* *Electronics*, October 1956.

The windings of transformers, electric motors and selsyns in this apparatus are wound from copper silver-plated conductors with insulation by a layer of heat resisting glass. Such a conductor is made with a diameter of from 0.12 - 1.8 mm. Test samples of the electric motors and transformers in which glass thread has been used for the external insulation have worked continuously for some hundreds of hours at temperatures of 520°C.

For the heating of conductors above 250°C, a copper wire becomes covered with a layer of copper oxide. For the preliminary experiments no particular importance was assigned to this effect. The ohmic resistance of the wire during the course of 260 hr at 300°C increased approximately 1 per cent, and after 103 hr at 400°C to 4 - 6 per cent. Here additional experiments are essential. It seems more dangerous, that for a very long exposure to a high temperature with periodic cooling of the conductors small pieces of detached copper start to project through the glass-fibre insulation and this latter darkens, as a result of which the insulation resistance of the winding is noticeably reduced. Attempts to prevent this by using an electroplated silver covered copper conductor did not give positive results. Evidently a thin porous layer of silver put on by electro-deposition does not give the desired protection against oxidation of the copper when the wires are exposed to high temperatures for long periods. It is possible that significantly better results may be achieved if the added layer achieves a greater thickness and additionally its penetrability can be reduced by a suitable filler. Aluminium coverings show themselves to be very resistant at temperatures of 300 - 400°C. However, if the copper conductor is covered with a melted layer of aluminium there is the fear that a brittle layer with higher electrical resistance may appear on the surface of the copper conductor. Better results may be attained if the aluminium envelope is put on a copper wire of large cross-section with a cold process and then the wire reduced to the desired size by drawing. When such an aluminium coated conductor is exposed to 300°C for 48 hr no change whatsoever in the ohmic resistance can be observed. Moreover, the requisite effect may be obtained if the aluminium covering is carried out not on a bare copper wire but on a wire previously covered with a thin layer of silver or nickel.

Translated by R.P. Froom

AN INVESTIGATION OF AN AUTOMATIC SYSTEM OF EXCITATION FOR LARGE TURBOGENERATORS USING SEMICONDUCTOR POWER RECTIFIERS*

IA.N. SHTRAFUN and M.S. ROSTOVTSEVA

Leningrad

(Received 31 October 1957)

The further growth of power systems in the Soviet Union has placed before the electrical industry the problem of the development of and putting into production and use of turbogenerators with powers up to 300 MW. The solution of this complicated problem of national economics has raised a series of serious scientific and technological questions, to the number of which is frequently added the development of an automatic regulating system for the excitation of turbogenerators which satisfied the demands of modern exploitation.

The desire for the utmost use of active materials and, connected with this, the application of forced draught hydrogen cooling with the hydrogen under a pressure of up to 3 atm in the body of the generator leads to a noticeable increase in the parameters of the excitation system of the generator (see Table 1).

TABLE 1

Turbogenerator power (*MW*)	Rotor current in rated conditions (*A*)	Rotor voltage in rated conditions (*V*)	Rotor voltage with forced excitation (*V*)
200	2250	400	800
300	3000	525	1000

As tests over many years have shown in use, a system of machine excitation has the greatest reliability in the case where the exciter is assembled on the same shaft as the turbogenerator. However, the given practical parameters of the system of excitation exclude the possibility of such a constructive solution if a d.c. machine is used as the exciter.

---

* *Elektrichestvo* No.8. 37-41, 1958.

The progressive increase in the production of semiconductor rectifiers gives favourable grounds for their use in the power circuits of excitation systems, and the availability of reliable sources of alternating current for supplying these rectifiers gives an especial perspective to such a system of excitation. To the total of such sources of supply may be added three-phase generators of increased-frequency alternating current (400 - 500 c/s) of the induction type which may be used for power circuits, and also generators with permanent magnets on the rotor for supplying the control circuit and the apparatus for automatic regulation. The absence of windings on the rotor and the need for connexion only to the stator of all the circuits substantially increases the reliability under working conditions of such arrangements. The necessity of increased-frequency a.c. generators of this type determined by constructional considerations may be expeditiously used for the reduction of the dimensions and the increase in the rapid action of the general elements of automatic excitation control, which gives the possibility of making a system compact and of small inertia.

With the aim of investigating the parameters of such a system of excitation in various conditions of use, and also of accumulating working experiments as separate elements, as well as of systems of excitation the exploitation of a new system of excitation of a turbogenerator with a power of 30 MW type TBF-30 was worked out by the whole factory "Elektrosil", prepared and handed over for operating tests in one of the electric stations LENENERGO. The technical details of the system are given in the appendix.

The main circuit of the excitation system is given in Fig. 1. A three-phase

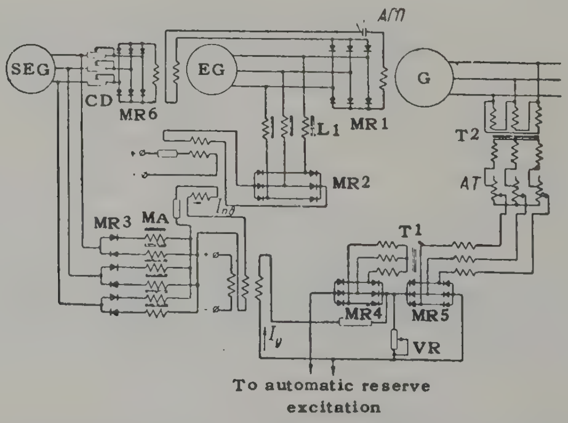

FIG. 1. Principal circuit for turbogenerator excitation

generator *EG* is used as a source of supply to the excitation system. This is of the induction type, having two excitation windings on the stator. The frequency generated is 500 c/s. The main excitation winding which is designed to make use of the compounding effect of the free current in the rotor is connected as a series self-excitation circuit. The second – auxiliary winding is connected as an independent excitation circuit. It is intended for the initial excitation of the generator and for adjustments of the circuit, and also may be used for forced excitation.

The independent excitation circuit receives a controllable supply from the high-frequency pilot exciter *SEG* through the rectifier *MR6*. The pilot exciter is itself excited by permanent magnets.

The generator and the pilot exciter are mounted on the same axle as the turbogenerator *G*.

The excitation winding of the generator gets its supply from the exciter of the generator through the Selenium Power Rectifier *MR1*.

To achieve great effectiveness in the rise of rotor voltage during the process of automatic regulation and forced excitation, the exciter of the generator is so calculated and constructed that with nominal rotor current for the turbogenerator, as a result of the consequent self-excitation, it produces a voltage at the exciter which exceeds the demands of a given condition and prepares the exciter for forced excitation. This produces a definite excess voltage at the exciter of the generator in this or another condition of the turbogenerator. The compensation of this excess of voltage is realized by switching an additional reactive load into the exciter circuit, automatically regulated in accordance with the conditions of working of the turbogenerator.

To this end power inductors *L1* are connected to the stator windings of the exciter in parallel with the output of the rectifier *MR1* with magnetization appearing in the main regulating element of the power part of the system. The automatic regulation of the turbogenerator excitation is achieved by means of a regulated fall in voltage on the stator windings of the exciter from the boost current of the power inductors. The degree of magnetization of the inductors is automatically changed by the excitation regulator.

Regulation of this kind seems effective in view of the character of generators type *BGT* which have relatively high values of reactance x_d, equal to $0.12\,\Omega$ in the given case. The necessary boost current is defined as the ratio of the excess voltage on the exciter to x_d.

Other variants of the automatic regulation of the excitation voltage of generators are possible, an analysis of which does not enter particularly, into the scope of the present article. It is only right to observe that, for a given rate of rise of voltage, and to attain the desired excitation power with forced excitation, the transition for example to a parallel self-excitation circuit demands the use of a rheostat, the losses in which increase the active boost losses in the inductors. The need for the use of relay forced excitation in this case also appears insufficient in comparison with a system of uninterrupted regulation for all the range of excitation current almost up to the maximum value.

As a possibility the use of a combined series-parallel circuit for self-excitation with automatic regulation in the circuit of the parallel self-exciter etc. may be considered.

The automatic regulator for the excitation operates as a function of the voltage across the intermediate amplifying element which is the Magnetic Amplifier *MA*. This is provided with an external return circuit for increasing the amplification factor. The a.c. windings of the magnetic amplifier are fed by the pilot exciter.

The metering element of the regulator consists of a three-phase saturated transformer *T1* which is connected across a variable autotransformer *AT*, *T1* gets its supply from the generator voltage transformer *T2*. The primary current of the metering transformer, appearing as the magnetizing current, is non-linearly dependent on the voltage of the generator to a marked degree.

The secondary windings of the metering transformer are only used for operating the automatic excitation regulator for the reserve excitation system. The magnetizing currents of the transformer are rectified by the rectifiers *MR5*; at their output the regulating resistance *VR* is established to which are connected the main control windings of the magnetic amplifier. For effective forced excitation the reduction of the no-load current both in the inductors and in the magnetic amplifiers must be substantial. With this in view the magnetic amplifier has an additional winding as well as the normal control windings the supply to which is from the operating current. As protracted tests have shown, the circuit may conveniently be supplied by the rectified exciter current.

The current flowing through this winding causes an initial magnetization directed towards the field by the condition of the external feedback, thanks to which the no-load currents of the magnetic amplifier are reduced. Moreover, the magnetic amplifier has an external winding of opposite sense which serves for adjustment of the circuit.

The current from the output of the magnetic amplifier is fed into the main magnetizing windings of the power inductors, having a winding external to the permanent return circuit. For the reduction of the no-load current in the inductors an additional winding is provided fed through a resistance from the operating current circuit. The direction of the m.m.f. of the additional magnetizing winding is in opposition to the direction of the m.m.f. of the normal winding of the external feedback. In this way under conditions of forced excitation the inductor current reaches a minimum value.

The process of automatic excitation regulation is achieved by use of the magnetizing current of the metering transformer as a function of the voltage of the turbogenerator, operating suitably on the magnetizing current of the power inductors.

In the event that it is necessary to maintain constant voltage and reactive power of the generator, the voltage of the measuring element is changed accordingly by the use of the variable autotransformer.

In the system of excitation relay blocking is provided which maintains the supply excitation of the generator in the event of rupture of the fuses on the high-voltage side of the voltage transformers by automatically connecting to the reserve.

Under working conditions the main direction of investigation was the determination of the following parameters of the system: the limits of voltage regulation, automatically maintained by the constants in the statistical regime; the steadiness of the regulation of excitation; the rapidity of voltage rise when the exciter worked on the excitation winding of the generator and the determination of the influence of the free rotor current under short-circuit conditions on the system.

For the preliminary stage of the investigations the optimum parameters of the elements of the system were determined. In addition, in the circuits for maintenance of forced excitation after extinction of the free rotor current, the effectiveness was determined of the additional relay forced excitation, which was achieved by means of adding to the independent exciting windings an additional current the magnitude of which depended on the value of the rectified excitation voltage of the generator *EG*.

The following stage was the investigation of the system of excitation and of automatic regulation when the turbogenerator was working in the no-load condition; by changing the load on the generator from zero to the normal value; by the transference of reactive power from the turbogenerator on test to the parallel working generators and back, with the sudden application of a three-phase short circuit to the stator of the turbogenerator, working on no-load at reduced initial excitation.

For reduction of the time constant of the control circuit of the magnetic amplifiers, an additional adjustable resistance is included in this circuit, the magnitude of which influences the steepness of the characteristics $I_u = f(U_g)$.

The characteristics were taken for various values of the resistance, but with a constant value for the resistance of the rheostat; they are shown in Fig. 2.

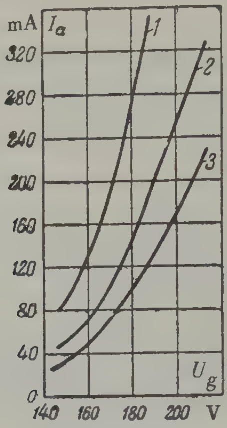

FIG. 2. Relationship of the control current of the magnetic amplifier to the generator voltage
(1) Without boost resistance. (2) and (3) Boost resistors 100Ω and 200Ω respectively

For reduction of the time constant of the circuits of the power inductors an additional variable resistance is included in this circuit also.

In Fig. 3 are shown the characteristics of a magnetic amplifier in its operation on the magnetization windings of the power inductors. The necessity for transference from no-load to normal power of the generator, the changing of the magnetizing regime of the power inductors and of the magnetic amplifier defines the regulation of the system which does not exceed 2-2½ per cent.

According to the results of the experiments performed on the elements of the automatic excitation regulator the parameters of the resistances in the magnetic amplifier and inductor circuits were chosen and these were left unaltered during the subsequent tests.

To define the effectiveness of the additional forced excitation of the exciter by means of the action on the independent winding as a function of the rectified voltage of the exciter, the regime of forced excitation was tested with operation of the exciter on a resistance equivalent to the resistance of the rotor winding.

The results of the regime of forced excitation without the additional effect of the independent excitation on the windings are given in Table 2.

In as much as with the extinction of the free rotor current of the turbogenerator there takes place some reduction in the effectiveness of the consequent self-excitation, so the effect was determined of the simultaneous action of the supplementary relay forced excitation.

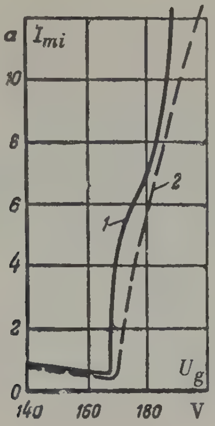

FIG. 3. Relationship between the output current of the magnetic amplifier (magnetizing current of the inductor) and the generator voltage
(1) Without a resistor in the magnetizing circuit. (2) With a resistor 10Ω. (Twice the resistance of the magnetizing winding)

TABLE 2

State	Magnetizing current in the inductors (A)	Equivalent load current (A)	Voltage on the equivalent load (V)
Initial	5.0	925	50
Forced excitation	0.8	3450	191

This forcing was achieved with the help of the feeding of the rectified excitation voltage to the independent winding of the excitation through a limiting resistor fixed at about 35 per cent of the additional m.m.f. of the excitation of the exciter in relation to the m.m.f. of the turbogenerator in its nominal running conditions. The results of the tests are given in Table 3, and the given working oscillogram in Fig. 4.

The rapidity of growth of the voltage on the equivalent resistance with the presence of additional forced excitation is 96 V/sec, and with forced excitation with additional operation on the independent winding, this speed equals 192 V/sec. The voltage on the independent winding appeared as given after 0.24 sec. Since the actual time of operation of the relay arrangement does not exceed 0.08 sec, this speed of growth of voltage of excitation in the second state is determined taking into account this time.

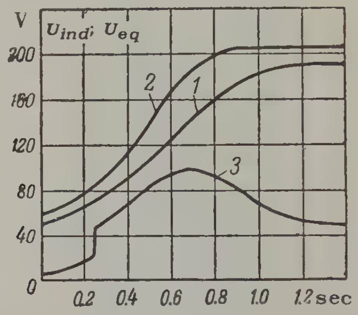

FIG. 4. Relationship between the voltage on the independent excitation winding of the exciter of the generator (U_{ind}) and on the resistance, equivalent to the resistance of the excitation winding of the generator (U_{eq}) and time with forced excitation.

(1) U_{eq} with the absence of additional forced excitation. (2) and (3) U_{eq} and U_{ind} with forced excitation with the additional effect on the independent winding

TABLE 3

State	Magnetizing current of inductors (A)	Voltage on independent excitation winding (V)	Equivalent load current (A)	Voltage on equivalent load (V)
Initial	4.5	6.7	1080	60.0
Forced excitation		100	3800	207

From the data given, it is seen that the additional action on the independent excitation winding, simultaneously with the increase in the rate of growth of the excitation, increases the maximum of excitation also.

The system of automatic regulation tested in a closed system worked as stably under no-load conditions as with the normal load on the turbogenerator without the use of the stabilizing transformer provided for the system of reserve excitation.

In the process of operation there takes place a transfer of reactive power from the turbogenerator on test to parallel working and back; the transfer proceeds evenly from almost full shedding of the reactive load of the turbogenerator on test to the limit of permissible load according to the conditions of operation.

For the testing of a system of series excitation with the appearance of free current in the rotor, a short circuit was suddenly applied to the output of the turbogenerator, with the generator voltage reduced to 2000 V. The change in generator stator current and voltage on the exciter are shown in Fig. 5.

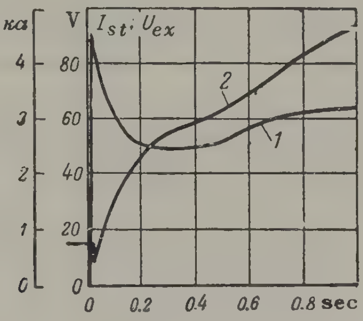

FIG. 5. A short-circuited generator
(1) Stator current (2) Exciter voltage

The speed of rise of voltage was determined graphically according to the stator voltage of the exciter and was found to be 128 V/sec which, in relation to the initial voltage (15 V) gives an 8.5 : 1 change in voltage in one second. If this parameter is calculated in relation to the generator voltage (6500 V) and the stator voltage of the exciter (100 V) running in normal conditions before the short circuit on the generator output a rate of change of voltage of almost 4 : 1 is found on the exciter.

Conclusions

A system of excitation built according to the parameters obtained above fully satisfies the given demands and guarantees the necessary statistical characteristics, in particular the range of regulation of voltage and reactive power of a generator with a low statism*. The process of regulation takes place stably. From tests of forced excitation on the equivalent resistance, the parameters of the system are found by the rapidity of voltage build-up. The effectiveness of the additional action is verified by the help of relay circuits on the excitation winding independent from its rectified voltage.

---

* Statism is the deviation of the controlled quantity at nominal load from its value at no load expressed as a percentage (of its value at no load).

Such an additional action is expedient, since it gives the possibility, in the event of forced excitation being necessary of obtaining stable forced excitation at the required level even after extinction of the free rotor current. Having obtained with this the additional saturation of the magnetic system of the exciter it leads in addition to the improvement of commutation of the rectifiers by means of the reduction of the reactiveness of the source of supply, and also guarantees a noticeable increase in the excitation maximum.

Experiments with suddenly applied three-phase short circuits with small initial excitation on a generator on no-load determined the rate of voltage build-up with the action of the free rotor current, stressing the expediency of series self-excitation for the exciter.

The experiments carried out give reason to conceive the development of the system as a project for large turbogenerators.

Translated by R.P. Froom

Appendix

Technical data of the arrangements.

1. Generator – Factory "Elektrosil", Type TVF-30-2; 30 MW, 3440 A; 6.3 kV; $\cos\phi = 0.8$; Nominal rotor current 1450 A; rotor resistance 0.0455 Ω.

2. Exciter – (for the turbogenerator), high-frequency generator. Type VGT-350-500 from the factory "Elektrosil"; 275 kVA; 110 V; 500 c/s; 1450 A; 3000 rev/min; Induction type, winding – delta connexion.

3. High-frequency pilot exciter – Type GSP-4.5, from the factory NIIEP; 118 A; 3.6 kW; 220 V; 3000 rev/min; 400 c/s; Permanent magnet excitation.

4. Automatic panel Type EPA-502 from the factory "Elektrosil"; with an assembled automatic regulator for the main and reserve excitation systems, with Selenium rectifiers type VS-59, rectifying the pilot exciter current, and with high-voltage Selenium rectifiers type TVS-100 for the feedbacks of the power inductors.

5. High power rectifier panel type PVS from the factory "Elektrosil" with high-voltage Selenium rectifiers type TVS-100 connected as a three phase bridge circuit with 150 parallel branches and 4 series branches in each arm; nominal rectified current 1500 A; nominal voltage 100 V; forced air draught cooling.

6. Power inductor panel type DS-1 from the factory "Elektrosil" 600 A; 500 c/s; power of the single-phase inductor.

THE EXCITATION OF SYNCHRONOUS MOTORS OF NORMAL CONSTRUCTION BY THE APPLICATION OF MECHANICAL RECTIFIERS*

N.S. SIUNOV, B.K. GAVRILOV and V.N. BREEV

Uralian 'Kirov' Polytechnic Institute

(Received 4 March 1958)

The problem of the replacement of the electromechanical exciter of synchronous machines by mechanical rectifiers is of great importance to low-and medium-power installations. Owing to the application of mechanical rectifiers [1] the construction is simplified and the cost of the plant is significantly decreased, (especially in the low-power range). The main cause of the inadequate introduction of mechanical rectifiers is the bad switching of current in these devices. Questions on the sparkless switching of the mechanical rectifiers of synchronous generators were most successfully resolved by Tamantsev [1]. In his proposed circuit a mechanical rectifier obtains its supply from an auxiliary winding situated in the recesses of the stator of the generator. The installation was provided with three single-phase current transformers, the secondary windings of which were shunted by small active resistors inserted into the circuit of the mechanical rectifier. Tamantsev's circuit enables us to obtain sparkless commutation of a mechanical rectifier and practically constant voltage for a synchronous generator with changes of load from zero to the nominal value.

As the experimental researches of Artanov showed [2], the circuit under consideration provides sparkless commutation in the motor only with an even load. Hence the pressing problem of the subsequent development of a circuit for synchronous motors with mechanical rectifiers, providing also satisfactory commutation of current with sudden loads. For this purpose one may employ a triple-wound transformer by means of which the supply is drawn via a mechanical rectifier to the circuit of the winding for starting the synchronous motor. Also, the synchronous motor is of normal construction as the manufacture of a supplementary winding on the stator is not required. As is known [3] triple-wound transformers in circuits for exciting synchronous generators were employed in one factory as far back as in 1947. The circuit for switching in the synchronous motor with a mechanical rectifier and triple-wound transformer is illustrated in Fig. 1.

---

* *Elektrichestvo* No. 8, 46-49, 1958.

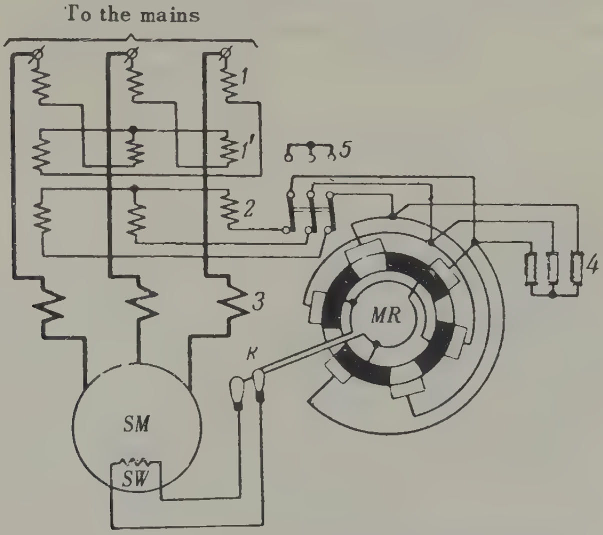

FIG. 1. Circuit of the switching of a synchronous motor with a mechanical rectifier and a triple-wound transformer

The three-phase regulating transformer has three windings. The primary winding *1-1′*, coupled "zigzag" is inserted in parallel with the stator winding of motor *SM*; winding *2* is supplied via the mechanical rectifier excitation winding *SW* of the motor. The series winding *3*, around which flows the full current of the stator, provides supplementary regulation of the current for exciting the synchronous motor with a change of its load. For changing the rate of the effect of current winding *3*, a transformer is provided with a movable magnetic shunt (Fig. 2).

On the same shaft with the motor is the mechanical rectifier *MR*, the width of an idle segment of which is equal to half of the width of a working segment. For improving the conditions of excitation, the brushes of the rectifier are shunted by the active resistors *4*. Change-over switch *5* locks the brushes during the starting period of the motor; after attaining hyper-synchronous speed, excitation is produced with the aid of a mechanical rectifier. As the load of the motor is increased, so the excitation current is automatically increased. The motor will work all the time with leading current and a practically hardly varying power factor.

As pointed out by Tamantsev, for flashless commutation during changes of working conditions from no load to full load, it is necessary to provide automatically for a constant position of the voltage vector on the rectifier brushes relative to the no load e.m.f. vector. In so far as the most essential factor for the practical application of the mechanical rectifier is the satisfactory commutation of current, so in the first instance, we shall consider the problem of rectifier operation in the circuit with the triple-wound regulating transformer.

The equivalent circuit of the commutator circuits is illustrated in Fig. 3

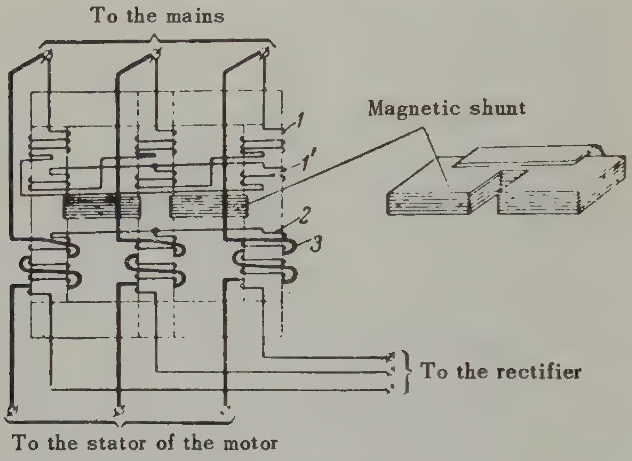

FIG. 2. Triple-wound transformer with a magnetic shunt

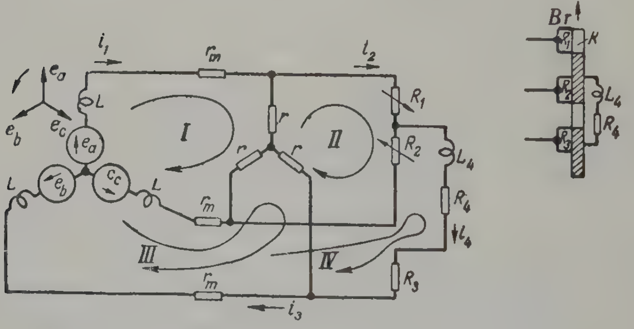

FIG. 3. Equivalent circuit of the commutator circuits

The direction of motion of the commutator in Fig. 3 is indicated by an arrow.

With the width of the brush equal to the width of an idle segment and equal to 60°, the period of commutation $T = 1/6f = 1/300$ sec. Since the picture of the commutation with motion of the commutator is periodically repeated, it is enough to consider the process for time equal to the period of commutation. The problem comes to the determination of the current in one of the brushes, as the current of a second brush is equal to the difference between the current of the winding for the excitation and the unknown value of the current. The value of the rectified current is assumed known and is practically constant. Taking into consideration that the resistance r_m of the secondary winding of the transformer is notably less than the resistance of the shunting brush, we may take it further that $r_m = 0$.

As a result of tracing circuits I and II we obtain the equation:

$$2L\frac{di_1}{at}+2ri_1-2ri_2-L\frac{di_3}{dt}-ri_3-ri_4=e_a-e_c; \qquad (1)$$

$$-2ri_1+(R_1+R_2+2r)\,i_2+ri_3-R_2i_4=0, \qquad (2)$$

where e_a and e_c are the resulting phase e.m.f. of the transformer; i_1, i_2, i_3 and i_4 is the current in the contours of the equivalent circuit; L is the equivalent inductance of a phase of the transformer device; r is the resistance shunting the brushes; R_1 and R_2 are the resistances of the brush contacts, dependent on time. Resolving equations (1) and (2) together, after simple conversion we obtain

$$\begin{aligned}&\frac{L}{r}(R_1+R_2+2r)\frac{di_2}{dt}+\\&+\left[\frac{L}{r}\frac{d}{dt}(R_1+R_2)+R_1+R_2\right]i_2-\\&-\left(\frac{L}{r}\frac{dR_2}{dt}+R_2\right)i_4=e_a-e_c.\end{aligned} \qquad (3)$$

We accept that resistances R_1 and R_2 depend only on the area of contact of the brushes with the working segments and, consequently, their dependence on time has the form:

$$R_1=\frac{T}{t}R;\quad R_2=\frac{T}{T-t}R,$$

where R is the resistance of a brush contact when a brush is completely situated on a working segment.

Having substituted in equation (3) the values R_1, R_2, dR_1/dt, dR_2/dt and having separated all the terms in the coefficient with derived current according to time, we obtain:

$$\frac{di_2}{dt}+\frac{RT^2[(2L+rT)\,t-rt^2-LT]}{Lt\,(T-t)\,[RT^2+2rt\,(T-t)]}\,i_2= \qquad (4)$$

$$=\frac{RT\,[r\,(T-t)+L]\,t}{L\,(T-t)\,[2rt\,(T-t)+RT^2]}+\frac{r\,(e_a-e_c)\,(T-t)\,t}{L\,[RT^2+2rt\,(T-t)]}.$$

Having produced integration and taking into consideration that $r \gg R$, we find the equation for determining the current i_2:

$$i_2=\frac{t\,(T-t)\left(\frac{t}{T-t}\right)^{-\frac{RT}{2L}}}{2rt\,(T-t)+T^2R}\left\{\int_0^t\left[\frac{RT\,[r\,(T-t)+L]}{L\,(T-t)^2}+\right.\right. \tag{5}$$

$$\left.\left.+\frac{r}{L}(e_a-e_c)\right]\left(\frac{t}{T-t}\right)^{\frac{RT}{2L}}dt\right\}.$$

For satisfactory working of the mechanical rectifier it is necessary to provide sufficient resistance for the brush contact, low equivalent inductance of the transformer device and a strictly fixed position of the brush cross-arm. One may join the first two conditions and in addition reduce to a formula in the following way. The transitory currents in the closed circuit, the operating segment – adjacent phase brushes – the external circuit, excited by the commutation processes will in practice damp during the period of commutation $T = 1/6f$, if the time constant of this circuit $T_{3.k}$ is 3 times less than the period of commutation, that is

$$T_{3.\kappa}\leqslant\frac{1}{3}T=\frac{1}{18f}. \tag{6}$$

The time constant T_y of the external part of the circuit from brush to brush in consequence of the practically clear active resistance of the brush contact may be considered greater than the time $T_{3.k}$, calculated in formula (6). Experiment shows that with a relatively large transitory fall of voltage in the brush contact of the order of 1.2 V and with effective line voltage on the brushes not exceeding 30-32 V the time constant T_y may be 3-4 times greater than $T_{3.k}$. In these conditions, with the correct setting of the brush cross-arm, the commutation of current flows satisfactorily.

In Fig. 4 are represented the calculated graphs of the change of current $i_2 = f(t)$ under the running brush for various values of the initial phase ψ with $e_a - e_c = 173 \sin(\omega t + \psi)$ V. The parameters of the circuit: $R = 0.1\ \Omega$, $r = 5\ \Omega$, and $L = 0.00833$ H, or brought to the voltage of the circuit and expressed in relative units, $R' = 1.15$, $r' = 57.5$ and $L' = 33.4$. From the graphs of Fig. 4 it is evident that flashless commutation of the current of a mechanical rectifier, connected according to the proposed circuit, is possible with the resulting e.m.f. of the first phase within the limits of from 15 to 30°.

The character of the change of the commutation current i_2 for a synchronous motor of 15 kW, 1500 rev/min, 220 V is represented on the oscillogram, (Fig. 5).

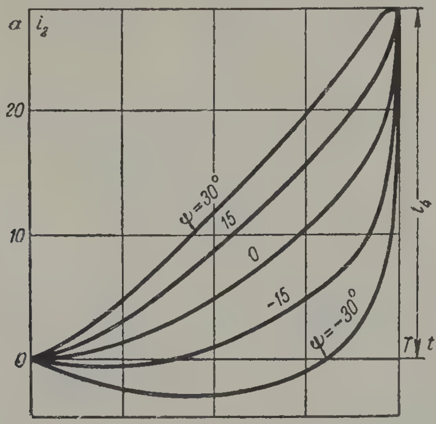

FIG. 4. Calculated graphs of the current under the running brush for various values of the initial phase ψ

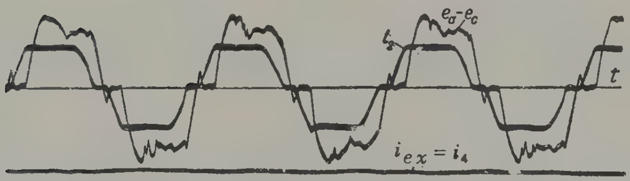

FIG. 5. Oscillogram of the change of commutation current

During experimental research on the synchronous motor with a mechanical rectifier its work was checked both with a smooth and with a sudden change of load.

With a smooth change of load in the range from idle running to nominal value the excitation current increased automatically, ensuring the operation of the motor with a given power factor. Numerous tests showed that during change of load of the motor in all ranges, commutation of current was satisfactory. As is clear from the oscillogram (Fig. 5), the rectified current i_4 is practically constant. The curve of current commutation has a trapezoidal form. At the beginning and end of the process the commutation of current does not exceed the arranged value, which testifies to the smooth running of the process. As the load of the motor increases simultaneously with the stator current, the excitation current winding is also increasing, (Fig. 6). The power factor of the motor with leading current in all ranges of load change remains constant in practice. The motor without sparking on the brushes of the rectifier works wholly satisfactorily up to 110 per cent of the rated load.

With sudden changes of load from zero to 70 per cent of the rated value the motor works soundly with practically sparkless commutation of current, (Fig. 7).

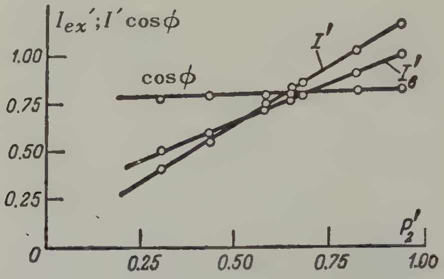

FIG. 6. The dependence of the stator current I', the current of excitation I'_B and cos ϕ on the load P_2 on the motor shaft, (all values in the relative units)

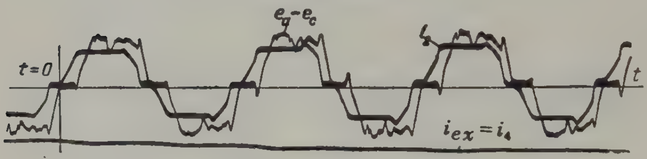

FIG. 7

The limits indicated above of the permitted change of the initial phase ψ of the resulting e.m.f. $(e_a - e_c)$ at the input to the commutator circuits testify to the possibility of a considerable displacement of the brush cross-arm, relative to its optimum position and to the possibility of a certain disharmony over the phase of the voltage system, applied to the brushes of the rectifier with an interior angle of the machine θ, which has considerable significance for reliable and steady work of the synchronous motor with a mechanical rectifier.

As investigations showed on a 15 kW motor which were carried out in the Electrical Machines Laboratory of the Uralian Polytechnic Institute, the displacement of a brush cross-arm by 8 - 10° does not result in a disturbance of the satisfactory commutation of current. Analogous results were also obtained from tests in industrial conditions of a synchronized 300 kW induction motor, the rotor circuit of which was supplied by current via a mechanical rectifier.

The possibility of a certain disharmony of work of a rectifier on the interior angle of the machine together with the possibility of the combination of the windings of a triple-wound transformer by a "zigzag" connexion, permits us to break the strict ratio of the parameters, adopted for generators in Tamantsev's system (1). With the operation of the machine by a motor this is still possible because there is no necessity to calculate the conditions of the machine for a wide range of changes of the power factor.

Conclusions

1. The excitation of synchronous motors of normal performance and of low and medium power may be accomplished with the aid of mechanical rectifiers attached to the output of a three-phase triple-wound transformer with a regulable magnetic shunt.

2. The proposed circuit provides an automatic increase of the excitation current with an increase of the load of the motor.

3. The commutation of the current of the mechanical rectifier is as satisfactory with slow as with sudden changes of load.

Translated by David Rex-Taylor

REFERENCES

1. S.G. Tamantsev; The synchronous generator with self-excitation from a mechanical rectifier. *Elektrichestvo* 3 (1952).
2. S.G. Artanov; *Issledovanie sinkhronnogo dvigatelya s mekhanicheskim vypryamitelyem (Investigation of the synchronous motor with a mechanical rectifier) Dissertatsia* NII MEP, (1954).
3. E.Yu. Movshin; The synchronous generator with excitation from selenium rectifiers in circuit with a triple-wound transformer. *Elektrichestvo* 7 (1947).

DIRECTIONAL PROTECTION FROM SHORT-CIRCUITS TO EARTH*

T.V. STEPNOV

(Received 5 July 1957)

In the design of protection gear for short-circuits to earth acting on transient process currents in a compensated network complications arise in the selection of settings on long out-going lines having a considerable natural capacitive current. As follows from a curve which has been previously published [1], when the earth-fault point is 7-12 km from the station bus-bars, the magnitude of the transient process current is reduced 3-5 times. This effect must be considered in the selection of the setting of protection gear.

The possibility of increasing the sensitivity of protection gear is limited by the presence of natural transient process currents in all faultless lines. In a network then, with a sustained capacitive current of 60-120 A, on outgoing lines with a natural capacitive current of more than 10 A the setting current can be less than the maximum possible natural transient process current which arises in the presence of a short-circuit to earth outside the given line, causing incorrect operation of protection gear. The maximum natural transient process current develops in faultless lines in the presence of short-circuits to earth at or near the station bus-bars. Strengthening of protection gear with the aim of increasing its selectivity leads to failures in cases of distant faults on the protected line.

Achieving the desired tuning out of natural currents and increasing protection sensitivity require a more detailed study of transient processes in unfaulted lines generally, and in "long distance lines" in particular. In this case, the term "long distance lines" is taken to mean lines with a sustained natural capacitive current of 10 per cent and more of the total capacitive current of the whole network, and with a distance of 7-12 km to the most distant points.

Information is presented below on working tests for an analysis of the operation of a previously described [1] directional protection gear in the light of the above-mentioned conditions. Current oscillographs were made in the network in the presence of artificial short-circuits to earth at various points. The latter, as a rule, were made across a spark gap. Each short-circuit lasted 0.7 - 1.2 sec. Here breakdown of the gap was repeated after 0.1 - 0.16 sec.

---

* *Electrichestvo,* No. 8, 75-79, 1958.

A simplified 3 - line circuit of the station and network with an indication of the earth-fault points is shown in Fig. 1. The parameters of its elements and the conditions in which the experiments were made are given in Table 1, and characteristic oscillographs are shown in Fig. 2.

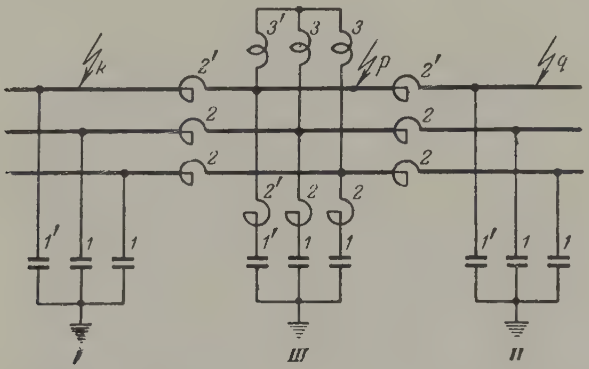

FIG. 1. Simplified circuit of station and network
I, II, III - outgoing lines
1 – capacitance of unfaulted phases of the line; *1′* – capacitance of earthed phase of the line; *2* – section and line reactors of unfaulted phases; *2′* – same for earthed phase; *3* – inductances of unfaulted phases of generating sources; *3′* – same for earthed phase.

Curve 7 is for the station where all the lines are equipped with reactors, and as a result, it corresponds in frequency and form with two other curves for long distance lines with approximately similar parameters.

In Fig. 3 a simplified equivalent circuit is given which is more suitable for analysis of the passage of currents in line II. In it the current directions in the earthed and unfaulted phases in the first half-cycle after the occurrence of a short-circuit to earth are shown under the action of which a resultant current develops in the secondary winding of the zero-sequence current transformer. Thus, this resultant current which is shown on the oscillographs is a superposition of the currents in the two unfaulted phases on the current in the faulty (earthed) phase.

The frequency and form of these currents are determined by the circuit which is formed in dependence on the location of the fault point. So when a short-circuit occurs at point *q* (Fig. 3), the following circuits are formed: for the earthed

TABLE 1

Line number in Fig. 1	Natural current of line, A	Length of cable, km, from bus-bars to		Cross-section of cable up to first reactor mm^3	Type of reactor		Power of generating sources, MW		Fault point in Fig. 1	Curve number in Fig. 2
		Most distant point	First reactor		Line	Section	Genera-tors	Trans-formers		
I	10.6	8.2	5.1	2×50	None	RB-1000-10	26	10	*q*	*3*
							10	25	*q*	*6*
							10	25	*k*	*5*
III	2	1.9	0.15	150	RB-600-6	same	26	10	*q*	*4*
II	14.6	5.6	1.8	2×120	None	same	26	10	*q*	*1*
							26	10	*k*	*2*
III	10.3	7.0	4.3	120	RB-600-6	2500a	108	40	*p*	*7*
I	6.6	6.4	2.7	70	None	None	0	27.5	*k*	*10*

phase $q-$earth$-o-$capacitance $1'-q$, the principal inductances (reactor and generating source windings) being absent in it; for the unfaulted phases $q-$earth$-o-$capacitance $1-$reactor $2-$generating source windings 3 and $3'-$reactor $2'-q$. All the principal inductances (the 2 reactors and the 2 windings of the different generating source phases) are connected in series in this circuit.

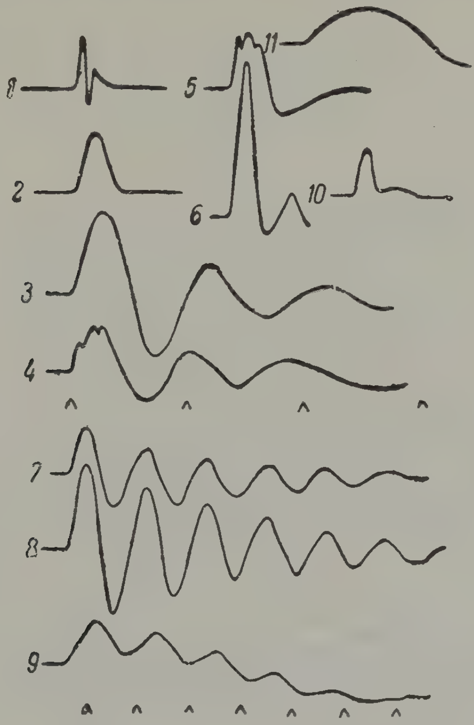

FIG. 2. Current and voltage oscillograms for various short-circuit to earth conditions

When a short-circuit occurs at point p, reactor $2'$ switches from the unfaulted phase circuit. In this case the inductances of the faulty and unfaulted phase circuits differ little in magnitude. When a short-circuit occurs at point k, an extra reactor is connected to the common branch for both circuits ($p-2'-$earth$-o$). The passage of currents in line I can be seen from Fig. 3 if the letters k and q are interchanged.

In considering the oscillograms, the sharp difference in the currents for the same line when a short-circuit occurs at different points is most noticeable (curves 1 and 2, 3, 5 and 6, Fig. 2). In curve 1 the frequency is considerably higher than in curve 2 since the earthed phased circuit current is predominant in the former where in this case the reactor is absent, whereas two reactors are connected in series to the unfaulted phase circuits. The current in the latter circuit (smaller both in frequency and in magnitude) is guessed according to the completion of the curve, (see dotted line on curve 1).

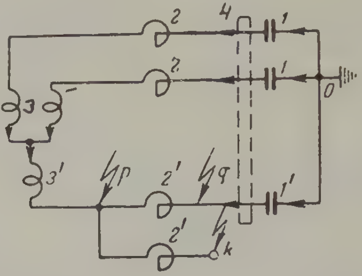

FIG. 3. Simplified equivalent circuit of test unfaulted line II, Fig. 1 *1* – capacitance of unfaulted phases; *2* and *3* – reactors and total inductance of generating sources of unfaulted phases; *1'*, *2'* and *3'* – same for faulty (earthed) phase; *4* – position of zero-sequence current transformers in the secondary winding of which the current oscillograms were taken

The current frequency is considerably lower in curve 2 since the earthed and unfaulted phase circuits include the same reactor; i.e., the inductances of both circuits differ little in magnitude and therefore the current frequencies differ little. Due to this, frequency divergence is not found in curve 2. The reactor connected to the common branch also affects the general reduction of frequency in this case.

Superposition of currents of dissimilar frequency is also clearly seen in curve 5. This occurs as the result of a considerable difference in the inductance of the earthed and unfaulted phases when a short-circuit occurs at point *k*, (line *I*, Fig. 1).

Frequency divergence of the earthed and unfaulted phase circuits is not found either in curve 3 or in curve 6, since when a short-circuit occurs at point *q*, the difference in the inductance of the earthed and unfaulted phases is not great.

However, curves 3 and 6, which are both for line *I* (Fig. 1), differ both in form and in current frequency when a short-circuit occurs at the same point *q*. As is seen from Table 1, this frequency divergence must occur due to the difference in the characteristics of the generating sources.

Curve 3 was taken during a predominance of generator (operating) power, whereas when curve 6 was taken there was a predominance of transformer power, other conditions being equal.

The same applies to curves 4 and 10.

As is seen from Table 1, the network line corresponding to curve 4 is considerably shorter and has a smaller capacitance. However, the frequency of its current is lower than in the line corresponding to curve 10. This is explained by the fact that curve 10 shows the natural current of the transient process in the unfaulted line supplied from a substation having no reactors and using only transformers as generating sources. Curve 4 is for an extremely short line; however, the presence of line and section reactors levels off the current form and lowers the frequency. This is an illustration of the considerable effect of reactor inductance on the frequency of the natural current of the line. The gradient of this curve (A/mm) is reduced approximately 10 times.

Simultaneously with the taking of oscillograms on "long distance lines", oscillograms were taken for the current at the earth-fault point and for the voltage at the secondary terminals of the voltage zero-sequence filter connected to the bus-bar section of line III, Fig. 1.

Curve 7, Fig. 2, is typical for the natural current of an unfaulted long distance line supplied from a station with reactor-equipped lines during a considerable predominance of power developed by operating generators (see Table 1), in the case of a short-circuit at the station bus-bars. Curves 8 and 9 were taken at the same time as curve 7 (curve 8 for the current at the earth-fault point, and curve 9 for the voltage at the terminals of the zero sequence voltage filter).

In the experiments, the first half-cycle of transient voltage exceeded the steady voltage by 1.5 - 1.7 times.

Curve 11 (Fig. 2) shows the current when a short-circuit occurs in the cable network at a distance of 12 km from the substation. It has a frequency of the order of 250 c/s, whereas when a short-circuit occurs at the substation bus-bars the current frequency at the fault point amounts to 1600 c/s.

Analysis of the oscillogram curves shows the most typical and all the remaining curves for a cable network of 6 kV with a capacitive current of 60 - 120 A permits the following conclusions:

1. When a short-circuit to earth occurs at or near the station bus-bars the frequency of the transient process current at the earth-fault point is determined by the frequency of the longest lines, (compare curves 7 and 8).

2. In a generator voltage network (for short-circuit conditions as in section 1) with lines fully equipped with reactors, the frequency of the transient process current at the earth-fault point and in the long distance lines lies within the narrow limits of 400 - 600 c/s.

3. In networks supplied from transformer substations (for short-circuit conditions as in section 1), without reactors, the frequency of the transient process

currents is higher and lies within the limits of 1000-1800 c/s.

4. When a short-circuit occurs at a distant point on the cable, the frequency of oscillations in all cases is lowered to 200-250 c/s, and the current as a rule is aperiodic.

5. From curves 7 and 8 it follows that the transient processes in long distance lines correspond in practice (excluding amplitude) with the transient processes at the earth-fault point. At the secondary terminals of the zero-sequence voltage filter a voltage is developed (curve 9) which corresponds to the transient process in a "long distance unfaulted line" with sufficient accuracy for all practical purposes.

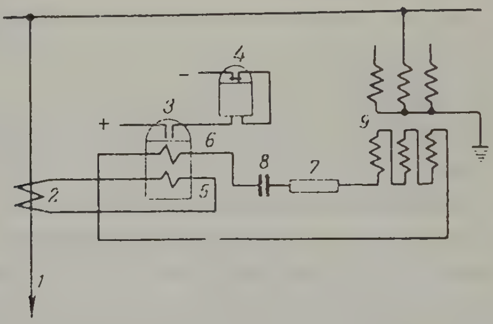

FIG. 4. Protection circuit
1 – protected line; *2* – zero-sequence current transformer; *3* – relay of type ET-521; *4* – signal relays; *5* – current (operating) winding; *6* – braking winding (additional); *7* – resistance; *8* – capacitance; *9* – zero-sequence voltage filter

The coincidence of these processes permitted the utilization of zero-sequence voltage for relay (type ET-521) braking in the presence of a short-circuit to earth outside the protected line. For this, relay *3*, Fig. 4, was provided with an additional braking winding *6* which was connected to the zero-sequence voltage filter *9* in such a manner that when a short-circuit to earth occurred outside the line, the additional winding created a demagnetizing effect and weakened the magnetic flux of operating winding *5*. It is necessary that the currents in both windings should be accurately displaced 180° in phase and coincide both in curve form and in magnitude. Therefore, capacitance *8*, which also locks a current with a frequency of 50 c/s, is connected to the circuit of winding *6*.

In addition to capacitance *8*, the current phase in the braking winding is also affected by the e.m.f. of the mutual inductance which is induced by the current of the operating winding *5*, so that during the braking process, i.e. when a short-circuit occurs outside the protected line, the e.m.f. of the mutual inductance and the self-inductance in the braking winding circuit are calculated, approximating the inductance of this circuit to zero. This occurs because the self-inductance factor of the braking winding circuit and the mutual inductance factor of the braking and operating windings are approximate in magnitude owing to appropriate parameter selection. Therefore, when a short-circuit occurs outside the protected line a capacitive current similar to the natural capacitive current in the protected line is developed in the braking winding circuit.

Due to the small difference in magnitude of the self-inductance and mutual inductance factors, the inductance of the braking winding circuit will also remain approximately zero and when short-circuit conditions vary causing a variation in the frequency and form of the natural current in the unfaulted line. The current in the braking winding in this case, remaining capacitive as before, will correspond in frequency and form to the altered natural current in the unfaulted line since the voltage at the terminals of the zero-sequence voltage filter also varies in accordance with the new conditions.

This is proven by the curves for the currents in the operating and braking windings and for the voltage supplied to the braking winding shown in Fig. 5 for the same relay in different short-circuit conditions outside the protected line and on two different lines.

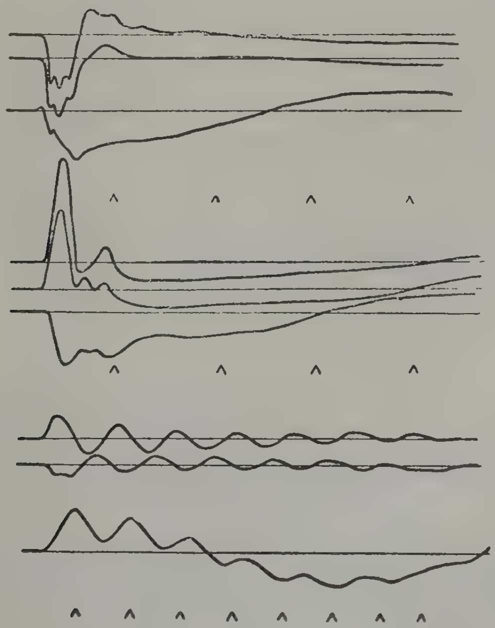

FIG. 5. Oscillograms of currents in braking and operating windings and of voltages at terminals of a zero-sequence voltage filter

In each of the three groups of curves in Fig. 5 the upper curve describes the current in the operating winding, the middle curve the current in the braking winding, and the lower curve the voltage at the terminals of the secondary winding of the zero-sequence voltage filter. The voltage filter on the primary side is connected to the bus-bar section of the test line.

The first two groups of curves are for line I which is connected to the station, a simplified diagram of which is given in Fig. 1: the upper group for the case of a short-circuit at point *k*, and the middle group for cases of a short-circuit at point *q*; the lower group is for line III, Fig. 1, for the case of a short-circuit at point *p*.

From what has been said it is seen that the relay in question can be applied on long distance lines of various networks without special changes in their parameters.

The relay should have the initial setting in order to compensate for a certain variance in magnitude of the currents in the braking and operating windings, (in different conditions). This setting, being determined by the condition of the longest line (according to Fig. 3, p.64 [1] without considering the natural current), is sufficient to compensate for the indicated variance of the processes.

When a considerable section of the line is tripped and when a short-circuit occurs outside the line, the braking current begins to predominate; however, incorrect operation is excluded by the presence of the same initial setting.

When a distant short-circuit occurs outside the line in question, the natural current in the given line is reduced; however, due to frequency reduction in this case, the braking current is also reduced.

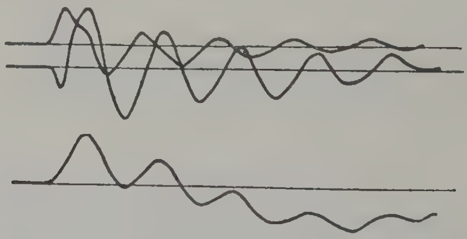

FIG. 6. Oscillograms of currents in relay when incorrectly connected

Curves are shown in Fig. 6 for the currents in the operating (upper curves) and the braking (mean curve) windings in the presence of an incorrect connexion of the leads of the operating winding, (the leads were crossed). This case reproduces a short-circuit at a distant point on the protected line. As is seen from the curves, the braking winding, increasing the sensitivity of the protection gear, came into operation.

The parameters of the relay circuit shown in Fig. 4 were selected for the most part by experiment.

Each coil of relay ET-520/0.2 consists of two windings of 250 turns connected by a PE-0.35 conductor. The lower winding of one coil is connected in series to the upper winding of the second coil, and vice versa. Thus, entirely separate windings (of 500 turns each) are obtained for a relay of 0.2 A.

With such a winding connexion the relay does not operate in the presence of counter-currents of 2.5 A in the braking and operating windings. The capacitor capacitance in the zero-sequence filter circuit amounts to 2 uF at 180 V and 3.3 uF at 100 V. The resistance in both cases amounts to 50 Ω.

At present, four such directional relays have been installed in the network. Here, there have only been two cases of incorrect operation but 12 cases of correct action.

The cases of incorrect operation were caused by two- and three-phase short-circuits to earth near the station bus-bars. They did not cause complications for the staff on duty since the fault was tripped with maximum protection. However, it must be remembered that in these cases incorrect operation of protection from short-circuits to earth is always possible; so, during a three-phase short-circuit to earth the protection gear operated incorrectly on 6 connexions which previously had not done so. Incorrect operation is eliminated in the presence of multi-phase short-circuits at distant points.

In the presence of a short-circuit to earth on 3 phases, due to their asychronization in phase, three transient process current pulses develop one after the other in the unfaulted lines causing incorrect operation of the protection gear.

In conclusion it must be noted that the operation of a network of 6 kV with almost total compensation of capacitive current (a simple metering device which has been developed has been installed in the stations allowing compensation control as required without any disturbances), over a number of years has shown positive results.

Such a type of fault as intermittent short-circuiting to earth has disappeared in practice since the current at the earth-fault point (including considerable higher harmonics), does not exceed 7-8 A.

Two forms of short-circuit to earth have remained: stable and transitory self-eliminating short-circuits, the latter in 1956 accounting for 75 per cent of the total number of short-circuits to earth. The number of short-circuits in cables has been halved.

The application of protection gear acting on transient process currents with the utilization of the given directional protection gear in networks of 6-10 kV is expedient, and also because, due to its quick action, directions are fixed automatically in the presence of transitory self-eliminating short-circuits to earth. The latter frequently precede stable short-circuits to earth.

Translated by F.J. Griffiths

REFERENCES

1. V.E. Darchenko and T.V. Stepnov; Zashita ot zamykanii na zemlyu v kompensirovannykh setiakh. (Protection from Short-Circuits to Earth in Compensated Networks). *Elektrichestvo,* No. 2, 1958
2. F.A. Likhachev; *Vybor, ustanovka i eksplutatsiia dugogasiashchikh apparatov. (The Selection, Setting and Operation of Arc-quenching Apparatus),* Gosenergoizdat, 1955.

ABSTRACTS OF PAPERS PUBLISHED IN ELEKTRICHESTVO NO. 8, 1958

High-molecular compounds in power engineering: K.A. Andrianov. (pp 1-4)

Many of the most important characteristics of electrical engineering equipment, for example, weight, dimensions and reliability in service, are determined mainly by the quality of materials, especially insulating material. The author argues at length for the advantages of high-molecular compounds, artificial fibres and plastics over non-thermostable electrical insulation and envisages an increase in the use of synthetic high-molecular compounds like phenolformaldehyde resins, silicone organic polymers and polyester resins in conjunction with fibre glass, asbestos and mica. The basic criterion for choosing from the great variety of polymers is thermal stability. He gives examples of the fields of application of high molecular compounds and tabulates the elasticity of polymers and the losses in weight (as a percentage) of polymers after 24 hr at different temperatures °C.

Plastic masses in power engineering: V.V. Baranovskii and Ia. L. Shugal. (pp 12-16)

The author considers the increasing use of plastics in electrical engineering. He tabulates certain electrical properties of plastic insulation; laminated plastics (genitex, tekstolite and glass textolite and organic and silicone-organic bonding); mounding plastics, (organic fillers and non-organic fillers with organic and silicone organic bondings) finally cast plastics. Photographs are shown of moulded components of the phenolformaldehyde type, arc-resistant moulded contactor chambers, and dry mining explosion proof transformer and its winding made of heat-resistant plastics, a mobile telescopic platform for repairing high-voltage lines without disconnecting them and miscellaneous insulating components of laminated plastics.

The author then reviews plans for developing these materials. Plastic masses to sustain over 200-220°C are envisaged. For obtaining glass textolites (suitable for service in tropical conditions), investigations are to be made into special types of glass cloth and special compositions of stekol. Cast plastics are to be investigated. Methods of radiation of hard rays and ultra-sound and the use of thermo-reactive bonds are to be investigated. The article closes with remarks on the organization of research, (mentioning the possibility of test stations in India or Viet Nam).

The electrical properties of artificial and synthetic fibres: P.A. Polonik. (pp 17-21)

This article examines (1), specific resistance as a property directly connected with the dispersion of the station electrical charges arising on the fibre and (2), electric susceptibility as the tendency for the fibre to generate and accumulate charges in defined conditions. The author concentrates on the effect of humidity on the specific resistance and electric susceptibility of fibre. He considers the method of measuring specific resistance and tabulates the results. He then proceeds with the method of investigating electric susceptibility. He concludes that all artificial synthetic fibres can be electrified, the charge depending on the relative humidity of the air and the speed of the movement of the fibre. There is no connexion between the specific resistance and the electric susceptibility of a fibre, but specific resistance and the rate of dispersion of the charges are completely interrelated. Only viscous and acetate fibre can be worked without considerable interference from static electricity when $\phi = 65\%$. To work′ synthetic fibres it is necessary to hold them 20-30 hr in conditions of $\phi = 75\%$ and more or to apply ionization of the air to neutralize the charges.

Synthetic polymers and micaceous insulation: L.A. Epshtein and A.I. Petrashko. (pp 21-27)

Synthetic polymers (alkide) resins, in particular, glypthal, are now being successfully used in the production of micanites. A new stage has been marked in the development of mica bonds by oil and bitumen-oil varnishes used in stator winding insulation of high-voltage machines and the slot insulation of low-voltage machines of humidity resistance design. But to reduce the consumption of vegetable oil required for food purposes the VEI developed new synthetic organic and silicone organic polymers of the TGF and TGF-8 types. The Stalin electromechanical works in Kharkov has developed epoxy resins. Also, silicone organic resins and varnishes with glass-mica materials have been developed to operate at 250-300°C for limited periods. The author then considers the properties of glass-mica-tape, flexible heat resistant micanite, flexible heat-resistant glass micanite, heat-resistant moulding mica, heat-resistant glass-micafolium, micanite, flexible heat resistant glass S-mica, moulding S-mica, glass S-mica tape.

The use of mica, glass-mica and S-mica materials in silicone organic varnishes increases heat resistance and prolongs the life of the equipment.

Varnish polymers in electrical insulation: K.I. Zabyrina and M.B. Fromberg. (pp 28-37)

Special interest is centred on replacing vegetable oils by new synthetic materials based on different polyesters, epoxy resins, melamineformaldehyde resins polyurethanes, polyamines, polyvinylacetal and other synthetic film-forming substances. These substances are then discussed in turn with tables of the electrical properties of certain varnishes and their compositions

Certain questions of the theory of the autodyne electrical machine: O.B. Benedikt. (pp 43 - 46)

It is desirable to create electrical machines combining the advantages of single armature converters (low weight, high efficiency and cos ϕ) with the good regulating features of motor-generators for direct current. To explain the method of operation of an autodyne the author considers the operation of a single armature converter without stator windings and the m.m.f. caused thereby. The theory expounded has been experimentally verified on specimens and models in the MIIT and NII ME P and the results of the investigations coincide with the results of the calculations. He presents an oscillogram showing that on a sudden increase in load current from 56 to 152 A the voltage remained practically constant. The effect of internal torques, assumed absent in the theory, is offset by the use of an amplifier or by a system of additional windings as illustrated.

Development of polyphase transformers and generator-transformers: R.S. Klimov. (pp 50 - 54)

For d.c. high-voltage transmission the publication of the rectified voltage (e.g., to values corresponding to a 24 phase scheme) can be reduced and the form of the current improved in generators by supplying several of a number of converters connected in series via phase-shifting transformers. The author describes three types of multi-phase transformer. Firstly, the method of a multi-phase transformer with a closed or other winding and the supply of the individual three phase (or single phase) transformers via phase-shifting transformers, the output of which amounts to 5 - 10% of the main transformers. Secondly, for a 48 phase transformer it is necessary to have three single phase transformers with a tertiary winding connected in star on each core (as illustrated) assuming the equality of the primary and secondary m.m.f. on every core. Thirdly, the author uses normal single - or three - phase transformers supplied direct from the stator coils of hydro - or turbogenerators the e.m.f. of which are shifted in relation to one another. The secondary windings are connected in the closed multi-phase winding. This principle underlying the third method has been extended to turbogenerators in the U.S.A. The author considers it expedient to divide the winding of each phase of a generator into two or more parts.

Currents and torques of asynchronous and synchronous machines when changing speed: L.G. Mamikoniants. (pp 54 - 63)

It is important to determine the conditions in which static characteristics can be used instead of dynamic and the method of deriving dynamic characteristics not only for induction motors but also for synchronous motors, especially in connexion with self-synchronization, re-synchronization and modelling. The author introduces formulae of currents and torques common to synchronous and asynchronous machines for an arbitrary known law of rotor movement. It is shown that in the presence of uniform acceleration the integrals entering the formulae can be found with the aid of known tables of special functions. The author concludes that it is necessary to take into account the effect of speed changes on currents or torques as a function of slip to analyse the processes (synchronization, swings), when the slip is relatively small or changes sign. For large machines the calculation of speed changes is as a rule necessary for lesser acceleration than for very small machines. These conclusions are qualitatively true for any laws of rotor motion.

Determination of the discharge voltage along column and garland insulators: A.M. Zalesskii. (pp 64 - 68)

The use of protective rings as armatures equalizing the voltage are very valuable for protecting insulators from corona and, in some cases, for increasing the discharge voltage of insulators. The use of protective armatures on the Kuibyshev G.E.S. to Moscow transmission line reduces the length of the garlands by 20%. The author proposes a method of calculating the effect of protective rings on the distribution of voltage in columns and garlands of insulators and determining the dimensions and distribution of the protective rings. The curve of the puncture voltage between the bar and the surface is used to determine the discharge voltage in the case of garlands of insulators of the "plate" type. In the case of columns of insulators of the rod or bar type, however, the discharge voltage is calculated from the voltage applied to the upper insulator and the puncture voltage between the ring and the flange of the upper insulator.

Control of frequency and output with the additional action of the first product of deviation: S.V. Usov, G.M. Pavlov and P.L. Shirshov. (pp 69 - 74)

The problem of maintaining frequency in the power system even by one station has yet to be settled for hydro-electric stations. The author introduces formulae to determine the structural scheme of the regulator which should have elements to reveal and measure the deviation of the frequency from 50 c/s, and the deviation of output from the desired value, an "executive" element for increasing the sensitivity of the regulator between the executive and metering elements and an intermediate amplifier for each group. Such a frequency regulator has been developed by the Leningrad Polytechnic Institute and produced and installed by the Leningrad Power Supply (Lepe ́nergo). The scheme and construction of the regulator is shown in Fig. 1. The author then investigates frequency and power regulation and concludes that the qualitative regulation can only be obtained by agreeing the parameters of secondary and tertiary regulators on condition that they operate jointly. Additional action of the first product effectively stabilizes the regulation process and in conjunction with a reduction in the constant T_u (time constant of the isodrome) can speed up the regulation process and maintain stability. An increased speed of regulation up to 40 - 50 MW/min obtained when testing two hydro-electric groups was the limit. He considers that with a correct choice of T_u and the amplification factor using the first derivative, loading speed can be raised to 80 - 100 MW/min as required in large power systems.

The Umov electromagnetic vector in the field of a transmission line: L.B. Slepian. (pp 79 - 81)

The Umov electromagnetic vector is a special value of the Umov vector which gives the density of any form of power flux and is determined by the relationship

$$U = vE_{\omega}$$

where U – the Umov vector;
V – the rate of power transfer;
E_{ω} – the volumetrical density of the power transferred.

The author considers how to establish the values of the rate of transfer of electromagnetic energy and the density of the transferred electromagnetic energy at all points of an electromagnetic field and whether the magnitudes derived equal the Poynting vector, (for the field around a power transmission line). He calculates that such an equality does exist although the Soviet editor points out that the article is controversial and in particular the author's assertion that the rate of power transfer along a line is in all cases equal to the speed of propagation of the free electromagnetic wave has yet to be substantiated.

The operation of carrier ducts of differential phase protection on long distance transmission lines: Mas Shi-Khe, Se Bo-En, Van Chzhu-Chun, Li Tsin-Cen and V.G. Kagan. (pp 82 - 85)

The Chinese People's Republic met with difficulties in installing PVZ - K carrier differential-phase protective gear on 220 kV lines 250 - 260 km in length. The simplest solution was the use of a double frequency variant of the duct and the scheme of double frequency receiver-sender was evolved, as illustrated in the text. The use of two frequencies is not always practicable however, and differential-phase protection is impossible on lines with branches.

SURFACE EFFECT IN SOLID FERROMAGNETIC BODIES TAKING NON-LINEARITY INTO ACCOUNT*

M.A. PANASENKOV

(Received 25 April 1958)

A great deal of attention is paid to the surface effect in ferromagnetic bodies. A considerable number of national and foreign works deal with this question. Soviet studies have made a large contribution to this field of science.

In 1913 Arkad′ev first introduced the concept of complex magnetic permeability. This was very useful for many investigations and calculations taking hysteresis loss into account, [1]. Fine steel plates and wires were the main object of Arkad′ev's investigations. A considerable part of the investigations made by him assumed constant complex magnetic permeability of the medium.

Neiman investigated electromagnetic processes in ferromagnetic bodies taking into account a variable magnetic permeability and hysteresis loss. On the basis of these investigations he proposed simple methods of calculating the electrical resistance of ferromagnetic material and the magnetic resistance of magnetic circuits. Larger solid bodies were the object of his investigations, [2].

The author of the present article selected relatively solid bodies as the object of his investigations, for example, ferromagnetic armatures of electrical machines (electromagnetic braking and induction motors), calendar shafts, cylinders of large dimensions and other units.

The presence of the air-gap, edge effect, unsatisfactory measurement of the temperature of the rotating armatures and a number of other factors interfere with the investigation of the basic characteristics in solid armatures of electrical machines. A solid steel ring was therefore investigated which excluded a number of the factors that could be subsequently taken into account more simply and with greater accuracy in individual cases. Fig. 1 shows an element of a solid steel ring of rectangular cross-section. The relationships of the dimensions of the ring are such that for solving the problem, use can be made of the equations of the electromagnetic field for a flat wave in rectangular co-ordinates:

---

* *Elektrichestvo* No. 9, 1-7, 1958.

$$-\frac{d\dot{H}}{dz}=\dot{\delta}=\gamma\dot{E}, \tag{1}$$

$$\frac{d\dot{E}}{dz}=-j\omega\dot{\mu}\dot{H}, \tag{2}$$

where H and E are the effective values of the voltages of the magnetic and electrical fields;
δ is the effective value of current density;
γ and $\dot{\mu}$ are the specific electrical conductance and the complex magnetic permeability of the steel of the specimen under investigation;
ω is the angle frequency of the eddy currents;
z is a co-ordinate.

The introduction into the equations of the electromagnetic field of complex magnetic permeability $\dot{\mu}$, as is known, is linked with the substitution of the effective non-sinusoidal periodic functions of the induction B and strength H of the magnetic field by equivalent sinusoids. As a rule, non-linearity I of the $b(h)$ kind is taken into account for complex magnetic permeability. That is, the non-linearity of the instantaneous values of induction b from the instantaneous values of the strength of the magnetic field h. This non-linearity, caused by hysteresis, leads to distortion (skewing) of the shape of the curves and itself determines the hysteresis losses. However, the main ferromagnetic characteristic is non-linearity II of the $B(H)$ type, (non-linearity expressing the basic magnetization curve). The latter non-linearity, caused by a different degree of saturation, generally leads to a non-sinusoidal state of the curves $B(t)$ and $H(t)$. Here, in weak and medium fields up to a maximum of magnetic permeability μ, the curve $B(t)$ has a pointed shape and a large amplitude factor, whereas the curve $H(t)$ is flattened and has a smaller amplitude factor. In powerful fields after the maximum of μ, the reverse phenomenon takes place. Besides taking into account non-linearity I it is also necessary to take non-linearity II into account. Here, the additional losses will also be taken into account which characterize this non-linearity and, apparently, the magnetic viscosity, in so far as the latter is caused by non-linearity II.

The total argument ψ of this complex permeability is a function of frequency. It can be represented in the form of two components:

$$\psi=\psi_{\mathrm{I}}+2\psi_{\mathrm{II}}, \tag{3}$$

where ψ_{I} is the argument caused by non-linearity I and taking hysteresis losses into account;

ψ_{11} is the argument caused by non-linearity II and taking the additional losses into account which characterize this non-linearity.

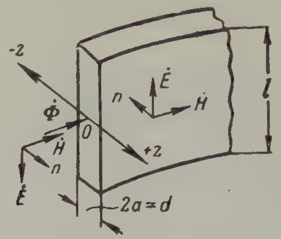

FIG. 1. Penetration of an electromagnetic wave into a steel ring
l, width of ring; $d = 2a$, thickness of ring. Z, co-ordinate; Φ, magnetic flux; E and H, strengths of the electrical and magnetic fields; n, vector of the direction of the electromagnetic wave

The argument ψ_1, equal to the hysteresis loss angle determined by static or quasi-static hysteresis loops, is only a function of the magnetic properties of the material. Argument ψ_{11} is a function of the process; that is, it is a function of all the parameters characterizing the electromagnetic process: $\psi_{\text{II}}(\omega, d, \mu, \gamma, \beta)$, where d is the thickness of the ring and β the angle between the induction and strength of the magnetic field, Argument ψ_{II} exists independently of the argument ψ_1. For example, in ferromagnetic bodies without hysteresis $\psi_1 = 0$, but argument $\psi_{\text{II}} \neq 0$, in so far as the basic non-linearity $B(H)$ is real. To determine argument ψ_{II}, it is necessary to solve the problem on the assumption that there is no hysteresis. It is, therefore, necessary to know the angle β.

Determination of the angle β

Fig. 2 shows the most characteristic (with two recurvatures) sections of the main d.c. magnetization curve. The curve $\mu(H)$ is also given there and the volume density of magnetic energy BH is plotted as a function of H. It is characteristic that from a certain value, the dependence of BH on H is practically a straight line and in a number of cases, this simplifies the calculations [3].

Assume a process where with a change of frequency within wide limits, the effective primary current of the ring I_1 is fixed. Here, the corresponding field strength H_1 will also be fixed. If the surface effect manifests itself sharply then H_1 will be the strength on the surface of the ring, but when $\omega \to 0$, H_1 will coincide with the average value according to the cross-section of the ring. Take a certain arbitrary point (4) of the $B(H)$ curve, Fig. 2. Here H_1 has a corresponding value of magnetic induction B_1 and an appropriate value of the volume density of magnetic energy B_1H_2, being a rectangle with the sides B_1 and H_2 in a system of co-ordinates (B, H). In the case of the quasi-static (i.e. slowly changing field), when the d.c. and a.c. magnetization curves coincide, the specific energy B_1H_1 is simultaneously both the effective and the average value according to the cross-section of the ring. Similarly, the corresponding value of the energy B_mH_m will be the amplitude and maximum value simultaneously. The connexion between these magnitudes is determined by the relationship;

$$B_1H_1=\frac{B_mH_m}{2}, \tag{4}$$

true both for the linear and non-linear dependence $B(H)$. If the dependence $B(H)$ should vary along the straight line 0-4, then the magnetic permeability would be substantially constant and equal to $\mu_1 = B_1/H_1$ for any values of H at any point of the ring cross-section. Here B and H would vary according to the sinusoidal law with the amplitudes $\sqrt{2B_1}$ and $\sqrt{2H_1}$, whereas the value of $\sqrt{2B_1}$ would lie along the straight line 0-4. At the point of intersection of the straight line 0-4 with the actual curve $B(H)$, the values B_1 and H_1 correspond to the effective values of the equivalent sinusoids for the actual curve, whereas $\sqrt{2B_1}$ and $\sqrt{2H_1}$ correspond to the amplitudes of these equivalent sinusoids. The amplitudes of the equivalent sinusoids are not as a rule severally equal to the actual amplitudes of B_m and H_m, but their products (i.e. the amplitude values of the energy), should be equal to one another, in so far as one and the same effective value of the volume density of magnetic energy corresponds to them: $B_mH_m = \sqrt{2B_1} \times \sqrt{2H_1} = 2B_1\,H_1$.

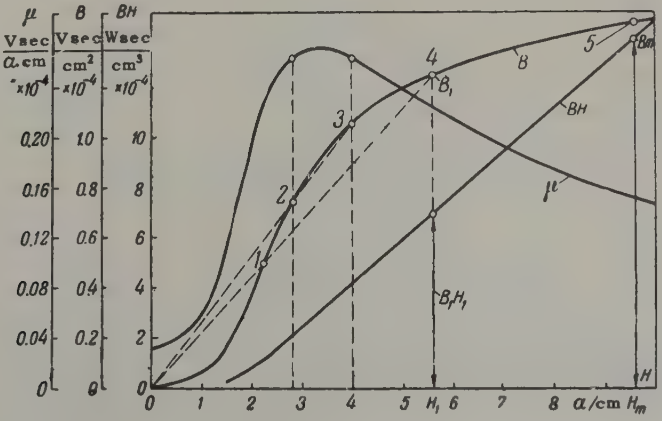

FIG. 2. Magnetic permeability μ, volume density of energy BH and induction B in relation to strength H, (direct current)

The method of determining the actual amplitudes B_m *and* H_m is derived from this. Given the value of H_1, we find the corresponding induction B_1 from the curve $B(H)$, and from the dependence $BH(H)$, the corresponding value of energy B_1H_1 and its doubled value B_mH_m, (Fig. 2). Induction B_m and strength H_m corresponds to this value of energy from curve BH at point (5).

Represent the amplitudes H_m and B_m in vector form, (Fig. 3). Their projections to the horizontal axis will correspond to their actual values. These vectors in relation to the horizontal axis, are then displaced through different angles ψ_H and ψ_B, the difference of which gives the angle β which characterizes the shift between H_m and B_m. The angles are analytically determined from the following relationships:

$$\cos\psi_H = \frac{H_1}{H_m} = \frac{1}{k_H}, \tag{5}$$

$$\cos\psi_B = \frac{B_1}{B_m} = \frac{1}{k_B}, \tag{6}$$

$$\beta = \psi_H - \psi_B, \tag{7}$$

where k_H and k_B are the amplitude factors.

After denoting the orthogonal components from B_m to the direction H_m by $B_s = B_m \sin\beta$ and $B_c = B_m \cos\beta$, but the orthogonal components from H_m to direction B_m by $H_s = H_m \sin\beta$ and $H_c = H_m \cos\beta$, respectively, we shall have:

$$\tan\beta = \frac{B_s}{B_c} = \frac{H_s}{H_c}, \tag{8}$$

whence we have a relationship similar to the expression for magnetic losses:

$$B_cH_c \tan\beta = B_1H_1 \sin 2\beta = B_1H_1 \cos\theta. \tag{9}$$

Here,

$$\theta = \frac{\pi}{2} - 2\beta.$$

The right-hand side of (9) is the actual part of the complex $H_1^2\mu$, where

$$\mu = \mu_1 e^{-j\theta} \tag{10}$$

is the complex magnetic permeability which must be introduced into (2) in order to find the solution for the argument ψ_n. However, the equation to determine ψ_n

can be obtained from the general solution by substituting θ into the corresponding equation of the argument ψ.

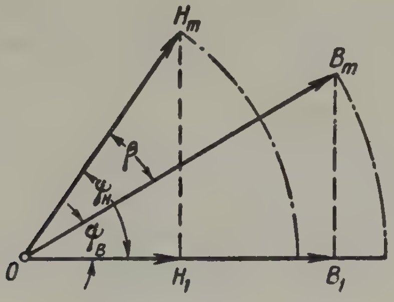

FIG. 3

Steel ring as a single-phase transformer with a short-circuited secondary turn

The solution of equations (1) and (2) in the presence of complex magnetic permeability $\mu = \mu_1 e^{-j\psi}$, taking into account the non-linearity of the magnetic characteristic of the material, gives:

$$\dot{H} = \dot{c}_1 e^{\dot{k} z_a} + \dot{c}_2 e^{-\dot{k} z_a} \qquad (11)$$

and

$$\dot{\delta} = -\frac{\dot{k}}{a} (\dot{c}_1 e^{\dot{k} z_a} - \dot{c}_2 e^{-\dot{k} z_a}), \qquad (12)$$

where

$$\dot{k} = a\sqrt{j\omega\dot{\mu}\gamma} = k_1 + jk_2, \qquad (13)$$

$$k_1 = k\cos\left(\frac{\pi}{4} - \frac{\psi}{2}\right), \qquad (14)$$

$$k_2 = k\sin\left(\frac{\pi}{4} - \frac{\psi}{2}\right), \qquad (15)$$

$$k = a\sqrt{\omega\mu_1\gamma}, \qquad (16)$$

$Z_a = Z/a$; $a = d/2$ is half the thickness of the ring.

Where $Z_a = 0$ the current density in the middle of the ring cross-section is zero and the constant integrations c_1 and c_2, as follows from (12), are equal one to another. Here, we have from (11):

$$\dot{H} = 2\dot{c} \cosh kz_a. \tag{17}$$

When $Z_a = 1$, we obtain the strength of the magnetic field on the surface of the ring:

$$\dot{H}_1 = 2\dot{c} \cosh \dot{k}. \tag{18}$$

Having excluded the constant $\dot{c}$ from (17) and (18), we shall have:

$$\dot{H} = H_1 \frac{\cosh \dot{k} z_a}{\cosh \dot{k}}, \tag{19}$$

$$\dot{\delta} = -\frac{\dot{H}_1 \dot{k}}{a} \frac{\sinh \dot{k} z_a}{\cosh \dot{k}}, \tag{20}$$

$$\dot{E} = -\frac{\dot{H}_1 \dot{k}}{\gamma a} \frac{\sinh \dot{k} z_a}{\cosh \dot{k}}. \tag{21}$$

Integrating (20) according to the square $radz_a$, where r is the length of the average magnetic path, we shall find the total current, equivalent to the eddy currents in the ring:

$$\dot{I}_e = ra \int_0^1 \dot{\delta} dz_a = -r\dot{H}_1 \frac{\cosh \dot{k} - 1}{\cosh \dot{k}} = r\dot{H}_0 - r\dot{H}_1, \tag{22}$$

Where $\dot{H}_0$ is the strength of the magnetic field in the middle of the ring cross-section, being obtained from (19) where $Z_a = 0$.

The values of the magnetizing forces are determined by the respective relationships:

$$\tau\dot{H}_1 = \dot{I}_1 w_1, \tag{23}$$

$$\tau\dot{H}_0 = \dot{I}_0 w_1, \tag{24}$$

the substitution of which into (22) gives

$$\dot{I}_1 w_1 + \dot{I}_e w_2 = \dot{I}_0 w_1, \tag{25}$$

whereas we have the value of the primary current

$$\dot{I}_1 = \dot{I}_0 - \dot{I}'_e = \dot{I}_0 + \dot{I}_{1e}. \tag{26}$$

Here $\dot{I}'_e = \dot{I}_e w_2 w_1$, is the eddy current applied to the turns of the primary winding of the ring w_1.

The number of the turns of the secondary winding $w_2 = 1$.

Analogously to the transformer, the primary current of the ring $\dot{I}_1$ has two components. One of them $\dot{I}_0$ goes to create the magnetic flux and the other $\dot{I}_{1e}$ compensates the demagnetizing action of the eddy current (the load current), $\dot{I}_e'$. The equivalent network and vector diagram will have the same form as in the case of the transformer on load.

Determination of resistance. Having taken the integral from strength $\dot{E}_1$ on the surface of the ring from the contour l_E which embraces the cross-section of the ring, we find the secondary e.m.f. $\dot{E}_2 = \dot{E}_1 l_E$. After multiplying it by the number of turns of the primary winding we obtain the applied e.m.f.

$$\dot{E}_1 = \dot{E}_2' = -w_1 l_E \frac{\dot{H}_1 \dot{k}}{\gamma a} \tanh \dot{k}. \tag{27}$$

The components of the primary current are:

$$\dot{I}_{1e} = (-I_e') = \frac{r\dot{H}_1}{w_1} \frac{\cosh \dot{k} - 1}{\cosh \dot{k}}; \tag{28}$$

$$\dot{I}_0 = \frac{r\dot{H}_1}{w_1} \frac{1}{\cosh \dot{k}}. \tag{29}$$

The resistances applied to the eddy current are:

$$Z_e' = \frac{-\dot{E}_1'}{\dot{I}_{1e}} = r_c' \frac{\dot{k} \sinh \dot{k}}{\cosh \dot{k} - 1} = r_e' + jx_e';$$

$$r_c' = \frac{l_E w_1^2}{\gamma r a} \tag{30}$$

$$r_e' = r_c' \frac{k_1 \sinh k_1 + k_2 \sin k_2}{\cosh k_1 - \cos k_2} \tag{31}$$

$$x_e' = r_c' \frac{k_2 \sinh k_1 - k_1 \sin k_2}{\cosh k_1 - \cos k_2}. \tag{32}$$

The resistances applied to the magnetization current are:

$$Z_0' = \frac{-\dot{E}_1}{\dot{I}_0} = r_c' \dot{k} \sinh \dot{k} = r_0' + jx_0'; \tag{33}$$

$$r_0' = r_c' (k_1 \tanh k_1 - k_2 \tan k_2) \cosh k_1 \cos k_2; \tag{34}$$

$$x_0' = r_c' (k_2 \tanh k_1 + k_1 \tan k_2) \cosh k_1 \cdot \cos k_2. \tag{35}$$

The equivalent resistance is:

$$Z_e = \frac{U_1}{I_1} = Z_1 + \frac{Z_0' Z_e'}{Z_0' + Z_e'} = Z_1 + Z'; \tag{36}$$

$$Z' = \frac{-E_1}{I_1} = r_c' \, k \tanh k = r' + jx'; \tag{37}$$

$$r' = r_c' \frac{k_1 \sinh 2k_1 - k_2 \sin 2k_2}{\cosh 2k_1 + \cos 2k_2}; \tag{38}$$

$$x' = r_c' \frac{k_2 \sinh 2k_1 + k_1 \sin 2k_2}{\cosh 2k_1 + \cos 2k_2}; \tag{39}$$

where Z', r' and x' are the full, active and reactive resistances which are applied to the current in the turns of the primary winding;

Z_1 is the full resistance of the primary winding;

U_1 is the voltage applied to the primary winding.

Argument $\psi_{\text{п}}$. Dividing equality (27) by $-j\omega w_1$, we find the expression for the magnetic flux:

$$\dot{\Phi} = l_E a \dot{H}_1 \mu_1 k_p (\sin \psi_1 - j \cos \psi_1) = l_E a_k \dot{H}_1 \mu_1 e^{-j\left(\frac{\pi}{2} - \psi_1\right)} \tag{40}$$

where

$$\sin \psi_1 = \frac{x'}{Z'} = \frac{k_2 \sinh 2k_1 + k_1 \sin 2k_2}{k\sqrt{\sinh^2 k_1 + \sin^2 2k_2}}; \tag{41}$$

$$\cos \psi_1 = \frac{r'}{Z'} = \frac{k_1 \sinh 2k_1 - k_2 \sin 2k_2}{k\sqrt{\sinh^2 2k_1 + \sin^2 2k_2}}; \tag{42}$$

$$a_k = ak_d = \frac{a}{k} \sqrt{\frac{\cosh 2k_1 - \cos 2k_2}{\cosh 2k_1 + \cos 2k_2}}; \tag{43}$$

$$k_d = \frac{1}{k} \sqrt{\frac{\cosh 2k_1 - \cos 2k_2}{\cosh 2k_1 + \cos 2k_2}}. \tag{44}$$

Here ψ_1 is the phase angle between $\dot{E}_1'$ and $\dot{I}_1$;

a_k is the equivalent depth of penetration of the alternating magnetic flux in the ferromagnetic body; that is, the depth to which the magnetic induction B_1 is distributed uniformly;

k_d is the demagnetization factor characterizing the decrease of the flux owing to the demagnetizing action of the eddy currents.

From the expression for the module of the magnetic flux

$$\Phi = S_k B_1 = S k_s B_1 \tag{45}$$

a connexion is derived between the a.c. and d.c. induction:

$$B_k = \frac{\Phi}{S} = \frac{S_k}{S} B_1 = k_s B_1, \tag{46}$$

where $S_k = L_E a_k$ and $S = 2al$ are the equivalent and actual cross-sections of the ring; L is its width; $k_s = k_E k_d$

In the general case, the coefficient $k_E = l_E/2l$ is a variable magnitude, but when $l \gg d$ it is approximately 1 and its effect is insignificant. Here, induction B_k for a given induction B_1 will only be a function of the coefficient k_d ($k_E \approx 1$). When $\omega = 0$, $k_d = 1$ and $B_k = B_1$. When ω increases, induction B_k diminishes with a decrease of k_d. Having substituted θ into argument ψ in (46) in accordance with (6), we shall have:

$$\cos \psi_{Bk} = \frac{B_{k1}}{B_{km}} = \frac{k_{d1} B_1}{k_{dm} B_m} = \frac{k_{d1}}{k_{dm}} \cos \psi_B, \tag{47}$$

where

$$\left. \begin{array}{c} k_{d1} = \dfrac{1}{k} \sqrt{\dfrac{\cosh 2k_3 - \cos 2k_4}{\cosh 2k_3 + \cos 2k_4}}; \\ k_3 = k \cos \beta; \quad k_4 = k \sin \beta; \end{array} \right\} \tag{48}$$

$$\left. \begin{array}{c} k_{dm} = \dfrac{1}{k_m} \sqrt{\dfrac{\cosh 2k_{m3} - \cos 2k_{m4}}{\cosh 2k_{m3} + \cos 2k_{m4}}}; \\ k_{m3} = k_m \cos \beta; \quad k_{m4} = k_m \sin \beta; \\ k_m = a\sqrt{\omega \mu_m \gamma}. \end{array} \right\} \tag{49}$$

Having determined the tangent of the secondary angle ψ_2 by the relationship of (32) to (31) and substituted ψ in the latter by θ and ψ_B by ψ_{Bk}, we obtain an analogous equation to determine the argument $\psi_{\text{п}}$

$$\tan \psi_{\text{п}} = \frac{k_6 \sinh k_5 - k_5 \sin k_6}{k_5 \sinh k_5 + k_6 \sin k_6}, \tag{50}$$

where

$$k_5 = k \cos \beta_k; \quad k_6 = k \sin \beta_k; \quad \beta_k = \psi_H - \psi_{Bk}.$$

When there is no surface effect ($k < 0.5$), $k_d = k_{dl} = k_{dm} = 1$, $\psi_{Bk} = \psi_B$ $\psi_{\text{п}} = 0$; $\psi_2 = 0$; $\psi_1 = \frac{\pi}{2} - \psi_1$. When the surface effect is sharp ($k > 3$) the coefficients

$k_{d_1} = 1/k = k_d$ and $k_{dm} = 1/k_m$ do not depend on the angle β. In this case, we have from (47), in accordance with (4):

$$\cos\psi_{Bk}=\frac{B_1}{B_m}\sqrt{\frac{\mu_m}{\mu_1}}=\sqrt{\frac{B_1H_1}{B_mH_m}}=\frac{1}{\sqrt{2}} \tag{51}$$

and, consequently, $\psi_{Bk} = \pi/4$. Here, from (50) and (41), respectively, we obtain $\tan\psi_{II} = \tan\beta_k$ and $\sin\psi_1 = \sin\left(\frac{\pi}{4}-\frac{\psi}{2}\right)$, whence it follows:

$$\psi_{II}=\beta_k=\psi_H-\psi_{Bk}=\psi_H-\frac{\pi}{4}; \tag{52}$$

$$\begin{aligned}\psi_1=(\psi_2)=\frac{\pi}{4}-\left[\psi_{II}+\frac{\psi_I}{2}\right]=\\=\frac{\pi}{2}-\left[\psi_H+\frac{\psi_I}{2}\right].\end{aligned} \tag{53}$$

Comparing (50) with (52) it follows that in (50), argument ψ_{II} depends on the coefficient k, and therefore is a function of all the parameters determining k. In (52) ψ_{II} only depends on the magnetic properties of the steel and on the degree of non-linearity of the magnetic characteristic. When μ is constant the arguments $\beta = \beta_k = 0$. Here, from (50 and (52), it follows that $\psi_{II}= 0$ for any manifestation of surface effect. This again proves that the argument ψ_{II} actually takes into account the non-linearity of the magnetic characteristic caused by the basic magnetization curve. On the magnetization curve there is a characteristic point at which $\beta = \beta_k = \psi_{II} = 0$. For example, in Fig. 2, this is point (2), the magnetic permeability at which μ_1 equals the magnetic permeability μ_m at point (3) with double magnetic energy in accordance with (4). At this point when there is a sharp surface effect, the angle ψ_1 is only determined by the difference $\pi/4 - \psi_1/2$, which can easily be verified by tests.

Fig. 4 shows the curves of the dependence of the individual arguments on H_1 for sheet steel, the magnetization curves of which are shown in Fig. 2 and below in Fig. 6. The curves of Fig. 4 enable us to establish that the arguments β and $\beta_k = \psi_{II}$ have clearly expressed negative minima, practically coinciding with the maximum ψ_1. In powerful fields (see Fig. 7), the arguments ψ_H and ψ_B and, consequently, β and $\beta_k = \psi_{II}$, are practically constant magnitudes, approximately equal to 57°, 22°, 33° and 12°. The argument ψ_1 in powerful and weak fields is negligibly small compared with ψ_H and, therefore, in accordance with (5), ψ_H has a decisive value for weak and powerful fields. When the surface effect is sharp, the phase angle ψ_1 in accordance with (53) does not depend on frequency, which also confirms the tests carried out at 50 and 500 c/s, (Fig. 5).

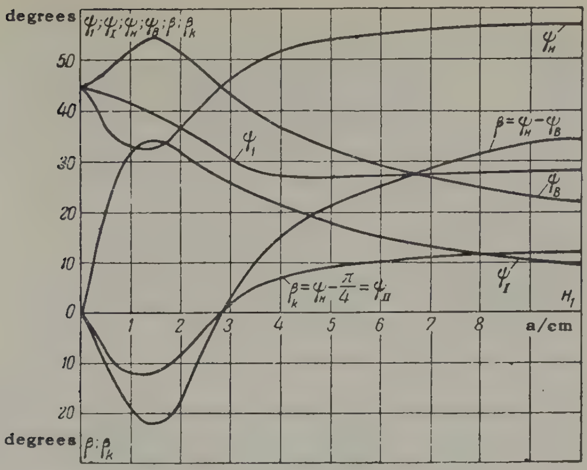

FIG. 4. The arguments in relation to the effective values of strength H_1

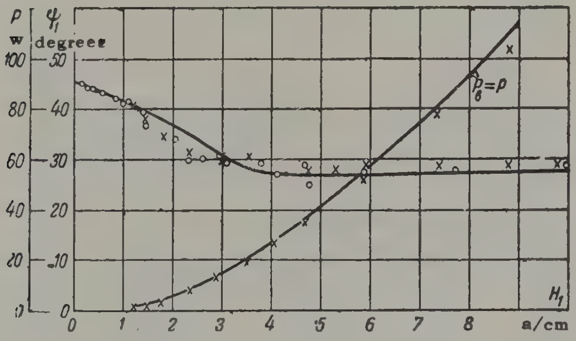

FIG. 5. Curves of the losses in the steel P and the angle of shaft ψ_1 between the current and the e.m.f. as a function of strength H_1.

o, test values at 50 c/s; ×, the same at 500 c/s

On passing from weak fields, the angle ψ_1 decreases from 45° to approximately 27° (when $H_1 = 4$) and then with a decrease of ψ_1, in accordance with (53) slowly increases to 33° when ψ_H increases to 57°, (see Fig. 7). Thus, when the surface effect is sharp, $\tan\psi_1$ is always less than unity and only in very weak fields when $H \to 0$, $\tan\psi_1 \to 1$. When the surface effect is poor, $\tan\psi_1 = \cot\psi_1$ and any values depending on the angle ψ_1 can be taken.

Determination of the losses in the steel

The losses in the steel are the sum of the electrical losses from eddy currents $P_e = I_e^2 r_e'$ (taking the hysteresis effect into account), and the magnetic

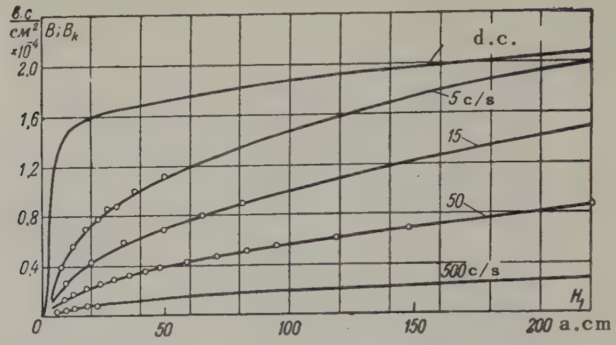

FIG. 6. A.C. magnetization curves at different frequencies ($\rho 20 = 0.225 \times 10^{-4}$ Ωcm), compared with test data. Upper curve experimental. ○ — test points

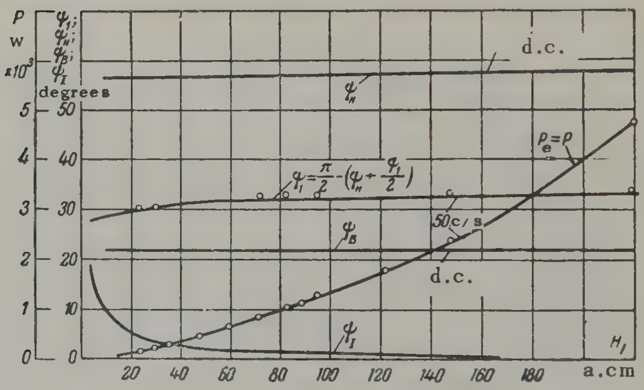

FIG. 7. Angles ψ and losses in the steel as a function of strength H_1. ○ — test points

losses caused by the magnetization current $P_0 = I_0^2 r_0'$, (taking the effect of eddy currents into account). The sum of these losses is

$$P = I_1^2 r' = E_1' I_1 \cos \psi_1 = \\ = \omega \Phi F \cos \psi_1 = \omega V_k B_1 H_1 \cos \psi_1, \tag{54}$$

where $F = \tau H_1$ is the magnetizing force;

$V_k = l_E a_k \tau$ is the equivalent volume of the ring.

Equation (54) can also be obtained with the aid of the Umov-Poynting vector. The special feature of equation (54) is that it generalizes in a simple and profitable form the total losses in the steel. For example when there is no surface effect ($k < 0.5$) and when the eddy current $I_e' = 0$, the electrical losses $P_e = 0$ and the magnetic losses P_0 equal the hysteresis losses, $(\Psi_n = 0)$:

$$\begin{aligned} P = P_0 = \omega V B_1 H_1 \sin\psi_1 = \\ = \omega V \frac{B_m H_m}{2} \sin\psi_1. \end{aligned} \tag{55}$$

Here,

$$\left.\begin{array}{r|l} r'_e = 2r'_c & r'_0 = r' = r'_c\, k^2 \sin\psi_1; \\ x_e = 0 & x'_0 = x' = r'_c\, k^2 \cos\psi_1. \end{array}\right| \tag{56}$$

where $l_E = 2l(k_E - 1)$ and $V = 2al\tau$ is the actual volume of the ring, $(k_d = 1)$.

In another limiting case when the surface effect is sharp $(k \geqslant 3)$, when $I'_e = I_1$, $I_0 \approx 0$ (which corresponds to short circuit conditions of the transformer), the magnetic losses $P_0 \approx 0$ and the total losses equal the electrical losses from eddy currents:

$$P = P_e = \omega V_k B_1 H_1 \sin\left(\psi_H + \frac{\psi_1}{2}\right) \text{ [w]}. \tag{57}$$

In this case,

$$\left.\begin{array}{r|l} r'_0 \to \infty, & r'_e = r' = r'_c\, k \sin\left(\psi_H + \frac{\psi_1}{2}\right); \\ x'_0 \to \infty, & x'_e = x' = r'_c\, k \cos\left(\psi_H + \frac{\psi_1}{2}\right). \end{array}\right| \tag{58}$$

Unlike (55), with a charge of ω in (57) the depth $a_k = a/k$ varies and, consequently, the equivalent volume

$$V_k = l_E a_k \tau = V \frac{k_E}{k} \text{ [cm}^3\text{]}. \tag{59}$$

The coefficient k_E, when the surface is sharp, can be determined with sufficient accuracy by the approximate formula

$$k_E = 1 + 0.65 \frac{d}{l}, \tag{60}$$

where the numerical coefficient 0.65 takes into account the curvature of the current path at the angles of the cross-section of the model, (when the surface effect is sharp).

A sharp manifestation of the surface effect has frequently to be dealt with in practice: for example, in the case of high frequency hardening of components, heating different installations and applications (calender shafts and cylinders etc.), and when investigating electrical machines with solid rotors and so on. Therefore, equations (57) and (58) are of practical interest owing to their simplicity. In so far as ψ_H and ψ_1 are functions of the magnetic properties of the material, so in accordance with curves ψ_H and $\psi_1 = f(H_1)$ (Figs. 4 and 7), it is easy to trace the effect of the arguments ψ_H and ψ_1 on the course of the process, for example, on the magnitude of the losses (57) when H changes from zero to the most powerful fields. In weak and powerful fields, where $\psi_1 \approx 0$, the argument ψ_H is the basic magnitude characterizing the process when ω is constant, for it also characterizes non-linearity II when $k > 3$. When $H \to 0$, the angle $\psi_H \to 45°$, which corresponds to the condition $\mu = \text{const}$. From the relationship:

$$\cos\psi_H = \frac{H_1}{H_m} = \frac{B_m}{2B_1} = \sqrt{\frac{\mu_m}{2\mu_1}} \tag{61}$$

it follows that in the case of powerful saturation, when $B_1 \to B_m$, the angle $\psi_H \to 60°$, but in so far as $B_1 \neq B_m$, so $\psi_H < 60°$. It also follows from (61) that beyond the limits of technical saturation when μ_1 and $\mu_m \to \mu_0$, the magnetic permeability of the air, $\psi_H \to 45°$. Thus, when H changes from zero to infinity, the changes of the angle ψ_H can be schematically represented in the form of the following chain: $45° - \psi_{H\ \min} - 45° - \psi_{H\ \max} - 45°$. It is analogous for ψ_B: $45° - \psi_{B\ \max} - 45° - \psi_{B\ \min} - 45°$. Consequently, the vectors B_m and H_m (Fig. 3), now converge and now diverge. The character of the divergence of these vectors beyond the characteristic point is inductive, but before the characteristic point, it is capacitive. However, in real conditions the capacitive divergence is smoothed out by the angle ψ_1 and the divergence of these vectors in all fields acquires an inductive character since the algebraic sum $(\psi_{\text{n}} + \psi_1/2$ is always positive, (Fig. 4).

The truth of the relationships (57) and (58) is the simplest to verify in tests on fields where $\psi_1 = 0$ and, consequently, where there is no error due to the angle ψ_1 because of inaccurate calculation with hysteresis loops. Experience fully confirms the truth of the definition of the angle ψ_H from (5).

The order of calculation. Using a value of H_1 given by the d.c. magnetization curve, first H_m and B_1. From (5) calculate ψ_H. From the curve $\psi_1 = f(H_1)$ for H_1, find ψ_1. Using (16), determine k. Here $\mu_1 = B_1/H_1$ is measured in (V.c/a.cm); B_1 in V.c/cm² or in Vb/cm², H_1 in a/cm; the specific conductance:

$$\gamma = \frac{1}{\rho} = \frac{1}{\rho_{20}\,[1 + \alpha_{20}\,(t - 20)]}\left[\frac{1}{\Omega\ \text{cm}}\right],$$

ρ 20 and α 20 are the specific resistance of the ferromagnetic body and its temperature coefficient at 20°C.

From (60) find k_E and from (59) V_k. Then from (57) and (58) determine the losses and resistances.

Experimental verification is carried out on a solid steel ring of rectangular cross-section which guarantees a sharp manifestation of the surface effect. The average diameter of the ring $D_c = 24$ cm; $\tau = \pi D_c = 75.5$ cm; $l = 8.7$ cm; $d = 2a = 1.5$ cm. Tests have been carried out using the E'pshtein apparatus with two windings (each with 440 turns), with a temperature of the steel at 20°C. The specific resistance of the steel at 20°C $\rho_{20} = 0.225 \times 10^{-4}\ \Omega$ cm. The fundamental magnetization curve is shown in Figs. 2 and 6 (upper). Comparison of the results of the calculation with test results is given in Figs. 5, 6 and 7. The angle ψ_1 in weak fields has been measured with the aid of an electronic-ray oscillograph. The curves $B_k = f(H_1)$ are calculated from (46), taking (60) into account.

Conclusions

The coincidence of the calculations with the test results testifies to the accuracy of the theoretical conclusions, taking into account the non-linearity of the magnetic characteristic. The formulae have been verified within the range of induction from 20 to 20,500 G at frequencies from 5 to 500 c/s. Overstatement of the losses by calculation (5-6 per cent), is only observed in medium fields in the region of maximum values of μ. In weak and powerful fields (Fig. 7), the results of the calculation practically coincide in full with the tests. Formula (46) enables a.c. magnetization curves to be plotted for different frequencies from the d.c. magnetization curve. It has been established that the phase angle between I_1 and E_1' when the surface effect is sharp does not depend on frequency. Its maximum value 45° and, consequently, the tangent of this angle will never be greater than unity, (when the surface effect is sharp). The division of the total current by I_e' and I_0 and the total resistance by Z_e' and Z_0' results in the equivalent circuit of the transformer. The method eases the transition to the analysis of the operation of an induction motor with a solid steel rotor such that when investigating induction motors of normal design, an equivalent circuit of a transformer is used as the starting point.

Translated by O. Blunn

REFERENCES

1. V.K. Arkad'ev; *E'lektromagnitnye protsessi v metallakh, (Electro-magnetic Processes in Metals).* pt. II United Scientific and Technical Press (1936).
2. L.R. Neiman; Poverkhnostnyi e'effekt v ferromagnitnykh provodakh i magnitnykh tsepiakh. (Surface Effect in Ferromagnetic Conductors and Magnetic Circuits). *Elekt. 1.* (1950).

3. M.A. Panasenkov; *Teoriia metodika rascheta i e'ksperimental'nye issledovaniia e'lektromagnitnykh tormozov, (Theory, Method of Calculation and Experimental Investigation of Electro-magnetic Braking).* Dissertation. ME'I. Jan. (1955).

AN EXPERIMENTAL TURBOGENERATOR WITH INTERNAL HYDROGEN COOLING OF STATOR AND ROTOR WINDINGS AT A PRESSURE OF THREE ATM*

L. Ia. STANISLAVSKII

(Received 2 April 1958)

In 1958 the Khar'kov turbogenerator works will produce the first two mark TGV-200 turbogenerators of 200 MW power which will come into regular production in 1959. Simultaneously, the plant is being prepared for the production of mark TGV-300 turbogenerators of 300 MW power. These generators will have internal hydrogen cooling of stator and rotor windings at increased pressure, and a number of other special design features.[†]

The mark TVO-30 experimental turbogenerator of 30 MW, 10-5 kV and 3000 rev/min, which in design is a prototype of the 200-300 MW turbogenerators, was planned as part of the preparation of the factory for the production of these large machines and was built in 1957. The generator was carefully tested with air and with hydrogen cooling on a specially constructed test stand at the works. After December 1957, detailed testing of this generator was continued in conditions of normal operation at one of the Mosenergo power stations.

Design of generator

The mark TVO-30 generator was planned and built to the overall dimensions of the mark TGV-25 turbogenerator in batch production, retaining its actual dimensions and assembly. The following new design features have been used in the experimental generator: the stator and rotor windings are internally cooled by hydrogen at a pressure up to 3 atm, eliminating the temperature drop in the winding insulation which occurs in machines having surface cooling of windings; the stator core, in contrast to usual machines, has axial ventilation only; a compressor is set inside the generator to build up the required pressure of gas; a new disk oil seal is used for the first time with piston rings between the housing and the seal plain bearings, making it possible to eliminate the diaphragm made of cable plastic or rubber which were unsatisfactory in operation.

---

* *Electrichestvo* No. 9, 30-34, 1958.

[†] L. Ia. Stanislavskii; Turbogenatory ot 30 do 300 MW zavoda KhETZ (Turbogenerators of 30 to 300 MW built by the Khar'kov Turbogenerator Works), Electrichestvo, No. 3, 1958.

The generator is excited by a turbine of 30 MW power. In order to test the generator thoroughly over a wide range of currents in the windings, its rated continuous output was taken as 50 MVA at $\cos \phi = 0.6$.

The generator bearings were situated in the external shields in which the disk oil seals were located. Since oil consumption in the body of the stator does not exceed 1 L/min when the hydrogen pressure is within the limits of 0.05 to 3 atm, vacuum purification of oil is not required, and therefore oil purification apparatus is unnecessary. The calculated excess of oil pressure over gas pressure in the stator casing is 0.3 - 0.5 atm. These values are substantiated by experimental data. The temperature of the babbit in the seal was 48 - 50°C with a total oil consumption of 50 l/min. The system developed for decreasing the load on the seals provides for a slight variation in oil consumption through the seals when the hydrogen pressure alters.

Cold rolled electrical steel was used for the stator core. The latter is cooled by the gas flowing through the axial channels in the teeth and back of the stator sections. There are no radial channels in the core. The stator sections are attached in the usual manner: with clamp bolts and non-magnetic steel retaining rings.

The stator winding is of the basket type. The design of the bars in the stator winding is new. Each bar consists of two series of transposed glass-insulated conductors. Stainless non-magnetic steel tubes carry the hydrogen which cools the bars are placed between the vertical series of conductors. The tubes have a specific resistance of 0.8 $\Omega\,\text{mm}^2/\text{m}$ and a magnetic permeability of not more than 1.5 in the presence of a field strength of 200 oersted. The hydrogen enters the ducts through silicone rubber caps from the turbine side and passes out through similar caps on the contact ring side. These caps serve as insulation between the bar heads. The ducts are insulated from one another and from the winding conductors by glass strip.

The greater portion of the winding bars have the usual compounded mica insulation in asphalt varnishes. A certain number of experimental bars of this type were inserted in the stator in order to gain experience in the manufacture and use of bars with silicone rubber insulation. These bars were developed in co-operation with the Lenin All-Union Electrical Engineering Institute (VEI). They were made from the same conductors and tubes, which were also compounded, but were insulated with glass mica in silicone-organic varnishes. Each bar was doubly insulated, baked and mounded in special pressure dies covering both the slotted and the front section of the winding.

The forging and also the banding rings, bushes and wedges of the mark TGV-25 generator were used in the rotor. The rotor winding turns consist of two U-shaped copper conductors forming the channel for the passage of the hydrogen coolant. The gas enters the hollow conductors from each side of the rotor and passes into the middle section of the latter through holes in the conductors and rotor wedges. The manufacture and applying of coils having such conductors differs little from usual practice. It was not necessary to cut up the coils in order to insert them into the slots. Accuracy in the matching of holes for the passage of gas in the coils and wedges was ensured with the aid of special appliances and conductors. Glass-textolite packing was used as the inter-turn insulation. Compressed sections of glass cloth in silicone-organic varnishes were used for the insulation under the bandings.

Forty-six thermocouples were installed for temperature measurement in various sections of the winding and sides of the rotor, as well as twelve thermo-anemometer pick-ups for measuring gas speed and consumption. Securing and insulating the pick-ups and thermocouples situated in the rotor, and, particularly, the withdrawal of the conductors presented a complex problem. A delicate operation was required in drilling blind holes 35 mm in diameter and 1500 mm in depth situated parallel to the central bore of the rotor occupied by the current conductor. One hundred and eight conductors were drawn through these holes to the terminal block connected to the slip ring. The production and arrangement of the pick-ups were carried out in co-operation with the Scientific Research Institute of the Electrical Industry.

A compressor with forward inclined blades was used to reduce the distance between the bearing axes, which is necessary in order to increase the vibration resistance of the rotor. This compressor, with overall radial dimensions determined by the position of the front sections of the stator winding, made it possible to obtain the required head of hydrogen.

In co-operation with the turbine department of the Khar'kov Aviation Institute, the compressor was examined on a specially constructed stand. By means of a suitable selection of diffuser blade pitch in the compressor, the zone of vibrationless operation was enlarged. At the same time a zone of noiseless operation was ensured by selecting the optimum clearances between the blades of the compressor flywheel and the diffuser. The disks and blades of the compressor flywheel were made of steel. Four vertical gas coolers were used for cooling the gas. In order to obtain a considerable rise in the rotor current and in order to use batch production contact rings, two pairs of contact rings with standard brush holders and two pairs of current-carrying bolts were installed in the rotor.

The generator is excited from a triple-phase current grid through ionic rectifiers with grid control. A d.c. motor-generator was used as a reserve group.

Experimental operations

When producing bars for generators with internal cooling the penetration of a compound into the ventilation tubes must be eliminated. After a number of experiments the introduction of a filler into the tubes and its removal after the end of the bar production process was found to be desirable.

The observance of requirements for tube strength and elasticity is important in order to obtain high-quality bars of uniform shape.

Lengthy experiments were carried out on the determination of the thermal parameters of the bars for a correct determination of their temperature. Here, the dependence of aerodynamic resistance on the velocity of the gas was established, making possible an exact determination of gas consumption and, consequently, of gas overheating. During internal hydrogen cooling the excess of the temperature of the stator copper is determined almost entirely by the heating of the gas, which is:

$$\Delta t = \frac{N}{C_p G},$$

where N is the losses in the stator copper, kW; C_p is the specific heat of the gas, kW. sec/kg. deg; and G is the gas consumption, kg/sec.

The gas consumption can be determined according to the formula

$$G = F \sqrt{\frac{2g\gamma_{cp}\Delta H}{1.5 + \zeta \frac{l}{d}}},$$

where F is the total area of the cross-section of the ventilation ducts, m²; γ_{av} is the specific weight of the gas in the mean cross-section of a bar, kg/m³; ΔN is the applied pressure mm hyd. col.; l is the tube length, m; d is the hydraulic diameter of a tube, m; ζ is the coefficient of friction of the gas in the tubes, $\zeta = \frac{0.3636}{Re^{0.25}}$ (Re – Reynolds number).

The results obtained are substantiated by experimental data with an accuracy up to 1°C.

As a result of these experiments, it was established that temperature drop from the walls of the tube to the gas when $Re = 4500 - 25{,}000$ (which corresponds to the whole possible range of turbogenerator operating conditions) amounts to 2.3°C, and 5.3°C considering the temperature drop in the duct and conductor insulation.

Dielectric losses for the bars with compound mica insulation coincided fully with the normal values for standard bars. The experimental bars with silicone rubber insulation had a dielectric loss angle tangent of 0.020 - 0.049 increasing within the limits 0.022 - 0.027 on a voltage increase from 0.5 U_n to 1.5 U_n. The electrical strength of this insulation is approximately the same as that of bars having the usual mica insulation.

It was interesting to determine the losses in the active steel of the stator and to determine its heating, since the stator core was made for the first time without radial ventilation channels, and had an active length of 2700 mm. Specific losses during induction of 10,000 G were equal to 1.24 W/kg, (1.26 W/kg according to calculations).

No less interesting were the tests of the electrical strength of the stator winding insulation, since the bar heads, where the silicone rubber caps separate the cooling ducts (which are under full voltage) of one bar from the other, are not insulated. Tests with a voltage of $2\,U_n + 3\text{kV} = 24$ kV confirmed the adequate reliability of these caps. There were no breakdowns or flashovers in the bar heads.

Testing the generator*

Factory tests of the generator were made on a reinforced concrete stand faced with iron plates allowing two turbogenerators of 300 - 500 MW each to be set up simultaneously. An oil supply system with an oil line pressure up to 5 atm, a water supply system, a gas supply station and a control panel for the regulation of hydrogen pressure from 0.03 to 4 atm were set up. During the course of sealing and the tuning of the generator at hydrogen pressures up to 3 atm, individual points of gas leakage were found and eliminated (it was necessary to scale the stator surface and the external shields), the reinforcement of the external shields was strengthened along the horizontal joint, and other gas leakage points were found and eliminated, (fine flanges, gas coolant reinforcement, etc.).

In addition to the thermocouples inserted in the rotor the following were also inserted in the active sections of the generator for the ensuing thermal tests in the process of manufacture of the generator: resistance thermometers and thermocouples for measuring the temperature of the stator windings and steel; thermocouples for measuring the temperature of the babbit in the oil seal; resistance thermometers and mercury thermometers for measuring the temperature of gas, water and oil. Thermal tests were made on the stand only in no-load conditions and during triple-phase short-circuit operation of the generator. Tests were made at the power station in conditions of the parallel operation of the generator with the Mosenergo system.

---

* The factory tests were made with the participation of the All-Union Scientific Research Institute of Electric Power and the Scientific Research Institute of the Electrical Industry; the tests at the Mosenergo power station were made with the participation of the works and the Scientific Research Institute of the Electrical Industry.

The temperature rises of the rotor and stator windings are shown in Tables 1 and 2 according to data from tests at the power station. These tests were carried out at rated generator voltage and at rated rotation speed.

TABLE 1

Mean excess of rotor winding temperature, °C
(by the method of measuring the winding resistance)

Output of generator MVA	Rotor current A	Hydrogen pressure atm				
		0.05	0.5	1	2	3
31.25	910	36	26	20.5	14	10.5
50	1320	–	62	43.5	28.5	20
62.5	1460	–	–	53	34.5	24.5
67	1580	–	–	–	40	29

TABLE 2

Maximum local excess of temperature in stator slot, °C
(measured by resistance thermometer placed between bars)

Output of generator MVA	Stator current A	Hydrogen pressure atm				
		0.05	0.5	1	2	3
31.25	1720	54	37	28	19	14
50	2750	–	–	57	40	29.5
62.5	3440	–	–	–	63	43
67	3680	–	–	–	–	49

The thermocouples placed in the rotor made it possible to determine both the maximum local temperature and the temperature distribution along the length of and around the rotor. Here, it was found that around the rotor there is a slight variation in temperature. In the coil nearest the large tooth of the rotor the temperature is 8°C less than in the coil farthest removed from it.

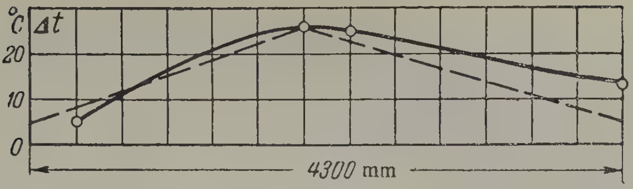

FIG. 1. Distribution of temperature rise along the conductor for the hottest coil in the rotor winding. Rotor current 907 A, hydrogen pressure 3 atm
—— experimental
– – – calculation

The distribution of temperature rise of the copper along the length of the rotor over the temperature of the cold gas is shown in Fig. 1. These results are somewhat better than the calculated results, according to which the maximum temperature of the winding at the mid-point of the rotor is approximately 1.85 times greater than the mean temperature of the winding. With the elimination of cold gas preheating when being supplied from the compressor (which does occur in the experimental generator), and the adoption of other measures, the ratio of maximum to mean temperature will be lowered to 1.6.

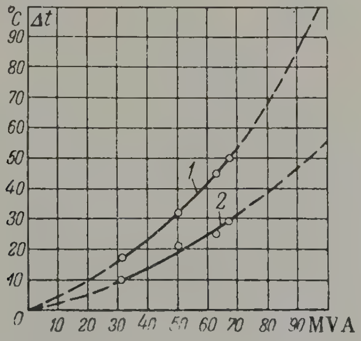

FIG. 2. Maximum temperature rise in stator slot (1), and mean temperature rise in rotor winding (2) over temperature of cold gas during variation in generator load. Hydrogen pressure 3 atm

The application of internal rotor winding cooling combined with an increase in gas pressure to 3 atm was very effective. As is known, the mean temperature rise in the presence of a load of 37.5 MVA amounts to 90°C in the rotors of mark TGV-25 or TV2-30-2 turbogenerators with the usual surface hydrogen cooling. In the test rotor of the TVO-30 generator which has the same active dimensions, the mean temperature rise in the presence of similar loading and a pressure of 3 atm was only 13°C (Fig. 2), and during double loading and a gas pressure of

3 atm the mean temperature rise was only 34°C. The temperature distribution along the length of the stator bars is shown in Fig. 3. Assuming linear dependence of the temperature of a bar on its length, it is easy to determine the maximum bar temperature from the readings of the hottest resistance thermometer. In the presence of a load of 50 MVA the maximum rise of the bar temperature over the temperature of the cold gas is only 39°C. Thus, the permissible load of the generator according to the heating conditions of the stator winding (the temperature rise at the hottest point is equal to 65°C) is 68 MVA. The dependence of the rise of the stator winding temperature on the hydrogen pressure is shown in Fig.4.

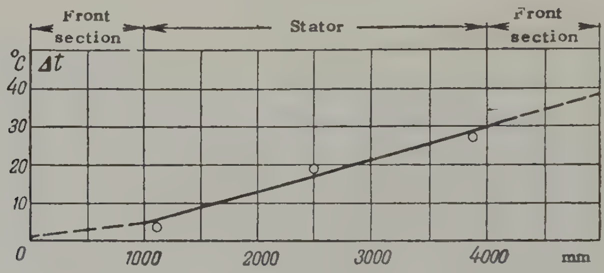

FIG. 3. Distribution of the temperature rise in rotor slot over temperature of cold gas along the length of the winding in the presence of a load of 50 MVA. Hydrogen pressure 3 atm

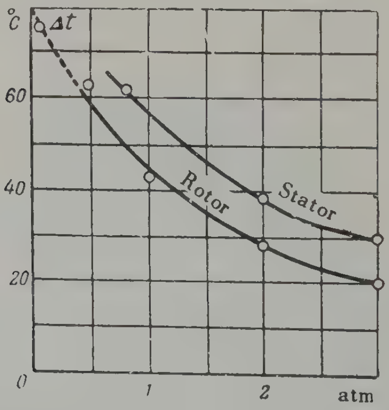

FIG. 4. Dependence of maximum temperature rise of the winding in the stator slot and the mean temperature rise of the rotor winding over the temperature of the cold gas during variation of hydrogen pressure. Load 50 MVA, rotor current 1320 A

The temperature rise of the remaining sections of the generator (the steel in the stator, bearings, seal, etc.) lay within the limits of normal values. Vibration of the generator bearings was within the limits of 0.02 - 0.04 mm, the vibration in the axial direction amounting to 0.02 mm.

During operation of the turbogenerator the hydrogen consumption (relative to normal pressure) at the various pressures was as follows:

TABLE 3

Hydrogen pressure in the generator, atm	Hydrogen consumption m^3/day
0.05	0.8*
0.5	0.8*
1	1.8
2	4.5
3	7.0

* Gas leakage is absent in practice. These values are an estimate of hydrogen consumption after taking tests and cleaning the drier.

Let us now dwell briefly on our experience in loading and mounting the TVO - 30 generator.

Arrangement of the bearings in the shields of the body of the stator made it possible to load the machine as assembled, i.e. with installed rotor, coolers, internal and external shields, oil seals and outlets. The generator was assembled and tested at the factory during hydrogen cooling. The total weight of the generator as assembled was approximately 85 tons. A standard flatcar of 100 tons load capacity which had previously carried only turbogenerator stators was used for its transportation (Fig. 5). In order to avoid axial displacements of the rotor during its transportation the half-sleeve of the rotor was fastened to the external shield of the generator, by a number of screws of sufficient cross-section. The erection of the generator at the power station including trial starting, connexion into the grid and conversion to hydrogen cooling was accomplished in 14 days, instead of the usual 3 - 4 months necessary for mounting turbogenerators sent from the plant in a dismantled state.

Conclusion

1. Tests of the mark TVO - 30 turbogenerator with internal hydrogen cooling of stator and rotor windings showed that it can develop twice the output of the 25 - 30 MW series of generator with the same overall dimensions. This corresponds to previously made calculations.

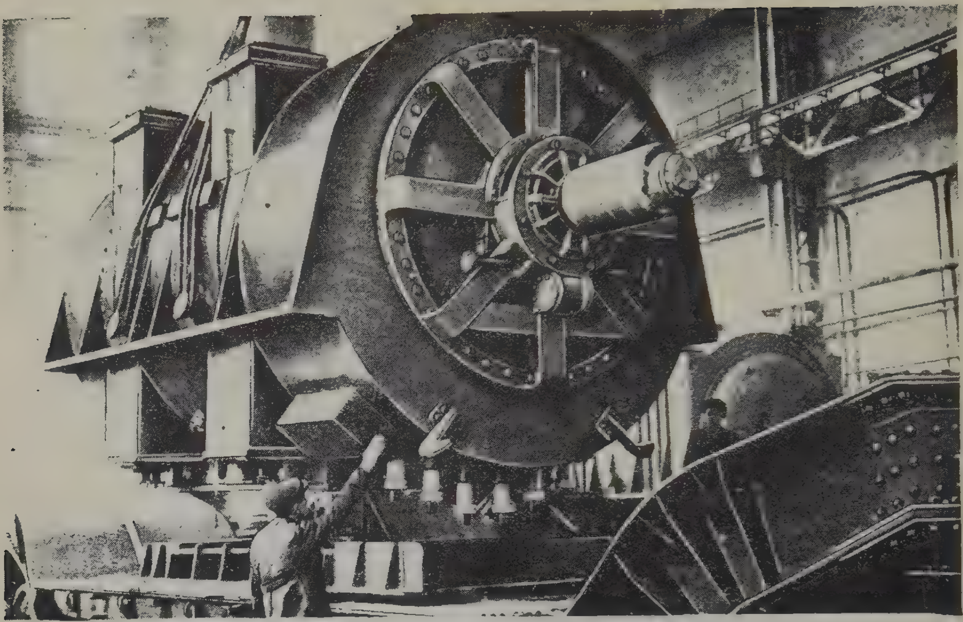

FIG. 5. Loading mark TVO-30 turbogenerator on railway flatcar

2. In manufacturing the generator a number of engineering problems were solved related to the regulation of the production of turbogenerators with internal cooling of windings, and additional requirements were made clear for the design of machines when increasing gas pressure up to 3 atm.

3. The possibility and economic expediency of transporting turbogenerators which have been assembled and tested at the works and also the possibility of mounting them rapidly on site were demonstrated.

Translated by F.J. Griffiths

CALCULATION OF THE REDUCTION OF VOLTAGE ON THE TERMINALS OF HIGH-POWER CURRENT COLLECTORS WITH STRONG ACTUATING CURRENTS*

G.M. KASPRZHAK

(Received 7 January 1958)

The calculation of the voltage loss in factory circuits supplying high-power current collectors with strong actuating currents (squirrel-cage motors and welding transformers), is usually undertaken with maximum actuating current using the well-known formula of approximation [1]:

$$\Delta U = kIL\,(r_n \cos\varphi + x_n \sin\varphi), \tag{1}$$

where r_n and x_n = the active and inductive resistance 1 km of the line Ω/km;
L = length of line km;
I = load current A;
$\cos\phi$ = power factor;
k = coefficient depending on the number of phases and equal to 2 or $\sqrt{3}$.

As can be seen from Fig. 1, such a calculation may give a most inaccurate and minimized result. In the example illustrated the inaccuracy amounts to 20/30 per cent when starting a squirrel-cage induction motor or when short circuiting the secondary circuit of a welding transformer supplied from a relatively weak low-power circuit; in other cases (c.f. appendix) it can amount to 100 per cent and above.

The error in calculation is explained by two factors. The first is that the power factor in activating circuits is very low (not more than 0.15 - 0.2) and as a result of this [2] the formula of approximation (1) is insufficient for calculations. The second factor is that the maximum reduction of voltage on the terminals of current collectors depends, as we know, not only on the strength of the load current but also on the angle of phase displacement between the load current and the short circuit current of the line. In the process of starting, the load current slowly decreases and the angle of phase displacement decreases rapidly. Consequently *the maximum voltage loss will be not in the short circuit but in another circuit* determined in the first instance by the angle of phase displacement.

---

* *Elektrichestvo* No. 9, 39-42, 1958.

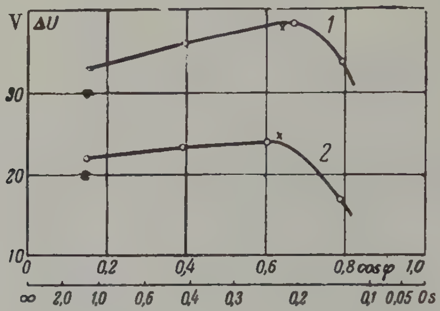

FIG. 1: The reduction of voltage on the terminals of current collectors when starting shown in relation to cos φ (for welding transformers), and to slip (for induction motors) 1 = for welding transformers type STE-34; 2 = for squirrel-cage induction motors with 28 kW output;
○ = test data; ● = data from calculations by equation (1);
X = data from calculations by the vector diagram

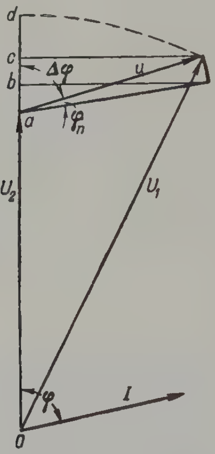

FIG. 2: Vector diagram
I = load current; U_1 = voltage at beginning of line; U_2 = voltage at end of line; u = voltage drop in the line

From the vector diagram shown in Fig. 2 it will be seen that with low power factors and considerable voltage drops in the conductors, the amount of voltage loss as computed from equation (1) (segment *ac*), can be appreciably different from the true value of that quantity, (segment *ad*). Consequently, when determining the maximum voltage loss in starting an induction motor and when welding, it is essential to state the mathematical relationships more precisely, (2). It will also be seen from the vector diagram Fig. 2 that the greatest voltage loss at a given current and consequently, with a given triangle of the voltage drop of a circuit, attains its maximum value when there is no phase displacement between the load current and the line current in the presence of a short circuit; that is, when $\Delta\phi = \phi - \phi_n = 0$.

This deduction, however, is true only when the load current is constant. In fact, it will decrease somewhat as soon as the motor is started. Consequently, conditions corresponding to the maximum voltage loss do not exactly fit the specification $\Delta\phi = 0$.

Let us determine analytically the conditions of maximum voltage loss having first of all studied the character of the change in the load current I of induction motors and welding transformers, and also the drop in voltage in the lines supplying them in systems from short circuit (starting) to no-load states. With this in mind, assume that the relation of current to load can be determined for medium and high power motors and transformers by a simplified equivalent network Fig. 3, in which, changing the system of operation from short circuit to rated load, we can disregard the conductivity of a parallel circuit of the equivalent network that is, ignore the no-load current. We know [5] that the relation of the current of a series circuit in the equivalent network I_n to the angle ψ between U_2 and I_n is as follows:

$$I_n = I'_{n\kappa}\sin\psi = I_{n\kappa}\frac{\sin\psi}{\sin\psi_\kappa}, \tag{2a}$$

Where I'_{nk} and I_{nk} are the current of the theoretical and the actual short circuit of the series circuit of the equivalent network; ψ_k = the angle of displacement between U_2 and I_{nk}

Consequently for high loads we obtain, with sufficient accuracy:

$$I \approx I_\kappa\frac{\sin\psi}{\sin\psi_\kappa} \simeq I_\kappa\frac{\sin\varphi}{\sin\varphi_\kappa}, \tag{2b}$$

where I_k is the current of the actual short circuit, ϕ and ϕ_k = the angle of phase displacement between the voltage and the current in the primary circuit in normal conditions and in the presence of a short circuit.

The angle ϕ_k can be determined for squirrel-cage induction motors from the parameters of the equivalent network of induction motors and consequently from the size of the critical slip of the machine S_k, such as

$$\cos\varphi_\kappa \approx \cot\varphi_\kappa \approx s_\kappa^{*} . \tag{3a}$$

For welding transformers the value of cos ϕ_k cannot be directly calculated from rating plate or catalogue data. Proceeding from data from the "Elektrik" factory the following approximate values of cos ϕ_k can be recommended for transformers made in our own country: for low-power transformers type STE-24, STAN-0, and STAN-1, cos $\phi_k = 0.2$; for medium power transformers type TSD-500, cos $\phi_k = 0.15$; for high-power transformers type TSD-1000, cos $\phi_k =$ 0.1.

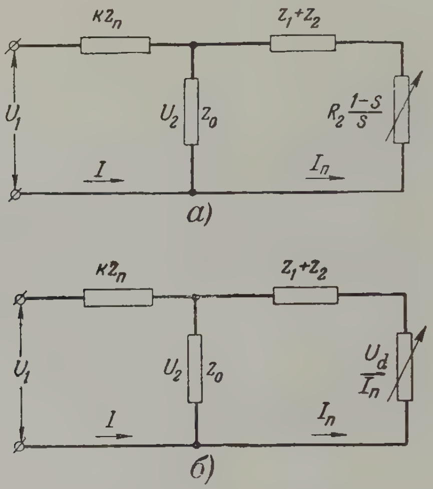

FIG. 3: Equivalent network of an induction motor (a) and of a welding transformer (b)

Z_0, Z_1, Z_2, R_2, $\frac{Ud}{I_n}$, = overall and active resistance of the equivalent network; kZ_n = total impedance of the line

Having determined current I let us determine the voltage drop in the line, the resistance of one conductor of which equals Z_n:

$$u = kI_\kappa \frac{\sin\varphi}{\sin\varphi_\kappa} z_n, \tag{3b}$$

Where $kI_k z_n/\sin\phi_k = u_k$ is the fall in voltage in a line in the presence of an ideal short circuit.

---

* The method of determining S_k is stated, for example in [4].

Thus,

$$u = u_{\kappa} \sin \varphi \tag{4a}$$

or, in relative units,

$$\varepsilon = \frac{u}{U_2} = \varepsilon_{\kappa} \sin \varphi. \tag{4b}$$

To calculate the voltage loss we shall use exact relationships where the unknown value of ΔU is defined, not as the sum of the distances *ab* and *bc*, but as *ab* + *bc* + *cd* Fig. 2, i.e., by calculating the transverse components of the voltage drop in the conductors. The expression is given a more convenient form if, for the initial value, we take the voltage drop in the conductors for a given current and angle of $\Delta \phi$, but express the initial and calculated values in relative units. Here, we obtain the mathematical formula introduced in [2]:

$$\delta = \sqrt{1 + 2\varepsilon \cos \Delta\varphi + \varepsilon^2} - 1, \tag{5a}$$

Where $\delta = \Delta U/U_2$: the voltage loss in relative units: $\Delta\phi = \phi - \phi_n$: the angle of phase displacement between U_2 and u.

Substituting in equation (5) the expression for ϵ from (4b) and changing the parameter $\Delta\phi$ for its value, we obtain:

$$\delta = \sqrt{1 + 2\varepsilon_{\kappa} \sin \varphi \cos (\varphi - \varphi_n) + \varepsilon_{\kappa}^2 \sin^2 \varphi} - 1, \tag{5b}$$

where $\epsilon_k = U_k/U_2$: the voltage drop in the system in the presence of short circuit current I_k.*

Let us determine the conditions under which the quantity δ attains its maximum value. After differentiation and a series of conversions we obtain:

$$\cot 2\varphi_{\kappa} = \frac{\varepsilon_{\kappa}}{2 \cos \varphi_n} - \tan \varphi_n. \tag{6a}$$

Thus, in the examples we have considered when the load current varies with angle ψ according to the sine rule the maximum voltage loss occurs not when $\phi = \phi_n$, but when the relationship between the angles ϕ and ϕ_n is determined by equation (6a). As can be seen from this formula, the relation between the parameters ϕ and ϕ_n is determined also by the amount of the relative voltage drop in the system ϵ_k with a short-circuit current I_k. However, in practice the function $\delta = f(\cos \phi)$ has no strongly expressed maximum. Consequently, the conditions where the voltage loss attains a maximum value can be determined approximately, disregarding the first term of the right-hand side of equation (6a); i.e., by the formula:

---

* With a considerable voltage drop on the terminals of current collectors, the quantity ϵ_k, estimated from the catalogue value of the short circuit current I_k, must be corrected, [1 and 6].

$$\cot 2\phi_k = -\tan \phi_n \tag{6b}$$

or, simpler still, by the following equality:

$$\varphi_k = 45^\circ + \frac{\varphi_n}{2}. \tag{7}$$

The relationships $\cos \phi = f(\tan \phi_n)$ for different values of ϵ_k are shown graphically in Fig. 4.

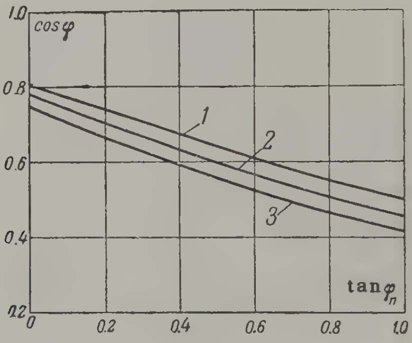

FIG. 4: Diagram to determine the conditions corresponding to maximum voltage loss
(1) $\epsilon_k = 0.6$; (2) $\epsilon_k = 0.4$; (3) $\epsilon_k = 0.2$

Here, it is essential to note that usually $\tan \phi_n < 0.5$. As a result, the maximum voltage loss in low-voltage distributing systems occurs when $\cos \phi = 0.5 \ldots 0.8$, i.e., far beyond the limits of starting conditions.

For cases frequently encountered in practice, when factory circuits are purely an active resistance, i.e. $\tan \phi_n \approx 0$, *the maximum voltage loss when starting an induction motor will occur when the slip is approximately critical.* Actually, in this case $\phi_k = 45^\circ$, but with considerable slip $\tan \phi \approx \tan \psi = s_k/s$, whence $s = s_k \tan \psi$. When $\tan \psi = \tan \psi_k = \tan 45^\circ = 1$ the unknown slip $s = s_k$.

When supplying a welding transformer from an analogous network, the maximum voltage reduction will be in the operating, and not the starting conditions; i.e. when the arc voltage $U_d \neq 0$. Actually, in this case, in accordance with the equivalent network shown Fig. 3b

$$\cos \phi = \cos \psi = \frac{U_d}{U_2}$$

whence

$$U_d = \cos \psi . U_2.$$

when

$$\tan \psi = \tan \psi_k = \tan 45^\circ, \ \cos \psi_k = 0.707$$

and, consequently, the arc voltage corresponding to the maximum voltage loss is $0.707\, U_2$.

Thus, with automatic welding (U_d up to 45 V) the maximum voltage loss occurs in practice in the presence of operating currents, and with manual welding ($U_d \approx 25$ V), when the arc is relatively low; i.e., with currents lower than operating strength, [5]. As the inductance of the supply system increases, so the conditions corresponding to maximum voltage loss will tend towards an increase in current: i.e. towards the short circuit system. Thus, for example, when starting a high-voltage induction motor directly and the line between the supply source and the motor is a purely inductive resistance [6], the maximum fall in voltage will occur in conditions close to starting conditions.

And so, knowing the conditions which correspond to the maximum fall in voltage on the terminals of the current collectors, and having used an accurate formula to calculate its value, we can calculate the voltage loss in electrical networks when supplied by high output squirrel-cage induction motors and welding transformers. It is not possible, however, to obtain a simple mathematical formula. Therefore, using in turn equation (6a) and (5b) we can plot a family of universal calculation curves. As is to be expected, the functions $d_{\max} = f(\epsilon_k)$ with the given tan ϕ_n are expressed by straight lines.

The approximate expression with which to determine the maximum voltage loss when starting high-power current collectors may be obtained by substituting the conditions for the maximum (7) into equation (5b). Here after conversion we obtain:

$$\delta_{\max} = \sqrt{\left(1 + \varepsilon_\kappa\left(\frac{1}{2} + \varepsilon_\kappa\right)(1 + \sin \varphi_n\right)} - 1. \qquad (8)$$

We can obtain an even more simple mathematical formula by assuming that with a given value of ϵ_k the relative voltage loss $d_{\max}$ increases in proportion to the value of $\tan \phi_n = x_n / r_n$ according to the sine rule. Then, when $\tan \phi_n \leqslant 1$:

$$\delta_{\max} = \varepsilon_{\kappa}\left[\frac{1}{2} + \frac{1}{3}\sin\left(\frac{\pi}{2}\cdot\frac{x_n}{r_n}\right)\right]. \qquad (9)$$

As has been shown by checking, equations (8) and (9) give sufficiently accurate results and they may be recommended for practical calculations.

It can be deduced from Fig. 5 and the mathematical formulae (8) and (9) that when $\tan \phi_n = 0$, $d_{\max} = 0.5\ \epsilon_k$; when $\tan \phi_n = 1$, $d_{\max} = 0.707\ \epsilon_k$; when $\tan \phi_n = \infty$, $d_{\max} = \epsilon_k$.

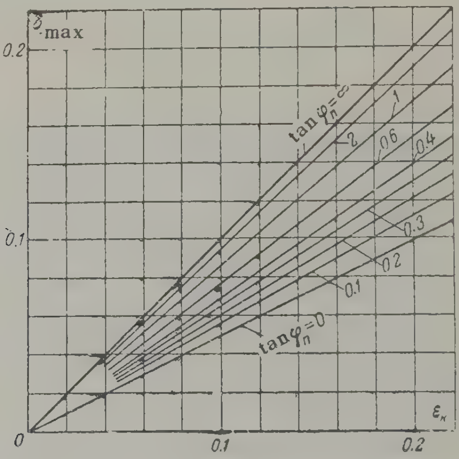

FIG. 5: Curves to determine maximum voltage loss

The relationships we have obtained may be used for approximate calculations. It can be seen from these relationships that with the standard method of calculating the voltage loss, the largest error is admitted in the case of a circuit with purely active resistance. When calculating the voltage loss in a line which only has inductive resistance, the method suggested in this article does not give greater accuracy in the calculations. In the appendix will be found examples of calculations confirming the need to use the suggested methods when calculating the voltage loss in low voltage factory circuits.

Appendix

As confirmation of the necessity to state the calculation of the voltage loss in conductors with large starting currents more precisely, we compare the results of a calculation by the standard method and by the method proposed. The calculations are shown in the table which may also be used as a model to study the sequence of the calculations of the voltage loss on the terminals of current collectors with large starting currents.

Initial data for the calculation:

Example 1: A squirrel-cage induction motor of 28 kW power (U_n = 380 V; I_n = 53.2 A; I_k = 265 A; cos ψ_k = 0.151) connected to an overhead line 52 m long with a copper conductor section 6 mm² (r_n = 3.06 Ω/kM; x_n = 0.37 Ω/kM).

Example 2: A welding transformer (U_n = 220 V; I_n = 345 A; I_k = 520 A; cos ϕ_k = 0.08) connected to a copper cable 188 m long section of a cable strand 70 mm²; r_n = 0.26 Ω/kM; x_n = 0.06 Ω/kM).

TABLE 1

Calculated value	Basis for calculation (equation diagram)	Example 1	Example 2
Voltage drop:			
In a theoretical short circuit	$\varepsilon_\kappa=\frac{kI_\kappa z_n\cdot L}{U_2\sin\varphi_\kappa}$	$\frac{\sqrt{3}\cdot265\cdot3,1\cdot0,052}{380\cdot0,99}=0,196$	$\frac{2\cdot520\cdot0,289\cdot0,188}{220\cdot0,997}=0,248$
In an actual short circuit	$\varepsilon'_k=\frac{kI_\kappa z_n L}{U_2}$	$\frac{\sqrt{3}\cdot265\cdot3,1\cdot0,052}{380}=0,194$	$\frac{2\cdot520\cdot0,289\cdot0,188}{220}=0,247$
Critical power factor ($\cos\phi_k$);			
Exact value	$\cot 2\varphi_\kappa=\frac{\varepsilon_\kappa}{2\cos\varphi_n}-\tan\varphi_n$	0,69	0,66
Approximate value	$\cot 2\varphi_\kappa=-\tan\varphi_n$	0,66	0,62
Maximum voltage loss:			
Exact value	Graphs $\delta_{\max}=f(\varepsilon_\kappa;\ \mathrm{tg}\, f_n)$ (Fig. 5)	0,112	0,157
Approximate value	$\delta'_{\max}=\varepsilon'_\kappa\left[\frac{1}{2}+\frac{1}{3}\sin\left(\frac{\pi}{2}\frac{x_n}{r_n}\right)\right]$	$0,194\left[\frac{1}{2}+\frac{1}{3}\times\sin\left(90^\circ\cdot\frac{0,37}{3,06}\right)\right]=0,125$	$0,247\left[\frac{1}{2}+\frac{1}{3}\times\sin\left(90^\circ\cdot\frac{0,06}{0,26}\right)\right]=0,172$
Voltage loss in short circuit			
Exact value	$\delta_\kappa=\sqrt{1+2\varepsilon'_\kappa\cos\Delta\varphi+\varepsilon'^2_\kappa}-1$	$\sqrt{1+2\cdot0,194\cdot0,27+0,194^2}-1=0,072$	$\sqrt{1+2\cdot0,247\cdot0,303+0,247^2}-1=0,105$
Approximate value	$\delta'_\kappa=\frac{kI_\kappa L}{U_2}(r_n\cos\varphi+x_n\sin\varphi)$	$\frac{\sqrt{3}\cdot265\cdot0,052}{380}(3,06\cdot0,151+0,37\cdot0,99)=0,052$	$\frac{2\cdot520\cdot0,188}{220}(0,26\cdot0,08+0,06\cdot0,997)=0,072$
Error in calculation	$\frac{\delta_{\max}}{\delta'_\kappa}\cdot100\%$	$\frac{0,112}{0,052}\cdot100=215\%$	$\frac{0,157}{0,072}\cdot100=218\%$

REFERENCES

1. V.N. Voronov and N.N. Lovtskii; *Proektirovanie silovovo elektrooborudovaniia promyshlennykh predpriiatii. (Designing the power equipment of industrial enterprises).* Gosenergoizdat (1950).
2. G.M. Kasprzhak; *Ob utochnenii rascheta poteri napriazheniia v provodakh. (More precise calculations of the voltage loss in conductors).* All-Union Correspondence Polytechnical Institute (1958).
3. G.M. Kasprzhak; *Individual'naia kompensatsiia reaktivnoi moshchnosti svarochnykh transformatorov. (The individual compensation of the reactive power of welding*

transformers). All-Union Institute of Scientific and Technical Information, Academy of Sciences U.S.S.R. (1958).

4. P.N. Solodovnikov; *O kriticheskom skol'zhenii asinkhronnykh dvigatelei. (The critical slip of induction motors).* VEP No. 11 (1956).
5. B.E. Paton and V.K. Lebyedyev; *Elementy raschetov tsepei i apparatov peremennovo toka dlia dugovoi svarki. (Elements for calculating a.c. circuits and apparatus for arc welding).* Publishing House of the Academy of Sciences of the Ukr. S.S.R. (1953).
6. I.A. Syromiatnikov; *Rezhimy raboty asinkhronnykh elektrodvigatelei. (The operating conditions of induction motors).* Gosenergoizdat (1955).

DIELECTRIC LOSSES IN CONDENSER PAPER*

V.T. RENNE, N.N. KALIAZINA and M.N. MOROZOVA

Kalinin Polytechnical Institute, Leningrad

(Received 13 December 1957)

Every year more uses are found in electrical engineering for paper condensers and in this connexion the manufacture of condenser paper in the U.S.S.R. is continuously increasing. At the same time there has been an improvement in its quality to correspond with the growth of demand for this dielectric from the point of view of the condenser industry in our country.

Furthermore, until recently such an important index of quality as the angle of dielectric loss could not be found in the All-Union State Standard on condenser paper, although in certain types of paper condensers, especially power ones, operating on alternating voltage, the magnitude of the losses in the dielectric determines the overheating of the condenser in operating conditions and the limiting value of its reactive power. In this connexion in recent years a series of investigations into dielectric losses in condenser paper have been carried out in the dielectric research laboratory of Leningrad Polytechnical Institute during which period contact was established with scientific research organizations of the paper industry (Central Paper Scientific Research Institute, Ukranian Paper Scientific Research Institute) and with the Chair of Cellulose Chemistry at Leningrad Technological Institute.

Methods of measuring the loss angle of the dry paper condensers described in foreign journals [1], are comparatively complicated, time consuming and difficult to utilize in the method of paper production, where it would be essential to be able to measure the loss angle of paper in connexion with the introduction of standards for this characteristic in the All-Union State Standard. We have, therefore, developed a special method of measuring the loss angle by means of a simplified system of electrodes, [2]. The method requires a paper specimen to be vacuum dried and eliminates the possibility of ionization developing in the

Elektrichestvo No. 9, 47-52, 1958.

test specimen. It was developed in the Ukranian Scientific Paper Research Institute and with certain modifications has been included in a new and recently approved edition of the All-Union State Standard on condenser paper. Use of this method enables us not only to establish the preliminary standard in the $\tan\delta$ of paper, but also to obtain certain facts about the dependence of the loss angle of condenser paper on various factors in order to devise means of improving this fundamental characteristic.

It is known that one can successfully use the simplest equivalent sequence method [3] to calculate the electrical properties of condenser paper by means of the familiar characteristics of cellulose, (i.e. the substances forming the fibre walls), and by means of the characteristics of the substances filling the pores of the paper. Using this method for the case of dry non-impregnated condenser paper [4] we may obtain an expression which connects the loss angle of paper with the dielectric permeability of cellulose ($\epsilon_k \approx 6.5$), its angle of dielectric loss ($\tan\delta_k \approx 60 - 70 \times 10^{-4}$ at a frequency of 50 c/s and at a temperature of 20°C) and its density $\gamma_k = 1.5 - 1.55$ g/cm³):

$$\tan\delta = \frac{\tan\delta_\kappa}{1 + \frac{\varepsilon_\kappa(\gamma_\kappa - \gamma)}{\gamma}},$$

where γ – density (volumetric weight), of test paper determined experimentally.

Thus, the loss angle of condenser paper must primarily depend on its density, which determines the intensity of the calendering process. Our rational paper industry manufactures two main kinds of condenser paper: KON-I, – normally compressed, and KON-II – highly compressed. According to the All-Union State Standard the density of paper KON-I must be between 0.97 and 1.03 g/cm³ irrespective of its thickness; the density of paper KON-II in small thicknesses can vary between 1.14 and 1.23 g/cm³ and in large thicknesses (12-15 μ) amounts to 1.18 – 1.26 g/cm³.

Experimental data concerning the influence of the degree of compression of paper on the size of its loss angle [5] are compared in Fig. 1 with the results of calculations with the formula introduced, (for calculation it is assumed that $\tan\delta_k = 65 \times 10^{-4}$ and $\gamma_k = 1.53$ g/cm³). The conformity of experimental with calculated data has proved to be adequately satisfactory, especially at a density of the order of 1 g/cm³ and above. Using this same data, [5] the dependence is shown in Fig. 2 of the loss angle on temperature for raw uncalendered paper, removed from the paper machine (1), for normally calendered paper (2) and for highly calendered paper (3). The density of the specimens amounted to 0.82, 1.0 and 1.22 g/cm³, respectively.

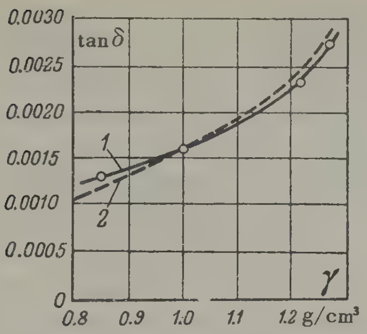

FIG. 1. Dependence of the loss angle on the density of paper, (50 c/s)
1 — experiment
2 — calculation

An increase in the density of paper, causing an increase in the tangent of the loss angle, at the same time leads to an increase in its electrical strength. Therefore paper KON-II is mainly used with direct current or with alternating current of low voltage, when its increased losses are not a special danger. Obviously it would be extremely desirable to produce such a paper Kon II, which would by conserving its electrical strength, reduce losses to the level of paper KON-I. In the new edition of the All-Union State Standard the following permissible maximum values of the tangent of the loss angle have been stipulated: for paper KON-II not greater than 0.002, but for paper KON-I not greater than 0.0017. These figures are appropriate for a frequency of 50 c/s and a temperature of 60°C, [range of minimum losses in the curve $\tan\delta = f(t)$].

It can be seen from the formula introduced that with a given density of paper, its loss angle can be reduced primarily because of the decrease in the magnitude of $\tan\delta_k$; i.e. the loss angle of the substance producing the paper's fibre wall in which there is inevitably an appreciable amount of organic ingredients and a certain amount of inorganic impurities (ashes) besides cellulose. One can primarily refer to the number of organic ingredients as "hemi-celluloses" (hexosans, pentroans and poly-uronic acids) and also lignin; the composition of the ashes includes silica, alumina, calcium oxide and magnesium oxide, and also the oxides of other metals (moreover, chlorides and sulphates are to be found in the ashes).

The contents of these substances obviously depend on the type of raw fibre from which the paper is manufactured; one might therefore assume beforehand that the value of $\tan\delta_k$, and consequently also the magnitude of dielectric losses in the paper can vary with the type of raw fibre. Experiment confirms this supposition. The data produced in Fig. 3 show that one can obtain a marked difference in the size of the loss angle of paper not only between such extremely diversified types of raw material as linen, rag and wood sulphate cellulose, but even for one type of material – wood sulphate cellulose. The kind of conifer from which cellulose is manufactured – fir and pine – can be of substantial importance. It is interesting to note that rag paper, in which the cellulose content proper (Alpha-cellulose) is greater than that in sulphate cellulose paper (i.e. the impurity content is less), provides not a lower but, on the contrary, a higher value of the loss angle than paper made from sulphate wood cellulose.

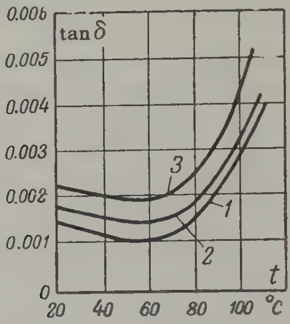

FIG. 2. Dependence of the loss angle on temperature, (50 c/s)
1 – uncalendered specimen of paper;
2 – paper KON - I;
3 – paper KON - II

In the U.S.S.R. and also abroad sulphate cellulose derived from pine wood is used as the basic raw material for the manufacture of condenser paper. Naturally the question arises: at what cost can one attain a reduction of the loss angle of paper in these conditions?

For an explanation of this, work has been carried out in the U.S.A. to study the influence which the cleansing of sulphate cellulose from non-cellulose ingredients has on the size of the loss angle of paper, [6]. The fundamental results of this work are shown in Fig. 4. The removal of inorganic substances and small amounts of foreign matter soluble in water and in organic solvents as well as lignin produces only a slight reduction of losses. When the hemi-cellulose content (mainly pentosans) was further reduced the losses began to decrease appreciably and reached a minimum with a certain optimum content of pentosans; a further elimination of pentosans was then accompanied by an increase of tan δ, whereupon the paper which had been prepared from almost pure alpha-cellulose showed a higher value of losses than in the case of the initial uncleansed sulphate cellulose. One should note that according to the data of this work the initial content of hemi-cellulose (pentosans) amounted to approximately 17 per cent in the American wood sulphate cellulose; minimum losses were reached with a residual content of pentosans of the order of 11 - 12 per cent.

Using cellulose with a decreased pentosan content, the Americans have produced a new kind of paper with reduced losses; the industrial use of such paper in the manufacture of power condensers has enabled losses in condensers to be reduced to 30 per cent and the reactive power of single condensers to be increased from 15 k var initially to 25, and eventually to 50 k var, [7].

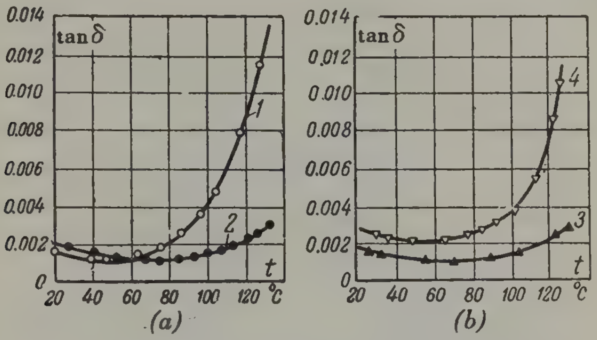

FIG. 3. Influence of type of raw fibre on the loss angle of condenser paper, (50 c/s)
1 — rag paper;
2 — sulphate-cellular paper;
3 — sulphate paper from pine cellulose;
4 — sulphate paper from fir cellulose

Analysis of national pine sulphate cellulose shows that the content of pentosan amounts to 11 - 12 per cent; i.e. without any further treatment it already lies within the limits of those values which were recognized in the U.S.A. as optimum from the point of view of obtaining minimum losses. Therefore, the purification of our cellulose for the purpose of reducing the hemi-cellulose content (pentosan) would not have to produce a decrease of tan δ. In fact, testing of experimental mouldings of purified cellulose produced in the Krasnogorodsk paper factory has shown that losses increase when the pentosan content in national KN type sulphate cellulose is reduced, (Fig. 5).

It was interesting to explain to what extent the residual lignin contained in KN cellulose and used in the production of national condenser paper can lead to a deterioration of its loss angle. For this purpose we measured the losses of that lignin which we obtained from the Central Scientific Research Institute of Paper in the form of powder and examined in the form of disks, cold-pressed at a pressure of 520 kg/cm². In view of the fact that it was impossible to make a direct comparison of the results of testing these disks with paper tests, for comparison, an experiment has been carried out with disks pressed out of low-molecular powdered cellulose (hydrate-cellulose), in these very same conditions, with a degree of polymerization of less than 200. The results obtained are shown in Fig. 6. In the range of temperatures of up to 80°C, losses were greater in lignin than in cellulose, but at higher temperatures the low-molecular cellulose produced a sharp increase in losses. These data indicate that the removal of lignin by purification of KN cellulose can produce a certain decrease of losses, but scarcely very great, as the lignin content in this cellulose is not very large – of the order of 3 - 4 per cent. Furthermore, there is reason to assume that a small residual content of lignin can even be useful with regard to an increase in the thermal stability of paper. In particular, it is known that rag paper, containing a sharply reduced quantity of residual lignin, (less than 0.5 per cent, has an appreciably lowered thermal stability in comparison with sulphate cellulose paper. It is, therefore, necessary to approach the question of reducing the content of residual lignin in KN cellulose very carefully.

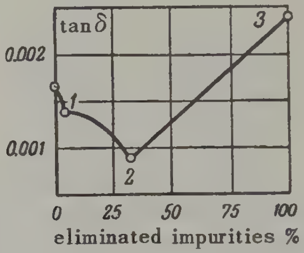

FIG. 4. Dependence of the loss angle on the degree of purification of paper from non-cellulose components, (60 c/s)
1 – without substances, extractable by solvents, of tannin lignin and ash; 2 – without part of the pentosan, (up to optimum); 3 – residual alpha-cellulose after every impurity has been removed

In the American work n special attention has been paid to the question of the influence of ashes and their composition on the size of the loss angle of paper. Moreover, there were reasons for supposing that even small changes in the composition of ash can have a considerable influence on the size of tan δ. Particularly, in one English work [8], it was shown that the presence of positively charged ions of monovalent metals in paper can substantially increase its conductivity. If the ash is analysed, we shall find in it metals in the form of oxides, However, before the specimen of paper is burnt to determine its ash content, metals can be found both in the paper and in another state, in particular, in the form of positively charged ions (cations) attached to the cellulose because of cation exchange reaction. In this connexion we have experimented with a solution of ash specimens of sulphate-cellulose condenser paper (solution is effected by treatment in a centi-normal solution of hydro-chloric acid with subsequent careful washing in distilled water), and we have also experimented with specially prepared specimens of paper, saturated after dissolving with various metallic cations, by producing a cation exchange reaction. These specimens were also carefully washed to remove that part of the metallic cations which had not become attached to the cellulose in the cation exchange. The quantity of connected cations was comparatively small and proved to be proportional to the atomic weight of the metal applied; for example, when saturated with magnesium the increase in weight of the sample amounted to about 0.05 per cent. The residual ash content of the specimens amounted to approximately 0.03 - 0.04 per cent. A spectrum analysis of the residual ash showed that it mainly consisted of compounds of silicon, aluminium and iron.

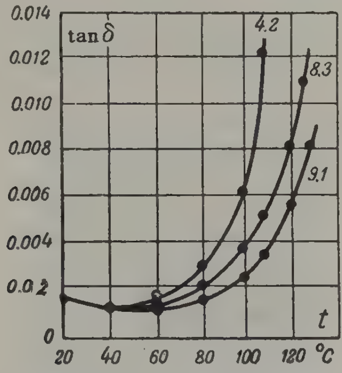

FIG. 5. The influence of a reduction of the pentosan content on the loss angle of experimental mouldings (50 c/s). The figures show the percentage content of pentosan

Measurements which were taken showed that the specific resistance of paper specimens appreciably decreases in comparison with decalcified (dissolved) samples, when cations of monovalent metal, such as sodium, are introduced into the paper; when cations of bivalent metals are introduced into paper, such as magnesium, there is little change in its specific resistance, (Fig. 7). In accordance with this, the loss angle of the specimens containing cations of monovalent metals sharply increases with temperature (Fig. 8), whereas the shape of the curve of the dependence tan δ on the temperature, representing the decalcified sample, remains practically unchanged, when cations of bivalent metals – magnesium, calcium, barium – are introduced. It is interesting to note that the deterioration of losses in paper is greater, the smaller the radius of the ion, when monovalent ions are introduced into it. Thus, losses of lithium, having the smallest ionic radius and to a lesser extent sodium and even less potassium, increase most of all; in this respect we have an interesting analogy with the behaviour of monovalent ions in inorganic glass, [9]. Evidently, in both cases the detrimental effect of monovalent ions is associated with their increased mobility.

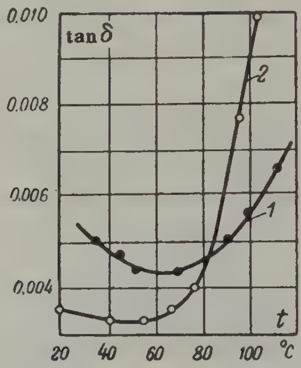

FIG. 6. Results of measuring losses (50 c/s) in lignin (1) and hydrate-cellulose (2)

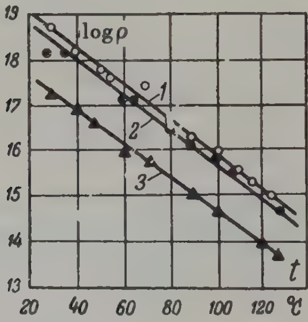

FIG. 7. Influence of cations on specific resistance of paper. 1 – decalcified sample; 2 – specimen, saturated with cations of bivalent magnesium; 3 – specimen, saturated with cations monovalent sodium

The influence of different types of ions on losses in paper at temperatures lower than zero is shown in Fig. 9. The minimum value of the dipole maximum of losses is seen in the case of the decalcified specimen. The introduction of metallic cations increases the dipole maximum all the more, the greater the radius of the ion and the higher its valency. Thus, in this temperature range the influence of bivalent ions on the amount of the losses is greater than the influence of monovalent ions in contrast to the range of temperatures above zero.

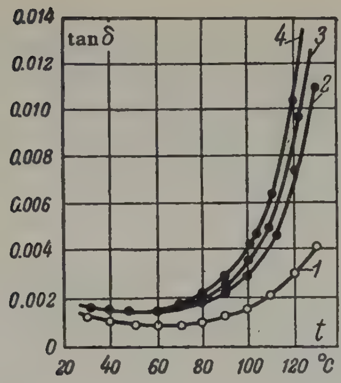

FIG. 8. Influence of cations on the loss angle of paper, (50 c/s)

1 – decalcified specimen; this particular curve agrees with curves for specimens saturated with bivalent cations of Ba^{++}, Ca^{++}, Mg^{++}; 2 – saturation of K^{+}; 3 – saturation of Na^{+}; 4 – saturation of Li^{+}

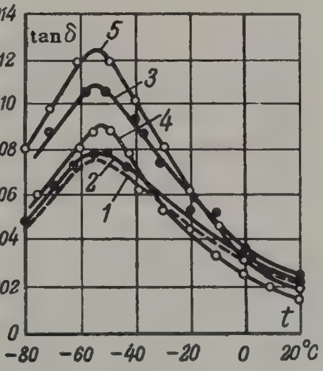

FIG. 9. Influence of cations on the loss angle of paper at low temperatures (1000 c/s)

1 – decalcified sample; 2 – saturated Na^{+}; 3 – saturated K^{+}; 4 – saturated Mg^{++}; 5 – saturated Ca^{++}

A study of the influence of metallic cations on the dielectric characteristics of condenser paper has enabled us to clarify the problem of selecting a system to purify the water used in processing this kind of paper. The introduction of a water-purifier at the "Kommunar" factory had, at first glance, a peculiar effect: paper, produced in purified water with its hardness sharply reduced, had appreciably worsened electrical characteristics compared with those groups of paper, which were previously produced in hard river water, (Fig. 10). Research into this problem showed that the sodium-cationic filter used in the water-purifying system introduced into the purified water cations of sodium, which passed from the water into the paper and worsened its dielectric properties. While retaining a little hardness in the water (ensuring an accelerated flow process compared with the use of hard river water), the removal of the sodium-cationic filter in the new water-purifying system enabled us to ensure that the electrical properties of the paper are no less than when river water is used.

These facts show that in solving the problem of reducing losses in paper one should pay attention not only to its organic composition but also to the volume of inorganic ingredients it contains, for which in the case in question the absolute content of ash in the paper is not so important as the ash's composition, in particular the presence of cations of monovalent metals.

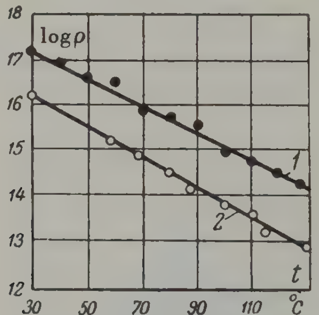

(a)

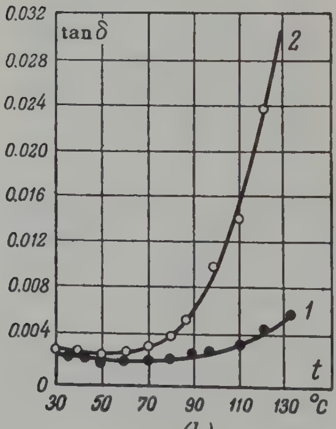

(b)

FIG. 10. Influence of the quality of the water used for production on the dielectric characteristics of condenser paper
A – specific electrical resistance; b – loss angle; 1 – river water; 2 – purified water (sodium-cationic filter in water-purification system)

In accordance with the prescription for boiling alkali, sulphate cellulose inevitably contains sodium, whose content practically remains constant in the process of pulverization and discharge of the paper, if additional portions of sodium cannot pass from the water used for production purposes into the paper in a defective water-purifying system. The possibility of eliminating sodium from raw cellulose to improve the characteristics of paper is an interesting proposition.

In the Moscow branch of the Central Scientific Paper Research Institute experiments have been carried out on the decalcification of paper by an electrodialysis method, [10]. The results of our measurements of the loss angle made on experimental mouldings from finely ground cellulose are given in Fig. 11. The data obtained show that electrodialysis is of short duration, which lowers the ash content to 0.12 per cent and practically rids the cellulose of its sodium content, appreciably reduces the loss angle; further decalcification ensuring a reduction of the residual ash content three times, but practically without changing the sodium content, does not reduce tan δ.

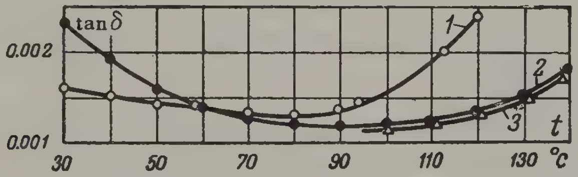

FIG. 11. Dependence of the loss angle on temperature for experimental mouldings of sulphate cellulose, purified by electro-dialysis
1 – raw cellulose, (ash content 0.53 per cent, sodium content 0.0590 per cent of weight of dry cellulose);
2 – cellulose after electro-dialysis of short duration, (ash content 0.12 per cent, sodium content 0.0017 per cent);
3 – cellulose after prolonged electro-dialysis, (ash content 0.04 per cent, sodium content 0.0013 per cent)

It is evident that the practical use of the electrodialysis method for eliminating the sodium contained in cellulose could assist the manufacture of paper with reduced losses.

Figure 3 shows a comparison of losses in paper prepared from different raw materials, a marked difference having been established between rag and sulphate cellular papers. In the light of data shown here regarding the influence of small changes in the composition of the ash on the dielectric characteristics of paper, one can imagine that the difference in the curves in Fig. 3 is caused not only by different raw material (from the point of view of the different organic composition), but also by a possible difference in the composition of the ash. To verify this supposition measurements were taken of the loss angle of specimens of rag and sulphate cellular paper, similar to that for which results of testing are shown in Fig. 3, but only after they had been subjected to a process of preliminary solution in hydrochloric acid and careful washing. Results which were obtained showed that, although the familiar difference between paper of different raw materials still subsisted, it did prove to be considerably less marked compared with that which had been observed before the samples were decalcified. This example confirms that the composition of ash exerts a great influence on the dielectric characteristics of paper.

Conclusions

1. The loss angle of condenser paper in a dried condition is an important criterion of its quality.

2. Purification of national sulphate cellulose in order to reduce its content of pentosans does not improve the paper's quality in so far as the reduction of its loss angle is concerned, but, on the contrary, leads to its increase.

3. An important factor, influencing the size of the loss angle of paper, is the composition of its ash; monovalent metals, in particular sodium, have a particularly detrimental effect.

4. A reduction of the loss angle of paper can be ensured by reducing the percentage of sodium using the electrodialysis method.

5. The use of sodium-cationic filters in systems for purifying the process water in the manufacture of electro-insulating types of paper should not be entertained.

Translated by J.F. Boyland

REFERENCES

1. H. Endicott; *Gen. El. Rev.* P. 28, No. 9 (1949).
2. V.T. Renne and N.N. Kaliazina; *Trud. LPI im. Kalinina (Works of the Kalinin Polytechnical Institute, Leningrad)* p. 343, No. 184 (1956).
3. V.T. Renne; *Raschet dielektricheskoi pronitsaemosti propitannoi bumagi. (Calculation of the dielectric permeability of impregnated paper). Elektrichestvo,* No. 1 (1949).
4. V.T. Renne; *Electrical Condensers.* Gosenergoizdat p. 303 (1952).
5. L.N. Kuligina; *Sbornik nauchno-issledovatel'skikh rabot studentov elektromekhanicheskovo fakul'teta LPI (Collection of the scientific research works of the students of the electromechanical faculty of Leningrad Polytechnical Institute)* p. 31 (1956).
6. H. Miller and R. Hopkins; *Gen. El. Rev.* P. 20, No. 12 (1947).
7. *El. World,* p. 241, No. 4 (1956).
8. H. Church; *J. Soc. Chem Ind.* p. 221. No. 7 (1947).

9. G.I. Skanavi; *Fizika dielektrikov, (Physics of Dielectrics),* Gostekhteore tizdat, p. 423 (1949).
10. S Kh. Kitaevai and V.V. Korolev; *Bumazhnaia promyshlennost' (Paper Production),* p. 4, No. 6 (1957).

ABSTRACTS FROM PAPERS PUBLISHED IN ELEKTRICHESTVO No. 9, 1958

Development of practical methods for designing low-frequency semiconductor amplifiers. I.L. Kaganov: (pp 8 - 15)

The author examines the methods of determining the operating conditions of (1) cascades of preliminary current amplification with RC and (2) current amplifiers with transformer coupling. As regards category (1), the formulae introduced are in respect of a voltage and current feedback scheme with different triodes and load resistances. As regards category (2), the author examines the choice of the coefficient of transformation n. He considers the case when the impedances cannot be agreed at the input and output to the cascade and proceeds to determine the resulting coefficient of amplification and the lower and upper limits of frequency.

Electrostatic field of a split phase. A.I. Darevskii: (pp 16 - 19)

Bi-polar co-ordinates are used and the Laplace equation directly solved for plane-parallel fields caused either by similarly charged double cylinders, or conducting double cylinders in a uniform field, or by two cylinders and an axis similarly charged and arranged at the points of an isosceles triangle.

Transformation method of circle representation and its use in solving electrostatic problems in a plane. G.N. Aleksandrov: (pp 20 - 23)

A field created by a linear charge q arranged in parallel to an axis of a conducting circular cylinder and outside it, can be found by superposing the fields of three linear charges without a conducting cylinder. The author's method implies the calculation of the distribution of field strength on the surface of split conductors.

Angular characteristic of a power directional device with phase sensitivity. Iu.G. Nazarov: (pp 24 - 30)

The angular characteristic represents the dependence of the average value of the voltage at the output of the scheme over a period on the angle between the current and voltage. The author examines distortions in the angular characteristic caused by (1), currents and voltages containing harmonics of the upper and lower frequencies and an aperiodic component and (2), by changes in the impedances of the rectifiers. In the event of impermissible distortions of the angular characteristic the author recommends the use of band filters which can be made sufficiently compact for detector-type relays.

A study of the heating of series A and AO 0.6 to 100 kW squirrel cage induction motors during continuous duty. P.A. Suiskii (pp 35 - 38)

Investigations have shown average values of the coefficients of heating losses can differ greatly from actual values. The author proposes formulae to determine the thermal parameters based on the regularities of a class of motors and the results of tests of a number of models. The method of equivalent heating losses is used to calculate the average temperature rises of the windings, illustrated in Appendix II. Apendix I shows the formulae for determining the air speed on different sections of the air conductor.

Industrial tests of a cable-bucket excavator with a new motor-drive system. V.P. Shafranov, A.I. Shishkov, V.D. Fursov and G.P. Petrenko: (pp 41 - 46)

The 1946 model with relay-contactor control and asynchronous drive did not ensure smooth starting and stopping, reliable operation and the required shape of the mechanical characteristic. In 1955 Novokramatorsk engineering works produced the E:Sh-4/40 excavators with drive mechanisms on the generator-motor system with a three-winding generator, but the cost was too high and the machines were unnecessarily powerful. In 1956 new electrical equipment was developed and in 1957 five excavators were built with the new system of asynchronous motor drive. The article then proceeds to discuss the most important results of tests on the drive mechanisms of one of these models. The use of powerful controlled saturation chokes in the circuit of the turning motor, the use of an inductive resistance in the rotor circuit of the main winch driving motor and the use of single phase braking of this motor has improved the technical and operating indices of the machine. In specified conditions the operating cycle of the excavator is 40 - 50 sec, its productivity 200 - 210 m^3/hr, the maximum volume of work per shift 1800 - 2000 m^3 and its specific power consumption 1 - 1.1 kW hr/m^3.

Portable electrical equipment and safety. M.R. Naifel' d: (pp 52 - 54)

Portable electrical equipment includes, electrical tools and production apparatus, domestic and laboratory appliances, children's toys and any electrical equipment connected to the mains by a flexible conductor and plug. The author states that the best guarantee of safety is the reliable construction and good insulation of the live parts of the equipment itself and the cables plugs and sockets. He reviews home and foreign practice and calls for a revision of the regulations governing this class of electrical equipment taking into account the different conditions in, for instance, schools, theatres, factories and homes.

The formation of static electricity charges and means of their neutralization.

V.N. Egorov: (pp 55 - 58)

A special piece of laboratory equipment is described and shown for determining the effect of factors causing the surface density of static electricity charges. The conditions causing the electrification of the materials in industrial conditions are reproduced on the apparatus. This consists of three driving and three driven rollers which move continuous tapes made of dielectric material. Each pair of rollers, as in industrial conditions, is made of metal, rubber, oak or organic glass. It is at the same time possible to measure the potential on tapes of three different materials with the same parameters (speed, tension, humidity, air temperature). Metering is effected by electro-static voltmeters both with the aid of a lamellar probe set up parallel to the surface of the belt and with the aid of foil brushes directly in contact with the surfaces of the moving tapes. The author then discusses his investigations with illustrations and tables of results and concludes that the speed of the tape in relation to the humidity of the air and the specific tension of the tape hardly affects the degree of neutralization and that temperature changes within the limits of 13 - 20°C do not really affect the process of de-electrification of the products. Soiling of the surfaces making contact likewise has little effect.

For neutralization of the static electricity charges he proposes new equipment. The surface of the grinding or driving organs rubbing the tape during operation should be intermittent strips made of material having a different permittivity, for example, rubber and plexiglass or of metal and plexiglass. The width of the strip on the rollers, with intermittent strips of different materials, should be inversely proportional to the potentials forming on the tape if the rollers are as a whole made of corresponding homogeneous materials. In this case, in the presence of friction at adjacent points of the products being electrified, charges arise which are the same in magnitude but opposite in sign. These are mutually compensated in the process of the passage of the product over the guiding or driving organ.

Calculating the power losses in a long line using the r.m.s. current.

T.B. Zaslavskaia (pp 58 - 59)

The author seeks to simplify the calculation of power losses in transmission lines by using the r.m.s. current method described in the text. Results are accurate within 2 - 4 per cent.

Electrical multiplication and division and its application to measurement and control. B.Sh. Bungin: (pp 60 - 62)

The author considers a method of obtaining the product or ratio of two or more electrical magnitudes based on the conversion of values into logarithms with subsequent addition or subtraction. As summing devices, use may be made of electrical machine or magnetic amplifiers with several control windings.

In the case of control using a logarithm of a function ϕ the absolute error ϵ corresponds in the whole range to an identical relative control error δ of the same function ϕ:

$$Y = \ln \varphi;$$
$$Y \pm \varepsilon = \ln \varphi \pm \varepsilon = \ln \varphi + \ln (1 \pm \delta) = \ln [(1 \pm \delta) \varphi].$$

If the absolute error ϵ of the function $Y = \ln \phi$ is a constant magnitude, then the relative error δ of the function ϕ is also constant.

Thus, logarithmic control of a magnitude can admit a lesser value of the coefficient of amplification of the system (for the desired relative error), or obtain a lesser relative error for small values of ϕ than in a system of control using the value of the function ϕ itself.

Measuring power by the equal temperature method. V.S. Popov: (pp 63 - 66)

The author's method is the direct measurement of the difference in power in the heaters of thermal converters or heating resistances; here the characteristics of each pair of converters or heating elements should be similar but the form of these characteristics can be quite arbitrary. The Electromechanical Institute of the Academy of Science has made a number of measurements of power with the aid of heating resistances. Here special equalizing heating resistances were developed consisting of two nichrome or constantan heaters, each of which was set in a glass insulation tube and a tungsten or platinum spiral mounted round the heater. Measurement of power by the equal temperature method is applicable to the measurement of power in the range of sound frequencies with an accuracy of hundredths of parts of a per cent, measurement and registration of power in a wide range of frequencies and the accurate measurement of power when the coefficient of power is low.

ELEKTRICHESTVO

Editor-in-Chief: N. G. Drozdov

Deputy Editor-in-Chief: I. A. Syromiatnikov

EDITORIAL BOARD

K. A. Andrianov, N. I. Borisenko, G. V. Butkevich, M. G. Chilikin, A. A. Glazunov, V. A. Golubtsova, E. G. Komar, M. P. Kostenko, L. R. Neiman, I. I. Petrov, V. I. Popkov, A. M. Fedoseev

Pergamon Press are also the publishers of the following journals:

Journal of Nuclear Energy (*including* The Soviet Journal of Atomic Energy *on behalf of Pergamon Institute*)

Reactor Technology (*Journal of Nuclear Energy, Part B*)

Health Physics (*The Official Journal of the Health Physics Society*)

Journal of Inorganic and Nuclear Chemistry

Tetrahedron (*The International Journal of Organic Chemistry*)

International Journal of Applied Radiation and Isotopes

Biochemical Pharmacology

*Biophysics

*Journal of Microbiology, Epidemiology and Immunobiology

*Problems of Hematology and Blood Transfusion

*Problems of Virology

*Problems of Oncology

*Sechenov Physiological Journal of the U.S.S.R.

*Radio Engineering

*Radio Engineering and Electronics

*Telecommunications

Archives of Oral Biology

Human Factors

*Pavlov Journal of Higher Nervous Activity

Electrochemica Acta

*The Physics of Metals and Metallography

*The Abstracts Journal of Metallurgy
  Part 1. The Science of Metals
  Part 2. The Technology of Metals

*Applied Mathematics and Mechanics

Chemical Engineering Science

Journal of Atmospheric and Terrestrial Physics

Planetary and Space Physics

Geochimica et Cosmochimica Acta

Bulletin Géodésique

Annals of the International Geophysical Year

Spectrochimica Acta

Journal of the Mechanics and Physics of Solids

Acta Metallurgica (*for the Board of Governors of Acta Metallurgica*)

International Journal of the Physics and Chemistry of Solids

Deep-Sea Research

Journal of Neurochemistry

Journal of Psychosomatic Research

Journal of Insect Physiology

Journal of Air Pollution

International Abstracts of Biological Sciences (*for Biological and Medical Abstracts Ltd,*)

Rheology Abstracts

Vacuum

Operational Research Quarterly

Annals of Occupational Hygiene

*Translations of the Russian journals published on behalf of Pergamon Institute.

Leaflets giving further details and subscription rates of each of these journals are available on request.

ELECTRIC TECHNOLOGY, U.S.S.R.

1959 VOLUME 3 NOVEMBER

CONTENTS

PAGE

V. L. **Fabrikant**: The utilization of semiconductors in relay protection 313

I. S. **Bruk**: Controlled reactors for long-distance transmission 322

I. K. **Khrustalev**: New methods of connecting starter-control resistances of asynchronous motors 334

R. A. **Lipman** and I. B. **Negnevitskii**: Transient processes in a magnetic booster working in a relay system 337

Abstracts of papers published in Elektrichestvo No. 7, 1958 353

V. A. **Prevezentsev**: Heat resistant winding conductors 358

Ia. N. **Shtrafun** and M. S. **Rostovtseva**: An investigation for an automatic system of excitation for large turbogenerators using semiconductor power rectifiers 373

N. S. **Siunov**, B. K. **Gavrilov** and V. N. **Breev**: The excitation of synchronous motors of normal construction by the application of mechanical rectifiers 384

T. V. **Stepnov**: Directional protection from short-circuits to earth 392

Abstracts of papers published in Elektrichestvo No. 8, 1958 403

M. A. **Panasenkov**: Surface effect in solid ferromagnetic bodies taking non-linearity into account 408

L. Ia. **Stanislavskii**: An experimental turbogenerator with internal hydrogen cooling of stator and rotor windings at a pressure of 3 atm 425

G. M. **Kasprzhak**: Calculation of the reduction of voltage on the terminals of high-power current collectors with strong actuating currents 435

V. T. **Renne**, N. N. **Kaliazina** and M. N. **Morozova**: Dielectric losses in condenser paper. 445

Abstracts of papers published in Elektrichestvo No. 9, 1958 458

NOTICE

Readers wishing to acquire translations or a copy of the original of any article abstracted or mentioned bibliographically in this journal, should sent their order or request for a quotation to:

The Secretary,
Pergamon Institute, Headington Hill Hall, Oxford
or
1404, New York Avenue, N.W., Washington 5, D.C.
where their order or enquiries will receive immediate attention

Made and printed in Great Britain by Pergamon Printing & Art Services Ltd.